22 | 1 | 04

Digestive Diseases
Clinical Reviews

Advanced Imaging Modalities

Editors
Steffen Rickes, Magdeburg
Peter Malfertheiner, Magdeburg

S. Karger
Medical and Scientific
Publishers
Basel • Freiburg
Paris • London
New York • Bangalore
Bangkok • Singapore
Tokyo • Sydney

KARGER

Digestive Diseases

Advanced Imaging Modalities

Editors
Steffen Rickes, Magdeburg
Peter Malfertheiner, Magdeburg

59 figures, 10 in color, and 28 tables, 2004

KARGER

Basel · Freiburg · Paris · London · New York ·
Bangalore · Bangkok · Singapore · Tokyo · Sydney

S. Karger
Medical and Scientific Publishers
Basel • Freiburg • Paris • London
New York • Bangalore • Bangkok
Singapore • Tokyo • Sydney

Drug Dosage
The authors and the publisher have exerted every effort to ensure that drug selection and dosage set forth in this text are in accord with current recommendations and practice at the time of publication. However, in view of ongoing research, changes in government regulations, and the constant flow of information relating to drug therapy and drug reactions, the reader is urged to check the package insert for each drug for any change in indications and dosage and for added warnings and precautions. This is particularly important when the recommended agent is a new and/or infrequently employed drug.

All rights reserved.
No part of this publication may be translated into other languages, reproduced or utilized in any form or by any means, electronic or mechanical, including photocopying, recording, microcopying, or by any information storage and retrieval system, without permission in writing from the publisher or, in the case of photocopying, direct payment of a specified fee to the Copyright Clearance Center (see 'General Information').

© Copyright 2004 by S. Karger AG,
P.O. Box, CH–4009 Basel (Switzerland)
Printed in Switzerland on acid-free paper by
Reinhardt Druck, Basel
ISBN 3–8055–7777–X

KARGER

Fax +41 61 306 12 34
E-Mail karger@karger.ch
www.karger.com

Vol. 22, No. 1, 2004

Digestive Diseases

Contents

KARGER

Fax +41 61 306 12 34
E-Mail karger@karger.ch
www.karger.com

© 2004 S. Karger AG, Basel

Access to full text and tables of contents, including tentative ones for forthcoming issues: www.karger.com/ddi_issues

Digestive Diseases

Dig Dis 2004;22:5
DOI: 10.1159/000079370

Editorial

Major progress in the diagnostic approach to diseases of the digestive system has been obtained by the introduction of new and refined noninvasive imaging technologies. Echo-enhanced sonography is a good example. This technique is based on the property of microbubbles to resonate and emit harmonic waves in an ultrasound field. The initial method, defined as 'second harmonic imaging', was completely limited by the inability to separate the signals obtained from the bubbles and tissue texture. Therefore this procedure was replaced by the pulse-inversion imaging technique which now gives much better picture quality. In this way echo-enhanced sonography enables the depiction of the vascularization pattern of distinct lesions in the liver and pancreas.

In a comparable way the other key imaging modalities, such as CT scan, magnetic resonance imaging, Doppler sonography, and endosonography, have also further improved in performance. In their complexity as well as selective applications, they represent a corner stone in the diagnosis and staging of benign and malignant lesions in the liver and pancreas. Although the methods do partly compete, they often need to be used in a complementary way to obtain optimal results for decision-making. An additional aspect addressed is the role of ultrasound imaging in inflammatory bowel diseases.

The aim of this issue of *Digestive Diseases* is to provide clinicians an insight into modern imaging modalities for the diagnosis, differentiation, and staging of gastrointestinal diseases.

Steffen Rickes
Peter Malfertheiner

KARGER

Fax + 41 61 306 12 34
E-Mail karger@karger.ch
www.karger.com

© 2004 S. Karger AG, Basel
0257–2753/04/0221–0005$21.00/0

Accessible online at:
www.karger.com/ddi

Review Article

Digestive Diseases

Dig Dis 2004;22:6–17
DOI: 10.1159/000078730

CT in the Differentiation of Pancreatic Neoplasms – Progress Report

Norbert Gritzmann Peter Macheiner Alois Hollerweger Erich Hübner

Department of Radiology and Nuclear Medicine, KH Barmherzige Brüder Salzburg, Austria

Key Words
Pancreas tumors · Ductal cell adenocarcinoma · Staging · Computed tomography · Functional tumors of the pancreas · Insulinoma · Serous cystadenoma · Mucinous tumors · Pancreatic tumors

Abstract
Today, computed tomography (CT) is the most commonly used imaging method in the assessment of pancreatic tumors. The sensitivity of CT in detection of pancreatic tumors is more than 90% when direct and indirect signs are used for diagnosis. However, the potential to differentiate exocrine (non-endocrine) tumors of the pancreas is limited. CT is used in these lesions to perform an adequate staging, especially for surgical purposes. The operative resectability, primarily in regard to vessels, lymph node metastasis and hepatic metastasis, has to be assessed. Keeping in mind the limitations of this macromorphological imaging procedure, CT has the best reproducibility and overall accuracy of all imaging methods. Using multislice CT it is possible to perform nonaxial reconstructions with high resolution. In functional endocrine tumors, multislice spiral CT will enhance the diagnostic capabilities, since the whole organ can be examined in thin slices, with high resolution during the rather short arterial phase of the contrast medium. Since some endocrine tumors are hypovascular, a scan during the portovenous phase is recommended too. The diagnosis of benign pancreatic tumors, like serous cystadenoma and pancreatic lipomas, is addressed. The most important pseudotumors of the pancreas are discussed.

Copyright © 2004 S. Karger AG, Basel

Introduction

Detection, classification and staging of pancreatic neoplasms are a challenge for radiologists. In recent years the technical and diagnostic performance of computed tomography (CT) has improved significantly [1]. Today, multislice spiral CT with 4–16 detector rows of simultaneous acquisition is state of the art. CT is the single best imaging modality in evaluation of pancreatic tumors in terms of overall accuracy, reliability and reproducibility [2]. In solid exocrine tumors an exact histologic classification is not possible using CT. However, approximately 80% of all epithelial neoplasms are ductal cell adenocarcinoma [3]. In these lesions the preoperative assessment and the ability of CT in regard to the clinical questions of resectability and staging will be addressed. In endocrine tumors that are often arterially hypervasculized, the impact of spiral and multislice CT will be discussed. In rare benign neoplasms of the pancreas, as microcystic adenoma or lipoma, typical radiological features are present. The radiological features of the most common pancreatic tumors are presented. Whenever present the characteristics of the lesions will be addressed.

KARGER

Fax + 41 61 306 12 34
E-Mail karger@karger.ch
www.karger.com

© 2004 S. Karger AG, Basel
0257–2753/04/0221–0006$21.00/0

Accessible online at:
www.karger.com/ddi

Norbert Gritzmann, MD
Professor of Radiology, Department Radiology and Nuclear Medicine
KH Barmherzige Brüder Salzburg, Kajetanerplatz 1
AT–5020 Salzburg (Austria)
Tel. +43 662 8088510, Fax +43 662 840464, E-Mail norbert.gritzmann@bbsalz.at

Exocrine Epithelial Neoplasms

Ductal Cell Adenocarcinoma

Ductal cell adenocarcinoma represents 75–85% of non-endocrine malignancies of the pancreas. These tumors predominantly occur in the seventh decade of life. 60–70% of the tumors are localized in the head of the pancreas. About 10% occupy the corpus of the pancreas, about 5% the tail, about 5% both the head and the corpus and about 10% corpus and tail [3]. Pancreatic carcinoma is the cause of 3–7% of all cancer-related deaths. The prognosis of this tumor still is very poor.

In the head of the pancreas the tumors usually show symptoms earlier than in the pancreatic tail. This is mainly due to symptomatic obstruction of the biliary or pancreatic duct. Usually ductal adenocarcinoma is diagnosed with a size of <10 cm in maximal diameter. The tumor often causes a desmoplastic reaction, especially when the gastrointestinal tract is invaded.

A focal mass is the most common CT finding. However, up to 5% of pancreatic cancers present as diffuse enlargement. In non-enhanced CT scans the tumor usually is isodense to the pancreatic tissue. Occasionally a slightly decreased attenuation is found. In multislice CT suspected adenocarcinoma, the contrast-enhanced scans are usually performed in two phases: first during the pancreatic phase that is approximately 40 s, and the portovenous phase 65–70 s after intravenous administration of iodinated contrast media. In many cases a moderately hypodense lesion with ill-defined borders will be seen (fig. 1a, b). Calcifications are only rarely seen in ductal adenocarcinoma. In some patients the tumor will be isodense even with an optimal intravenous bolus of contrast media. Due to these limitations, small-sized tumors (<2 cm) will frequently be missed by CT since these lesions do not alter the contour of the organ [4]. Overall, the sensitivity of CT in detection of pancreatic carcinoma is reported to be between 90 and 99% depending whether only signs of direct evidence or both direct and indirect signs are taken into account [2]. Only indirect signs as dilatations of the major pancreatic or the main biliary duct are often visualized in small tumors. In some early cancers of the papilla vatteri or the head of the pancreas, the only sign of a tumor is an abrupt obliteration of the pancreatic or the common bile duct.

Usually the main pancreatic duct measures <2 mm in transverse diameter. A dilatation of the pancreatic duct proximal to the obstructing tumor will be seen in 50–75% of cases. The dilatation of the pancreatic duct is better seen on narrow slices. Neoplasms of the head of the pan-

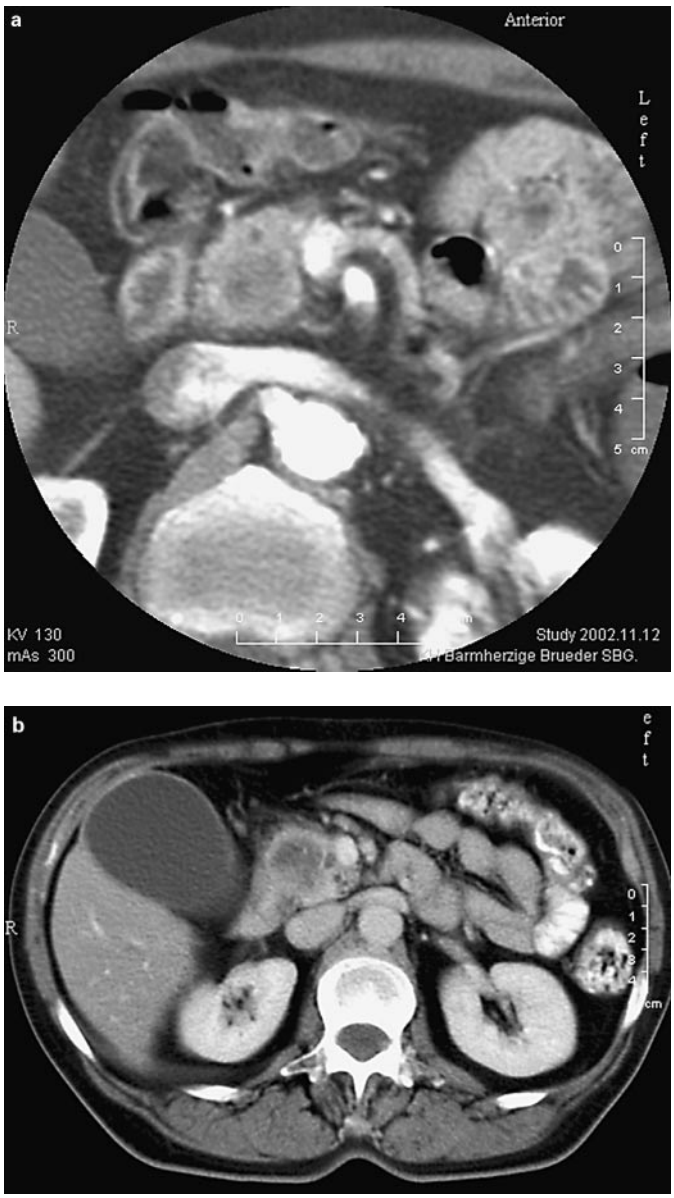

Fig. 1. a CT of the pancreatic head. A hypodense lesion is seen in the pancreatic head without enlargement of the organ. Moderate dilatation of pancreatic duct: ductal cell adenocarcinoma. **b** Section of the head pancreas. A hypodense lesion is visualized in the pancreatic head. Note that there are no fat planes between the tumor and the superior mesenteric vein. Also in normal pancreas no fat planes are found in this location. The dilated main pancreatic duct and small dilated ducts in the uncinate process are displayed. The gallbladder shows a hydrops. Histologically a ductal cell adenocarcinoma without vascular invasions was diagnosed.

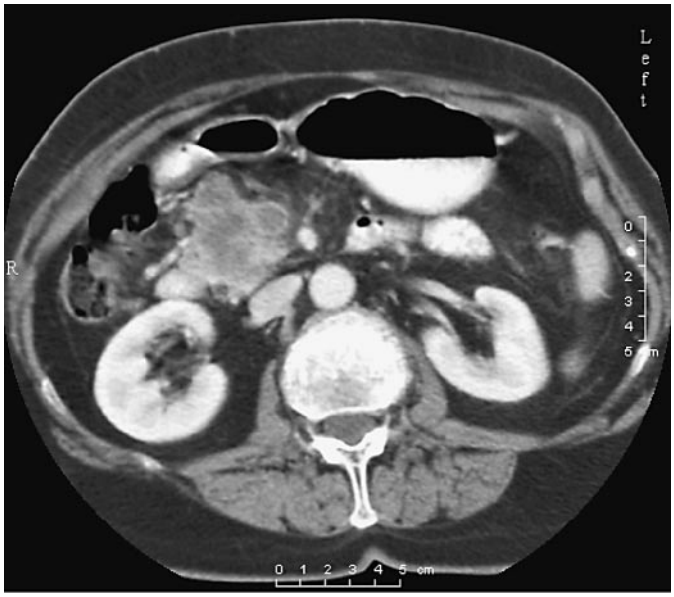

Fig. 2. CT of the pancreatic head. A hypodense, ill-defined tumor is visualized, the superior mesenteric vein is thrombosed: adenocarcinoma of the pancreatic head with venous invasion.

creas frequently show a dilatation of the main pancreatic duct. Often an atrophy of the pancreatic parenchyma is found in the surrounding area of an obstructed pancreatic duct. A concomitant chronic pancreatitis is found histologically in up to 50% of these patients. In the non-operated biliary system a transverse diameter of the choledochal duct of up to 6 mm is regarded as normal sized. The non-dilated intrahepatic bile ducts are not seen using CT. Hypodense tubular structures running parallel to the portal system are regarded as dilated bile ducts.

The combination of dilated bile and pancreatic duct is regarded as very suspicious for a pancreatic neoplasm (double duct sign). However, benign diseases like chronic inflammatory pseudotumor of the pancreatic head may also obstruct the ductal systems. Abrupt obstruction of the ductal systems is typical for tumors. However, a non-calcified concrement may cause the same CT feature.

Staging of Pancreatic Cancer Using CT

CT is the single most important imaging method for staging of pancreatic cancer [2, 5–7]. Multislice spiral CT has become the standard in CT. Using this technique, narrow slices of the abdomen can be obtained within seconds. Hence the bolus of the contrast medium can be used in an optimal way.

Compared with single-slice CT, multiplanar reconstructions can be performed, even in a curved manner with a high resolution. Due to nearly isotropic acquisition of volumetric data, CT has become a real multiplanar imaging technique as MRI. The application of intravenously iodinated contrast media is obligatory in the assessment of pancreatic tumors. 2 ml/kg body weight of non-ionic contrast media are needed for an adequate contrast. Usually in the assessment of non-endocrine tumors the scans are performed in the pancreatic phase to obtain the best tumor/pancreas contrast. The liver and the surrounding vessels are best evaluated during the portovenous phase.

In small cancers, that do not alter the contour of the pancreas, it may be difficult or even impossible to detect the lesion since pancreatic cancer may be isodense to the pancreatic parenchyma. Extrapancreatic infiltrations are present in 40–70% of cases.

Vascular encasement is extremely important to diagnose preoperatively [8, 9]. Normally the arteries (superior mesenteric artery, celiac trunk, aorta) are surrounded by retroperitoneal fat planes. The obliterations of these fat planes by (solid) structures are indicative of infiltrations of the wall of the vessels or vascular encasement.

Lu et al. [9] reported four categories regarding the circumference of vessels contiguous with the tumor. In pronounced cases, narrowing or even occlusion of the vessels can be seen. In these situations, collateral vessels may be depicted. Especially in assessment of the vascular situation, multislice spiral CT has advantages over single-slice spiral CT since very narrow slices may be obtained.

On the venous side it is important to detect infiltrations of the superior mesenteric vein, portal vein, vena cava inferior, or the renal veins. The assessment of the splenic vessels is less important since in a Whipple procedure these vessels are resected together with the pancreas. In venous occlusion, collateral veins can be detected too. Generally, CT is more accurate in the assessment of venous encasement than in arterial infiltrations. Limited venous invasion does not represent absolute exclusion from surgery, but increases the operation time significantly. Thrombosis of the vessels is detected with high accuracy (fig. 2). However, it is very difficult to differentiate tumor thrombosis from appositional thrombosis. Due to the high resolution of multislice spiral CT, clinically anatomic variations of the vascular anatomy can be diagnosed preoperatively.

Invasion of continuous structures occurs in advanced disease most commonly involving the duodenum and the stomach. The colon, spleen, and left adrenal, rarely the

left kidney or the spine, may be affected. When ascites is found, tumor resectability is highly unlikely. Most often, ascites is a sign of peritoneal carcinomatosis. The small peritoneal implants are rarely depicted by CT. As discussed above, CT is accurate in detection of obstruction of the biliary or the pancreatic duct.

Peripancreatic lymph nodes are the primary lymph node stations of the pancreas. However, the lymph nodes in the hepatoduodenal ligament or the paraaortal nodes may be involved in pancreatic cancer too. In ductal adenocarcinoma, CT demonstrates enlarged retroperitoneal lymph nodes in 15–30%, and usually these nodes are metastatic. However, it is not possible to diagnose metastasis in normal-sized retroperitoneal lymph nodes by CT [7].

Hepatic metastases are present on CT at the initial evaluation in 20–50% of cases. Hepatic metastases of pancreatic cancer are frequently relatively small and therefore difficult to detect. Most of the hepatic metastases of ductal cell adenocarcinoma are hypodense lesions compared with the normal liver parenchyma. Extraabdominal metastases are only rarely found during the initial staging of pancreatic cancer. The accuracy of CT in assessment lack of resectability of pancreatic cancer is about 84–96 % [7]. However, 25–30% who are reported to be respectable on CT have unresectable disease at surgery [2].

Pleomorphic Giant Cell Carcinoma

Pleomorphic giant cell carcinoma is a highly malignant variant of ductal cell carcinoma, comprising 2–7% of non-endocrine tumors of the pancreas. Histogenesis favors sarcomatoid transformation of ductal cell carcinoma. Prognosis is extremely poor with a median survival of 2 months. CT depicts this neoplasm as large thick-walled cystic masses with a ragged inner contour, due to central hemorrhagic necrosis. Otherwise, solid masses with a relatively low attenuation center are found [10–11]. No distinctive CT features that allow the differentiation from ductal adenocarcinoma have been reported. Massive retroperitoneal lymph node metastasis and hematogenous metastasis are frequently found.

Adenosquamous Carcinoma

This neoplasm represents about 3% of all non-endocrine pancreatic neoplasms. Adenosquamous carcinomas are large masses that are either solid with a desmoplastic response or partially necrotic without desmoplasia. When necrotic areas are present, CT will display cystic regions that may communicate with the pancreatic duct. No distinctive CT features that allow the differentiation from ductal adenocarcinoma have been reported [13, 14]. Prognosis is slightly worse than in ductal cell carcinoma.

Fig. 3. CT of the pancreatic head. A large ill-defined tumor is seen in the pancreatic head with a very hypodense structure. The vessels are encased by dense structures. Dilatations of the intrahepatic bile ducts are preset. Histology revealed a mucinous adenocarcinoma.

Histologically, *microadenocarcinoma* and *anaplastic carcinomas* can also be differentiated. No distinctive CT features that allow the differentiation from ductal adenocarcinoma have been reported.

Mucinous Adenocarcinoma (Colloid Carcinoma, Mucin-Hypersecreting Carcinoma)

The presence of a great amount of mucin characterizes this rare tumor. About 2% of the non-endocrine tumors are caused by this type of tumor. Mucinous adenocarcinomas are often larger than ductal cell carcinomas. CT may demonstrate low density areas consistent with necrosis or mucin. The mucin-filled ducts have a homogeneous or a slightly low inhomogeneous attenuation. These areas of mucin do not enhance after contrast (fig. 3). Enhancing tumor nodules may be depicted within the dilated ducts [15, 16]. In cases limited to the ducts a better prognosis than in ductal cell carcinoma has been reported.

Microcystic Adenoma (Serous Cystadenoma)

80% of patients with microcystic adenoma are older than 60 years. There is a female predominance of 3:2 to 9:2. There is no predilection for any location within the gland. Microcystic adenomas are on average 10 cm in diameter and usually have a lobulated contour. Microcystic adenomas are composed of innumerable cysts, the vast

Fig. 4. CT of the pancreatic head. A lesion with an inhomogeneous structure with a honeycomb appearance is seen in the pancreatic head. Histology revealed a serous, microcystic adenoma.

Fig. 5. CT of the pancreatic tail. A multicystic lesion with cysts of 3–4 cm is visualized in the pancreatic tail. Histology revealed a mucinous adenoma.

majority vary from 1 mm to 2 cm in diameter. Calcifications can be present, are mostly central and rarely have a typical sunburst pattern [3]. After intravenous contrast the lesions show a Swiss cheese/honeycomb pattern caused by tiny non-enhancing cysts and the markedly vascularized stroma and septae (fig. 4). Furthermore, a central fibrous scar that may calcify is regarded as typical. More than 6 cystic spaces are usually visualized [17–20]. Cysts >2 cm may be present in some cases. Solid masses may enhance as islet cell tumors [17].

A variant is macrocystic serous adenoma of the pancreas, were a uni- or bilocular cystic process is found [21]. Usually these cysts are thin-walled and indistinguishable from mucinous cystadenoma by CT. A female prevalence is reported too. The prognosis of benign serous cystadenoma is good. Serous cystadenocarinomas are very rare tumors [17, 22].

Mucinous Cystic Neoplasm (Mucinous Cystadenoma, Cystadenocarcinoma)

There is a 9:1 female to male ratio. 50% are in the 40- to 60-year age group. 90% are located in the corpus or tail of the pancreas. The average diameter is 12 cm. Their external surface is smooth. They are composed of uni- or multilocular large cysts [23–25]. The average number of cysts is <6. However, smaller cysts with a diameter of <2 cm may also be present. Calcifications may be found. Solid papillary nodules may be observed, which are enhanced after intravenous contrast administration. Calcifications, thickened walls or septa are signs of malignancy [25]. Mucinous tumors may be diagnosed by fine needle aspiration biopsy [26, 27]. It is not accurately possible to differentiate benign from malignant forms with any imaging method (fig. 5, 6). The prognosis is better than in duc-

Fig. 6. CT of the pancreatic tail. A multicystic lesion with several cysts and some solid structures and tiny calcifications is found. Histology revealed a macrocystic mucinous carcinoma.

tal adenocarcinoma even in frankly malignant cases. All lesions should be treated by complete excision.

Ductectatic cystadenoma/cystadenocarcinoma is a variant of mucinous cystic neoplasm. There is no female predilection in these lesions. Often the tumor occurs in the uncinate process [28, 29]. Solid tumor nodules are found within a conglomerate of 2–4 cm communicating cysts. There is a poor discrimination between benign and malignant forms by CT.

Acinar Cell Carcinoma

This neoplasm comprises up 1–10% of non-endocrine pancreatic carcinomas. There is a male prevalence of elderly men. Acinar cell carcinoma show less demoplastic reaction than ductal adenocarcinoma. Usually they are large than these. In CT they show a greater tendency to central necrosis. Cases with subcutaneous fat necrosis due to excessive lipase production and osteolytic features have been described [12]. No clear differentiation criteria to other solid exocrine tumors have been reported for CT.

Pancreatoblastoma (Infantile Carcinoma of the Pancreas)

This tumor is very rare. The patients are younger than 7 years. They are located typically in the head of the pancreas. CT shows a well-demarcated solid mass of variable size containing low density areas corresponding with hemorrhage and necrosis [30]. The prognosis is good if no distant metastases are present. The lesion is usually curable by complete resection. However, many children have hepatic or nodal metastasis. In these patients the prognosis is poor.

Solid and Papillary Epithelial Neoplasms

Solid and papillary epithelial neoplasms mainly occur in young women [31–33]. They are predominantly located in the pancreatic tail. The tumors contain signs of hemorrhage or cystic areas, sometimes with a fluid-debris level [31]. Calcifications are frequently seen. The prognosis is better than in ductal adenocarcinoma.

Osteoclast-Type Giant Cell Tumor, Mixed Carcinomas

These rare histological forms exhibit no distinctive CT features that allow the differentiation from ductal adenocarcinoma.

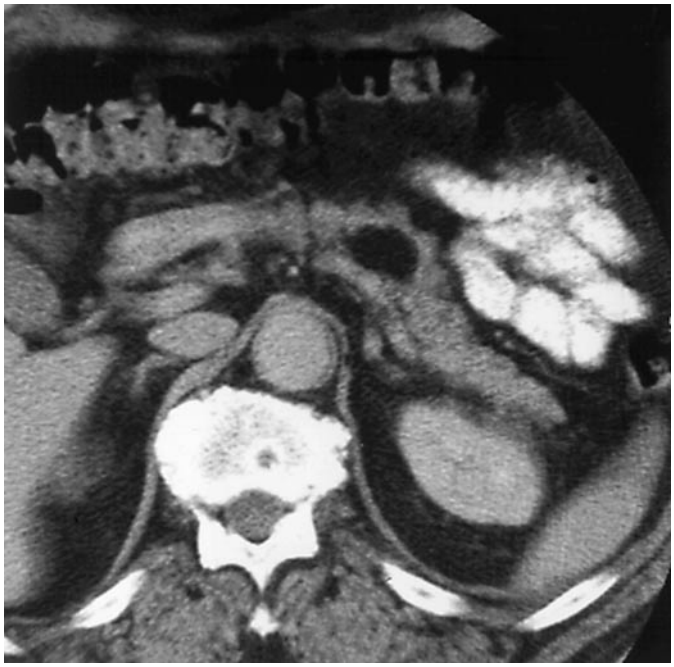

Fig. 7. CT of the corpus of the pancreas. In the corpus of the pancreas a 2-cm very hypodense lesion with fat equivalent density values is visualized. Lipoma of the pancreas.

Lipoma

Lipoma of the pancreas is a rare benign tumor. Due to the unique negative density values (–20 to –100 HU) this lesion can be diagnosed rather specifically [39, 40]. Usually these lesions measure 2–3 cm in diameter and are clinically unapparent (fig. 7). The differential diagnosis of fat-containing pancreatic tumors would be retroperitoneal liposarcoma or a dysontogenetic tumor like a dermoid.

Lymphoma

Non-Hodgkin lymphoma rarely involves the pancreas. Less than 0.5% of all pancreatic tumors are lymphomas. However, in Burkitt's lymphoma the involvement of the pancreas is not unusual [3]. Features favoring lymphoma versus ductal carcinoma are large size, lack of bile duct dilatation and multifocality. Diffuse lymphomatous infiltration is occasionally present that can mimic acute pancreatitis on CT. Sometimes it is difficult to differentiate enlarged peripancreatic nodes from intrinsic pancreatic involvement. Bulky disease is often present in the retroperitoneum.

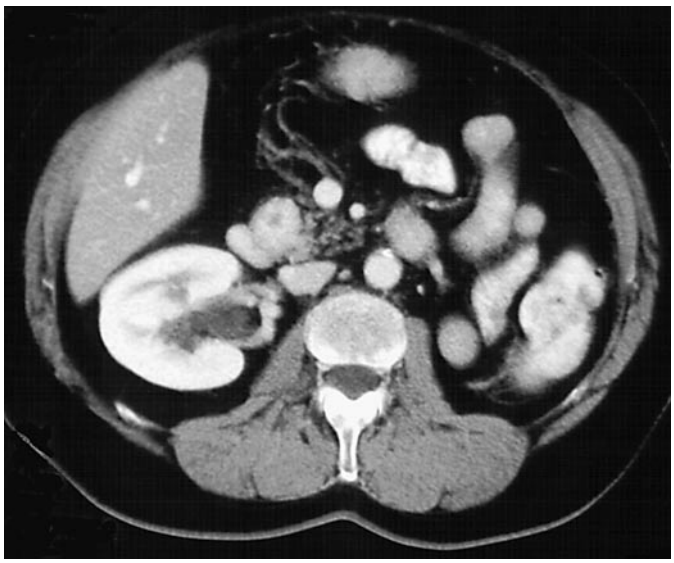

Fig. 8. CT of the pancreatic head. Shown is a patient after left-sided nephrectomy due to hypernephroma. A small-sized hyperdense lesion with central hypodensity is visualized. Histology revealed metastasis of a hypernephroid carcinoma of the kidney.

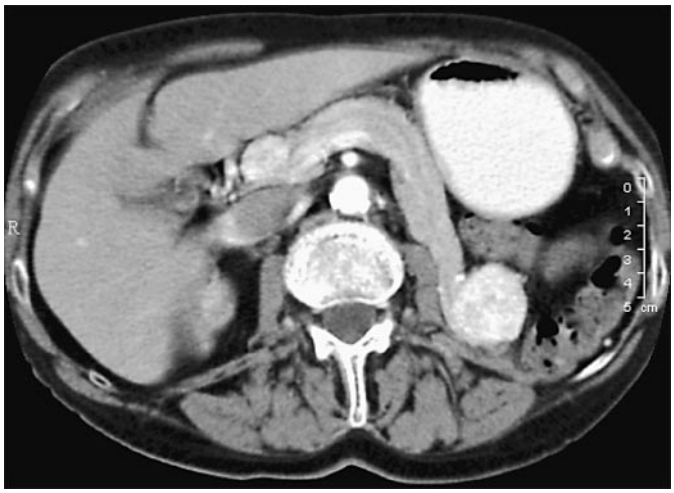

Fig. 9. CT of the pancreas. Two hyperdense lesions are visualized: one is smaller in the pancreatic neck and one larger in the pancreatic tail. Histology revealed multiple insulinomas.

Metastases

Metastases to the pancreas are relatively rare. However, several cases of metastases in the pancreas caused by hypernephroma have been reported [34]. In these tumors arterial-enhancing lesions are seen within the gland, sometimes with central necroses (fig. 8). Most often these lesions measure about 3 cm in diameter. They are usually detected during a follow-up investigation without symptoms.

Other tumors that may cause metastasis in the pancreas are bronchial carcinoma, melanoma, gastric cancer or breast cancer [34–38]. Widespread metastases are often present in these tumors.

Tumors of the Endocrine Pancreas

Tumors of the endocrine pancreas are rare neoplasms. They are divided into functional and non-functional tumors and often referred to as *APUDomas* (amine precursor uptake and decarboxylation).

Islet Cell Tumor

Islet cell tumors are classified as either functional or non-functional tumors. Functional tumors produce an excessive level of insulin. Laboratory tests can measure these hormones. These tumors may be either single or multiple. They may be benign or malignant. Malignancy may be difficult to determine even by histology; evidence of adjacent organ invasions or metastasis are the most reliable signs of malignancy. Their size may vary considerably at the time of clinical presentation. In functional tumors the aim of radiology is to localize the lesion within the gland and to diagnose possible multinodularity.

Insulinomas

Insulinomas are the most frequent islet cell tumors. They occur most often after the age 40 years, except in patients with MEN-1 syndrome who are younger at presentation. The vast majority of tumors are <2 cm in diameter, solitary and benign. Most patients with multiple tumors have MEN-1 syndrome. Patients with Hippel-Lindau disease also have an increased prevalence of islet cell tumors and pheochromocytoma [42]. Insulinomas are distributed evenly throughout the pancreas. Insulinomas are recognized by a typical clinical picture of significant hypoglycemia. Rarely, hyperinsulism may develop in neonates and young children secondary to islet cell hyperplasia or due to excessive differentiation of pancreatic epithelial cells to islet cells (nesidioblastosis). In these patients no lesions are found radiologically.

Using CT it is important to investigate functional endocrine tumors during the arterial phase, since the le-

Table 1. Typical CT densities after contrast media of pancreatic tumors

Cystoid	Hyperdense	Hypodense, isodense
Serous cystadenoma (Swiss cheese)	Endocrine tumors	Most exocrine tumors
Macrocystic mucinous adenoma/carcinoma	Metastasis (hypernephroma)	Lymphoma
Necrotic carcinomas (giant cell carcinoma)	Non-functional endocrine tumors	Endocrine tumors (mostly non-functional)
Neuroendocrine tumors (hyperdense parts)	Leiomyoma	
Ductectatic mucinous papillary tumor		
Lymphangioma		

sions may reveal only a short enhancement (fig. 9) [41, 43–45]. Multislice spiral CT is capable of investigating the whole gland in thin sections during the arterial phase, which lasts only 10–15 s. Most of the insulinomas are hyperdense during the arterial phase (table 1); however, scans during the parenchymal phase of the pancreas are also recommended, since some lesions may be found only during this phase [43, 44]. Insulinomas >1 cm are usually detected using spiral CT. A minority of secretory islet cell tumors are hypovascular or even cystic and therefore are not readily detected with CT. Generally, multiple tumors are more difficult to detect since they are usually smaller in size. Larger tumors may show central necrosis or calcifications [46, 47].

Gastrinomas

Although the majority of gastrinomas are localized in the pancreas, up to 10% may arise in an extrapancreatic location (table 2). Most of them are found in the region of the common bile duct, cyst duct and descending duodenum. They are usually found on the right side of the junction of pancreatic corpus and tail, in the triangle below the cystic duct and the descending duodenal wall. Approximately 60% of all gastrinomas are malignant. A typical clinical presentation (hyperactivity, hypersecretion and atypical ulcers) was first described by Zollinger and Ellison. 20–40% of patients with Zollinger-Ellison syndrome are estimated to have MEN-1. Today, diagnosis is made by measurement of the gastrin levels. CT is commonly used to localize gastrinomas. Lesions >3 cm are localized with high accuracy. Tumors <1 cm are difficult to diagnose by CT. Scanning during the arterial phase is important to detect these transient hypervascular tumors [48].

Table 2. APUDomas and their frequency in pancreatic localization

Histology	Pancreatic localization, %
Insulinoma	100
Glucagonoma	100
Gastrinoma	90
PPoma	100
Somatostatinoma	56
GRFoma	30

Delayed scanning (4–6 h after contrast administration) has especially been recommended to detect liver metastasis. In hepatic metastasis of functional endocrine tumors, multislice CT will probably optimize the accuracy of CT, since the whole liver can be examined during the short arterial phase.

Glucagonomas

Glucagonomas are rare islet cell tumors and generally large, malignant masses [49]. Patients often present with characteristic skin diseases known as migratory necrolytic dermatitis commonly associated with stomatitis. Diabetes mellitus may be present.

VIPomas (Vasoactive Intestinal Peptide)

Hormone-active VIPomas often cause watery, secretory diarrhea, hypokalemia, and hypochlorhydria. Usually these tumors are large and often localized in the head of the pancreas. Most of them are malignant [50]. Like other

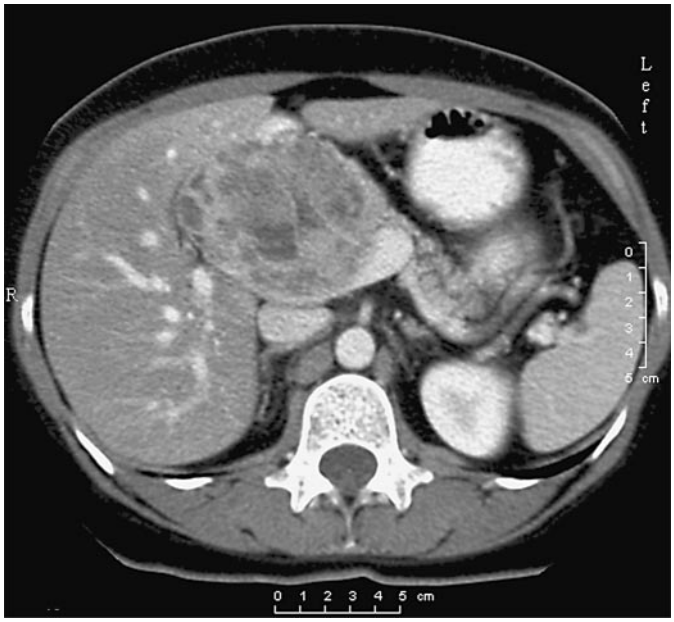

Fig. 10. CT of the pancreatic head. In the head of the pancreas a big lesion with an inhomogeneous structure with hyperdense areas are seen. There is no dilatation of the bile ducts: VIPoma was reported histologically.

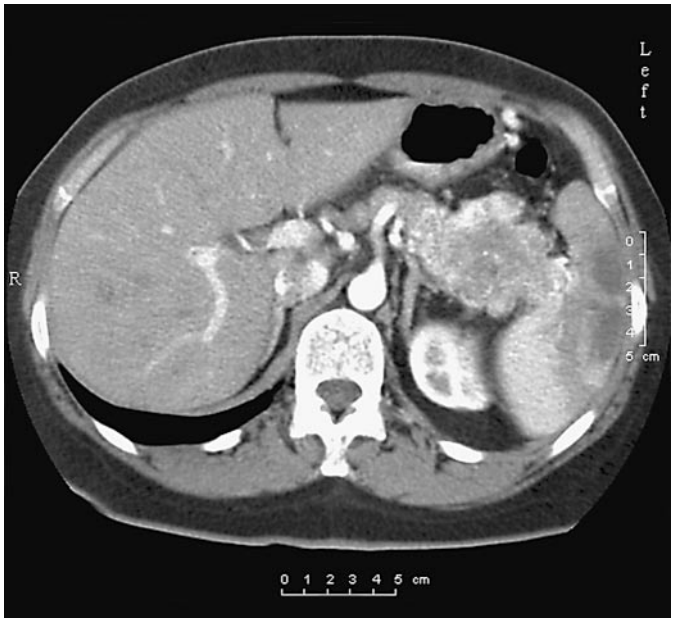

Fig. 11. CT of the pancreatic tail. A large ill-defined marginal hyperdense tumor is seen. Hypodensities in the spleen are indicative of obstruction of the splenic veins. Histology revealed a neuroendocrine carcinoma.

functional pancreatic tumors, they are at least partially arterial hypervascular. VIPomas sometimes show calcifications [51]. Despite their large size they often do not cause dilatation of the biliary system (fig. 10).

There are several other uncommon hormone-active tumors of the pancreas, for instance PPomas and somatostatinomas. However, they are too rare to provide any systematic data about the CT morphology.

Non-Functional Endocrine Tumors of the Pancreas

Non-functional tumors are generally larger than functional tumors, therefore they are detected with high accuracy [52, 53]. These lesions frequently demonstrate central necrosis. In 70%, contrast enhancement will be seen in the solid walls of the tumors or the tumors are diffusely hyperdense after contrast (fig. 11). However, some of the tumors may be isodense or even hypodense compared with the normal enhancing pancreas. These tumors most times cannot be differentiated from pancreatic adenocarcinoma by CT. Due to their large size they will cause deformity of the pancreas. Most of the non-functional tumors are malignant and therefore their general prognosis is less favorable than for functional tumors.

Pseudotumors of the Pancreas (table 3)

Sometimes it is impossible to differentiate a chronic inflammatory pseudotumor in the head of the pancreas from a ductal carcinoma, since the CT signs overlap in many cases [54–56]. Calcifications are more common in chronic inflammatory pseudotumors (fig. 12). Even biopsy is not highly accurate regarding this differentiation. Only the positive biopsy result has a high predictive value. Normal variants like a pancreas divisum or a pancreas annulare may simulate a tumor of the head of the pancreas [57].

Tuberculosis or sarcoidosis of the pancreas may also mimic a tumor [58–60]. In rare cases, fat necrosis may simulate a tumor. Pseudoaneurysms of arteries can be accurately diagnosed by contrast-enhanced CT (fig. 13) [61, 62]. It should be mentioned that pseudocysts (fig. 14), especially during their early stage, can be rather thick-walled with an inhomogeneous content, and they may simulate a cystic neoplasm. However, these patients usually have significant pancreatitis in their medical anamnesis.

Diverticles of the duodenum may mimic a cystoid lesion in the head of the pancreas. To avoid this pitfall, diluted contrast media can be given orally and a careful search for little air bubbles within the diverticles should

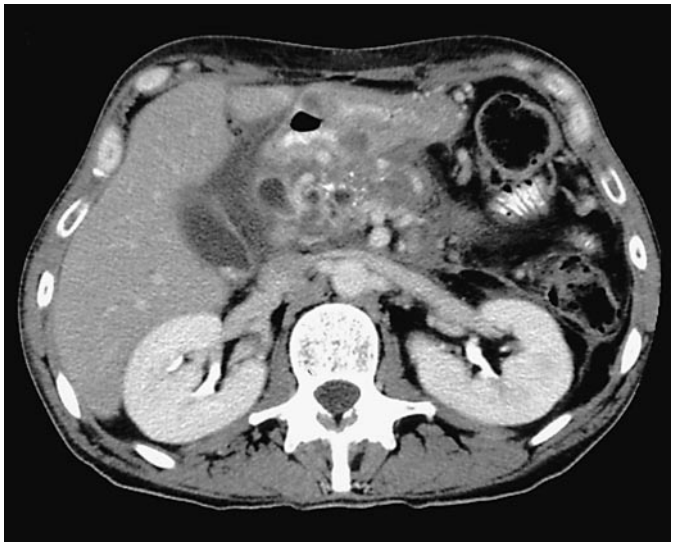

Fig. 12. CT of the pancreatic head. A large ill-defined lesion is seen with cystic and solid portions, some calcifications were visualized. Dilatations of the bile and pancreatic ducts were present: chronic inflammatory pseudotumor of the pancreatic head.

Fig. 13. CT of the head of the pancreas. A lesion with dense, contrast media equivalent density values and a thrombosed wall is seen in the pancreatic head. Pseudoaneurysm of the gastroduodenal artery.

Table 3. Pseudotumors of the pancreas

Chronic inflammatory pseudotumor
Peripancreatic fat necrosis
Tuberculosis
Sarcoidosis
Pseudoaneurysm
Atypical pseudocyst
Pancreas divisum
Pancreas annulare
Duodenal diverticle

be performed. Water is usually given as a negative contrast in staging of a pancreatic tumor in order to visualize duodenal infiltrations.

CT after Tumor Operations of the Pancreas

The investigating radiologist must be informed which operative procedure has been performed [63–64] (Whipple operation, gastrointestinal anastomosis, left resection of the pancreas, tumor enucleation). The upper intestinal tract has to be opacified in order not to misread bowel structures for a recurrent tumor. One major clinical question after radical operation of a pancreatic tumor is whether there is obstruction of the biliary system. If an aerobilia is present, a significant obstruction of the biliary

Fig. 14. CT of the pancreatic tail. A sharp-bordered cystic lesion is seen, no signs of mural thickening or enhancement: pancreatic pseudocyst was diagnosed.

tract is unlikely. The patency of biliary stents or catheters can be evaluated only in an indirect way, by judging the width of the biliary system.

To sum up, small exocrine tumors that do not alter the contour of the pancreas are difficult to detect by CT; furthermore, exocrine neoplasms are difficult to subclassify with CT. It should be kept in mind that 80% of the nonfunctional pancreatic tumors are ductal cell adenocarcinomas. The aim of CT in exocrine pancreas tumors is to perform an adequate staging with respect to the operatively vital structures. However, CT together with clinical history can give some hints for an unusual histology of a pancreatic tumor. Lipomas exhibit rather typical density values. Often serous microcystic adenoma shows the typical Swiss cheese or honeycomb appearance. Cystoid lesions of the pancreas reveal a broad differential diagnosis. The aim of CT in functional endocrine tumors is to localize the lesion and to diagnose singularity or multinodularity.

References

1 Fishman EK, Horton KM: Imaging pancreatic cancer: The role of multidetector CT with three-dimensional CT angiography. Pancreatology 2001;1:610–624.
2 Megibow AJ, Zhou XH, Rotterdam H, Francis IR, Zerhouni EA, Balfe DM, Weinreb JC, Aisen A, Kuhlman J, Heiken JP, et al: Pancreatic adenocarcinoma: CT versus MR imaging in the evaluation of resectability – Report of the Radiology Diagnostic Oncology Group. Radiology 1995;195:327–332.
3 Friedman AC: Pancreatic neoplasms; in Taveras JM, Ferrucci J (eds): Diagnostic Radiology. Philadelphia, Lippincott, 1993, vol 4, chapt 72, pp 1–23.
4 Ishikawa O, Ohigashi H, Imaoka S, Nakaizumi A, Uehara H, Kitamura T, Kuroda C: Minute carcinoma of the pancreas measuring 1 cm or less in diameter – Collective review of Japanese case reports. Hepatogastroenterology 1999;46: 8–15.
5 Bluemke DA, Cameron JL, Hruban RH, Pitt HA, Siegelman SS, Soyer P, Fishman EK: Potentially resectable pancreatic adenocarcinoma: Spiral CT assessment with surgical and pathologic correlation. Radiology 1995;197: 381–385.
6 Imbriaco M, Megibow AJ, Camera L, Pace L, Mainenti PP, Romano M, Selva G, Salvatore M: Dual-phase versus single-phase helical CT to detect and assess resectability of pancreatic carcinoma. AJR Am J Roentgenol 2002;178: 1473–1479.
7 Zeman RK, Cooper C, Zeiberg AS, Kladakis A, Silverman PM, Marshall JL, Evans SR, Stahl T, Buras R, Nauta RJ, Sitzmann JV, Al-Kawas F: TNM staging of pancreatic carcinoma using helical CT. AJR Am J Roentgenol 1997;169: 459–464.
8 Cunningham JD, Glajchen N, Brower ST: The use of spiral computed tomography in the evaluation of vessel encasement for pancreatic cancer. Int J Pancreatol 1996;19:9–14.
9 Lu DS, Reber HA, Krasny RM, Kadell BM, Sayre J: Local staging of pancreatic cancer: Criteria for unresectability of major vessels as revealed by pancreatic-phase, thin-section helical CT. AJR Am J Roentgenol 1997;168:1439–1443.
10 Ichikawa T, Federle MP, Ohba S, Ohtomo K, Sugiyama A, Fujimoto H, Haradome H, Araki T: Atypical exocrine and endocrine pancreatic tumors (anaplastic, small cell, and giant cell types): CT and pathologic features in 14 patients. Abdom Imaging 2000;25:409–419.
11 Yamamoto T, Hirohashi K, Tanaka H, Uenishi T, Shuto T, Kubo S, Kinoshita H: Resectable pleomorphic giant cell carcinoma of the pancreas. Int J Pancreatol 2001;29:63–67.
12 Radin DR, Colletti PM, Forrester DM, Tang WW: Pancreatic acinar cell carcinoma with subcutaneous and intraosseous fat necrosis. Radiology 1986;158:67–68.
13 Komatsuda T, Ishida H, Konno K, Sato M, Watanabe S, Furuya T, Ishida J: Adenosquamous carcinoma of the pancreas: Report of two cases. Abdom Imaging 2000;25:420–423.
14 Ueno N, Sano T, Kanamaru T, Tanaka K, Nishihara T, Idei Y, Yamamoto M, Okuno T, Kawaguchi K: Adenosquamous cell carcinoma arising from the papilla major. Oncol Rep 2002;9:317–320.
15 Gustafson KD, Karnaze GC, Hattery RR, Scheithauer BW: Pseudomyxoma peritonei associated with mucinous adenocarcinoma of the pancreas: CT findings and CT-guided biopsy. J Comput Assist Tomogr 1984;8:335–338.
16 Whang EE, Danial T, Dunn JC, Ashley SW, Reber HA, Lewin TJ, Tompkins RK: The spectrum of mucin-producing adenocarcinoma of the pancreas. Pancreas 2000;21:147–151.
17 Zirinsky K, Abiri M, Baer JW: Computed tomography demonstration of pancreatic microcystic adenoma. Am J Gastroenterol 1984;79: 139–142.
18 Procacci C, Graziani R, Bicego E, Bergamo-Andreis IA, Guarise A, Valdo M, Bogina G, Solarino U, Pistolesi GF: Serous cystadenoma of the pancreas: Report of 30 cases with emphasis on the imaging findings. J Comput Assist Tomogr 1997;21:373–382.
19 Itai Y, Ohhashi K, Furui S, Araki T, Murakami Y, Ohtomo K, Atomi Y: Microcystic adenoma of the pancreas: Spectrum of computed tomographic findings. J Comput Assist Tomogr 1988;12:797–803.
20 Fujiwara H, Ajiki T, Fukuoka K, Mitsutsuji M, Yamamoto M, Kuroda Y: Serous adenoma of the pancreas with multiple microcysts communicating with the pancreatic duct. HPB Surg 1998;11:43–49.
21 Khurana B, Mortele KJ, Glickman J, Silverman SG, Ros PR: Macrocystic serous adenoma of the pancreas: Radiologic-pathologic correlation. AJR Am J Roentgenol 2003;181:119–123.
22 Widmaier U, Mattfeldt T, Siech M, Beger HG: Serous cystadenocarcinoma of the pancreas. Int J Pancreatol 1996;20:135–139.
23 Lundstedt C, Dawiskiba S: Serous and mucinous cystadenoma/cystadenocarcinoma of the pancreas. Abdom Imaging 2000;25:201–206.
24 Procacci C, Graziani R, Bicego E, Bergamo-Andreis IA, Mainardi P, Zamboni G, Pederzoli P, Cavallini G, Valdo M, Pistolesi GF: Intraductal mucin-producing tumors of the pancreas: Imaging findings. Radiology 1996;198: 249–257.
25 Procacci C, Carbognin G, Accordini S, Biasiutti C, Guarise A, Lombardo F, Ghirardi C, Graziani R, Pagnotta N, De Marco R: CT features of malignant mucinous cystic tumors of the pancreas. Eur Radiol 2001;11:1626–1630.
26 Gupta RK, Scally J, Stewart RJ: Mucinous cystadenocarcinoma of the pancreas: Diagnosis by fine-needle aspiration cytology. Diagn Cytopathol 1989;5:408–411.
27 Vellet D, Leiman G, Mair S, Bilchik A: Fine needle aspiration cytology of mucinous cystadenocarcinoma of the pancreas. Further observations. Acta Cytol 1988;32:43–48.
28 Kobayashi H, Itoh T, Itoh H, Konishi J: Duct ectasia due to mucus-producing cancers with intraductal extension: Histopathologic correlation with radiologic imagings. Abdom Imaging 1995;20:341–347.
29 Taouli B, Vilgrain V, Vullierme MP, Terris B, Denys A, Sauvanet A, Hammel P, Menu Y: Intraductal papillary mucinous tumors of the pancreas: Helical CT with histopathologic correlation. Radiology 2000;217:757–764.
30 Roebuck DJ, Yuen MK, Wong YC, Shing MK, Lee CW, Li CK: Imaging features of pancreatoblastoma. Pediatr Radiol 2001;31:501–506.

31 Balthazar EJ, Subramanyam BR, Lefleur RS, Barone CM: Solid and papillary epithelial neoplasm of the pancreas. Radiographic, CT, sonographic, and angiographic features. Radiology 1984;150:39–40.
32 Buetow PC, Buck JL, Pantongrag-Brown L, Beck KG, Ros PR, Adair CF: Solid and papillary epithelial neoplasm of the pancreas: Imaging-pathologic correlation on 56 cases. Radiology 1996;199:707–711.
33 Savci G, Kilicturgay S, Sivri Z, Parlak M, Tuncel E: Solid and papillary epithelial neoplasm of the pancreas: CT and MR findings. Eur Radiol 1996;6:86–88.
34 Ng CS, Loyer EM, Iyer RB, David CL, DuBrow RA, Charnsangavej C: Metastases to the pancreas from renal cell carcinoma: Findings on three-phase contrast-enhanced helical CT. AJR Am J Roentgenol 1999;172:1555–1559.
35 Merkle EM, Boaz T, Kolokythas O, Haaga JR, Lewin JS, Brambs HJ: Metastases to the pancreas. Br J Radiol 1998;71:1208–12014.
36 Cunningham JD, Cirincione E, Ryan A, Canin-Endres J, Brower S: Indications for surgical resection of metastatic ocular melanoma. A case report and review of the literature. Int J Pancreatol 1998;24:49–53.
37 Mountney J, Maury AC, Jackson AM, Coleman RE, Johnson AG: Pancreatic metastases from breast cancer: An unusual cause of biliary obstruction. Eur J Surg Oncol 1997;23:574–576.
38 Ferrozzi F, Bova D, Campodonico F, Chiara FD, Passari A, Bassi P: Pancreatic metastases: CT assessment. Eur Radiol 1997;7:241–245.
39 Itai Y, Saida Y, Kurosaki Y, Kurosaki A, Fujimoto T: Lipomas of the pancreas. Acta Radiol 1995;36:178–181.
40 Katz DS, Nardi PM, Hines J, Barckhausen R, Math KR, Fruauff AA, Lane MJ: Focal fatty masses of the pancreas. AJR Am J Roentgenol 1998;170:1485–1487.
41 Rossi P, Baert A, Passariello R, Simonetti G, Pavone P, Tempesta P: CT of functioning tumors of the pancreas. AJR Am J Roentgenol 1985;144:57–60.
42 Binkovitz LA, Johnson CD, Stephens DH: Islet cell tumors in von Hippel-Lindau disease: Increased prevalence and relationship to the multiple endocrine neoplasias. AJR Am J Roentgenol 1990;155:501–505.
43 Van Hoe L, Gryspeerdt S, Marchal G, Baert AL, Mertens L: Helical CT for the preoperative localization of islet cell tumors of the pancreas: Value of arterial and parenchymal phase images. AJR Am J Roentgenol 1995;165:1437–1439.
44 King AD, Ko GT, Yeung VT, Chow CC, Griffith J, Cockram CS: Dual phase spiral CT in the detection of small insulinomas of the pancreas. Br J Radiol 1998;71:20–23.
45 Chung MJ, Choi BI, Han JK, Chung JW, Han MC, Bae SH: Functioning islet cell tumor of the pancreas. Localization with dynamic spiral CT. Acta Radiol 1997;38:135–138.
46 Sohaib SA, Reznek RH, Healy JC, Besser GM: Cystic islet cell tumors of the pancreas. AJR Am J Roentgenol 1998;170:217.
47 Stair JM, Schaefer RF, McCowan TC, Balachandran S: Cystic islet cell tumor of the pancreas. J Surg Oncol 1986;32:46–49.
48 Tjon A Tham RT, Falke TH, Jansen JB, Lamers CB: CT and MR imaging of advanced Zollinger-Ellison syndrome. J Comput Assist Tomogr 1989;13:821–828.
49 Breatnach ES, Han SY, Rahatzad MT, Stanley RJ: CT evaluation of glucagonomas. J Comput Assist Tomogr 1985;9:25–29.
50 Tjon A Tham RT, Jansen JB, Falke TH, Roelfsema F, Griffioen G, van den Sluys Veer A, Lamers CB: MR, CT, and ultrasound findings of metastatic vipoma in pancreas. J Comput Assist Tomogr 1989;13:142–144.
51 Fassbender CM, Buchsel R, Seelis R, Hofstadter F, Matern S: Liver calcifications in metastasizing vipoma (in German). Dtsch Med Wochenschr 1989;114:1445–1449.
52 Secil M, Goktay AY, Oksuzler Y, Sagol O, Dicle O, Igci E, Pirnar T: CT findings of nonfunctioning neuroendocrine pancreatic tumors. Comput Med Imaging Graph 2002;26:43–45.
53 Stafford Johnson DB, Francis IR, Eckhauser FE, Knol JA, Chang AE: Dual-phase helical CT of nonfunctioning islet cell tumors. J Comput Assist Tomogr 1998;22:59–63. Erratum: J Comput Assist Tomogr 1998;22:335–339.
54 Neff CC, Simeone JF, Wittenberg J, Mueller PR, Ferrucci JT Jr: Inflammatory pancreatic masses. Problems in differentiating focal pancreatitis from carcinoma. Radiology 1984;150:35–38.
55 Kim T, Murakami T, Takamura M, Hori M, Takahashi S, Nakamori S, Sakon M, Tanji Y, Wakasa K, Nakamura H: Pancreatic mass due to chronic pancreatitis: Correlation of CT and MR imaging features with pathologic findings. AJR Am J Roentgenol 2001;177:367–371.
56 Yamaguchi K, Chijiiwa K, Saiki S, Nakatsuka A, Tanaka M: 'Mass-forming' pancreatitis masquerades as pancreatic carcinoma. Int J Pancreatol 1996;20:27–35.
57 Soulen MC, Zerhouni EA, Fishman EK, Gayler BW, Milligan F, Siegelman SS: Enlargement of the pancreatic head in patients with pancreas divisum. Clin Imaging 1989;13:51–57.
58 Demir K, Kaymakoglu S, Besisik F, Durakoglu Z, Ozdil S, Kaplan Y, Boztas G, Cakaloglu Y, Okten A: Solitary pancreatic tuberculosis in immunocompetent patients mimicking pancreatic carcinoma. J Gastroenterol Hepatol 2001;16:1071–1074.
59 Fischer G, Spengler U, Neubrand M, Sauerbruch T, Fischer G, Spengler U, Neubrand M, Sauerbruch T: Isolated tuberculosis of the pancreas masquerading as a pancreatic mass. Am J Gastroenterol 1995;90:2227–2230.
60 Soyer P, Gottlieb L, Bluemke DA, Fishman E: Sarcoidosis of the pancreas mimicking pancreatic cancer: CT features. Eur J Radiol 1994;19:32–33.
61 Gavin PM, Matalon TA, Petasnick JP, Roseman DL: Congenital hepatic artery aneurysm simulating pancreatic carcinoma. Radiology 1984;152:607–608.
62 Kittredge RD, Gordon RB: Pseudoaneurysm with rupture in pancreatic pseudocyst wall as demonstrated by computed tomography. J Comput Tomogr 1987;11:35–38.
63 Coombs RJ, Zeiss J, Howard JM, Thomford NR, Merrick HW: CT of the abdomen after the Whipple procedure: Value in depicting postoperative anatomy, surgical complications, and tumor recurrence. AJR Am J Roentgenol 1990;154:1011–1014.
64 Heiken JP, Balfe DM, Picus D, Scharp DW: Radical pancreatectomy: Postoperative evaluation by CT. Radiology 1984;153:211–215.

Review Article

Digestive Diseases

Dig Dis 2004;22:18–25
DOI: 10.1159/000078731

ERCP and MRCP in the Differentiation of Pancreatic Tumors

Dirk Hartmann[a] Dieter Schilling[a] Boris Bassler[b] Henning E. Adamek[c]
Günter Layer[b] Jürgen F. Riemann[a]

Departments of [a]Medicine C (Gastroenterology) and [b]Diagnostic and Interventional Radiology, Klinikum Ludwigshafen gGmbH, Academic Hospital of the Johannes Gutenberg University of Mainz, Ludwigshafen, and [c]Department of Gastroenterology, Klinikum Leverkusen, Academic Hospital of the University of Cologne, Leverkusen, Germany

Key Words
Magnetic resonance imaging · Magnetic resonance cholangiopancreatography · Endoscopic retrograde cholangiopancreatography · Pancreatic cancer · Epithelial cystic neoplasms · Islet cell tumors

Abstract
The introduction of endoscopic retrograde cholangiopancreatography (ERCP) in the early 1970s provided gastroenterologists with a number of diagnostic as well as therapeutic possibilities for examining biliopancreatic systems. In the meantime, magnetic resonance cholangiopancreatography presents a non-invasive alternative to diagnostic ECRP providing the advantage of a lower rate of possible complications. This article addresses the two methods presently available for differentiating pancreatic tumors. The objective of this article is to describe the advantages and disadvantages as well as the possibilities inherent in both methods.

Copyright © 2004 S. Karger AG, Basel

Introduction

The development of endoscopic retrograde cholangiopancreatography (ERCP) in the early 1970s revolutionized the possibilities available to gastroenterologists in the diagnosis and therapy of pathologies relating to the biliopancreatic system [1, 2]. Twenty years later, Wallner et al. [3] described for the first time the possibility of non-invasively displaying the biliopancreatic system by means of magnetic resonance tomography. Since then, magnetic resonance cholangiopancreatography (MRCP) has been continuously developed and is today one of the standard methods for diagnosing the biliopancreatic system [4–7].

This article focuses on the two methods available for differentiating pancreatic tumors. It describes the advantages as well as disadvantages, including the possibilities of these two methods.

Technical Aspects of MRCP

The principle of MRCP is based on the signal generated by stationary fluids in T2-weighted sequences [8]. Adjacent solid structures, stones or vessels generating a very weak signal in these sequences are used as contrast. A sufficient image quality is obtained with a number of dif-

KARGER
Fax + 41 61 306 12 34
E-Mail karger@karger.ch
www.karger.com

© 2004 S. Karger AG, Basel
0257–2753/04/0221–0018$21.00/0

Accessible online at:
www.karger.com/ddi

Prof. J.F. Riemann, MD
Department of Medicine C, Klinikum der Stadt Ludwighafen gGmbH
Bremserstrasse 79
DE–67063 Ludwigshafen am Rhein (Germany)
Tel. +49 621 5034100, Fax +49 621 5034114, E-Mail MedCLu@t-online.de

ferent systems and magnetic field strengths. Tomographs with a modern high or medium field (1.0–1.5 Tesla) are considered standard today. Images are optimized by using fat suppression pulses as well as surface coils.

A large number of protocols have been introduced for MRCP. Today, turbo spin-echo (TSE) sequences are increasingly used since they offer a good signal-to-noise as well as contrast-to-noise ratio. In addition, interferences relating to field inhomogeneities, metal clips or bowel gas are minimal. To avoid respiratory artifacts, images are generated using the breath-hold technique. The acquisition time per slice was reduced to 4–20 s with the event of the especially fast RARE (half-Fourier rapid acquisition with relaxation enhancement) or HASTE (half-Fourier acquisition single-shot TSE) sequences [9]. Maximum intensity projection (MIP) algorithms and multiplanar reformatting techniques allow for the generation of three-dimensional images [10]. The exact anatomic display of the biliopancreatic duct system provides for an exact planning of invasive surgery or radiation therapy. The technical aspects of ERCP have been intensively described previously [11].

Complications of ERCP and MRCP

The most frequent complication encountered with ERCP is the occurrence of pancreatitis in 5–7% with usually mild effects. For diagnostic ERCP, the rate of complications is slightly lower than for therapeutic indications; serious complications are present in 1–2% with a mortality rate of 0.2% [12, 13]. In case of sphincterotomy to the bile duct, the complication rate is 9.8% (bleeding in 2%, pancreatitis in 5.4%). In this case, the rate of complication is a consequence of the endoscopic technique used and the indication (e.g. sphincter of Oddi dysfunction) [14].

Complications with MRCP are rare. Side effects to contrast agents are of a low percentage only. Serious reactions occur in 1 out of 350,000 cases [15]. In 5% of all patients, claustrophobia restricts a complete MRI examination [16]. Absolute contraindications apply to wearers of pacemakers, clips of a cerebral aneurysm, wearers of cochlear or ocular implantations or the presence of foreign bodies in the eye. Implantation of a cardiac valve replacement, a neurostimulator or metal prostheses represent relative contraindications [17].

Table 1. Sensitivity of ERCP in the diagnosis of pancreatic carcinoma

Author	n	Sensitivity, %
Gilinsky et al., 1986 [24]	117	80
Bakkevold et al., 1992 [25]	442	79
Niederau and Grendell, 1992 [26]	565	92
Burtin et al., 1997 [27]	68	92
Rösch et al., 2000 [28]	184	89

Diagnostic ERP and MRP

Pancreas Carcinoma

Ductal adenocarcinomas are among the most frequent malignancies of the pancreas. This malignant tumor is clinically characterized by the absence of specific early symptoms as well as minimally invasive, sensitive screen diagnostics. Typical symptoms involve epigastric pain as well as back pain, jaundice, premature feeling of fullness or weight loss. Eighty percent of patients diagnosed with a pancreatic carcinoma show an advanced tumor stage. Curative treatment is not possible due to metastases or the invasion of blood vessels [18, 19]. The prognosis for pancreatic carcinoma is poor, even if the survival rate for the patient increases after curative surgery. The 5-year survival rate lies between 19 and 26% [20–22]. Diagnosis rarely involves small pancreatic carcinomas. However, the size of the tumor, lymph nodes, retroperitoneal or serosal infiltration are of prognostic relevance [23]. For this reason, early diagnosis plays a decisive role in the outcome for patients suffering from pancreatic carcinoma.

In several series, ERCP reaches a sensitivity of 80–92% in the diagnosis of pancreatic cancer [24–28] (table 1). In addition to cholangio- and pancreatography, ERCP provides the possibility of intraductal ultrasound (IDUS). The mini probe is advanced into the pancreatic or cystic duct via the work channel of the duodenoscope. This allows for the staging of smaller carcinomas and also the sensitivity for displaying vessel invasion [29].

Using a cohort of 26 patients (14 carcinoma, 12 strictures involving chronic pancreatitis), Furukawa et al. [30] was able to demonstrate the superiority of the IDUS as compared to endoscopic ultrasound (EUS), computed tomography (CT) and endoscopic retrograde pancreatography (ERP) in the differential diagnosis of strictures in the pancreatic duct. The sensitivity as well as specificity obtained for IDUS were 100 and 91.7%, for EUS 92.9 and 58.3%, for CT 64.3 and 66.7%, and for ERP 85.7 and

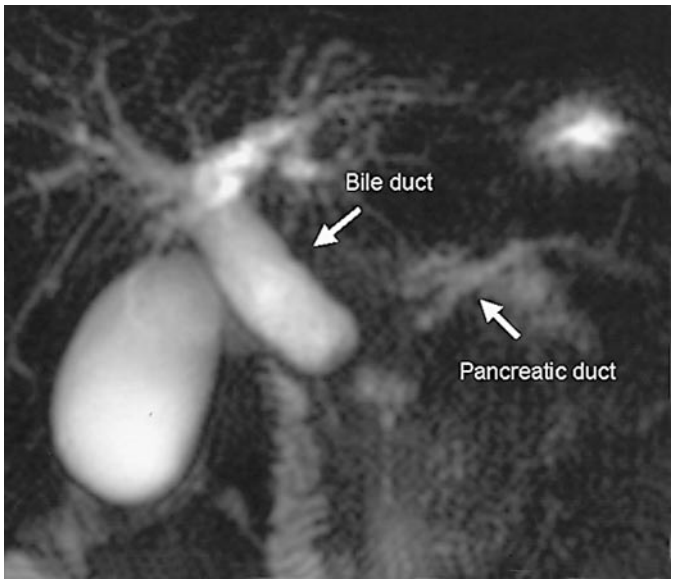

Fig. 1. Cancer of the pancreatic head. Double duct sign in MRCP: dilated bile and pancreatic duct.

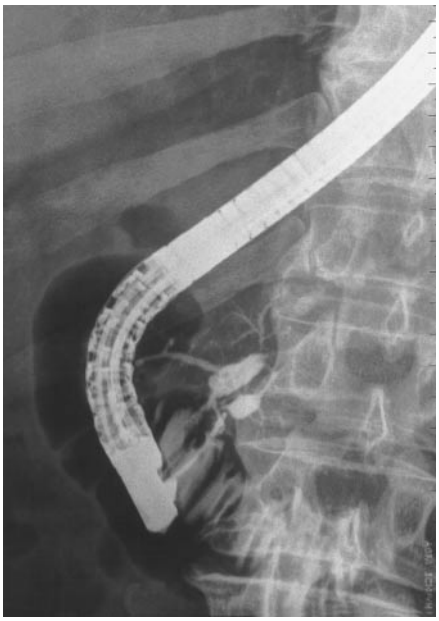

Fig. 2. Cancer of the pancreatic head. Double duct sign in ERCP.

66.7%. However, additional prospective histopathologically controlled studies are not available to date.

MRCP also shows a high diagnostic accuracy in the detection of pancreatic carcinoma [31–35] (table 2). Using the current work of Lopez Hanninen et al. [31], an MRI including MRCP was performed in 66 patients with suspected pancreatic tumors. For a total of 44 patients, the histology of the follow-up showed a malignant tumor. Magnetic resonance tomography was able to provide the correct pre-diagnosis for 42 out of 44 patients.

To date there are only a few prospective examinations that compare ERCP with MRCP in the diagnosis of pancreatic tumors [36, 37] (table 3). With respect to a cohort of 125 patients examined in a study by Adamek et al. [37], it was shown that 37 (30%) were diagnosed with a pancreatic carcinoma, 17 (14%) showed other neoplasia of the pancreas, 57 suffered from chronic pancreatitis, and for 13 the pancreatic duct did not show any pathological findings. With respect to the diagnosis of pancreatic carcinoma, the sensitivity of MCRP was 84% while its specificity reached 97%. Compared to these findings, the corresponding values for ERCP were 70 and 94%.

Through additional imaging in the axial and transverse plane, MRCP was able to provide further information regarding tumor size and resectability with the same or improved diagnostic accuracy as modern CT [38, 39].

An additional advantage of MRI is the possibility of magnetic resonance angiography in one session ('one-stop shopping'). This eliminates the need of conventional angiography preceding planned surgery. In series including between 44 and 46 patients, vessel invasion of pancreatic carcinoma detected through MRI was confirmed intraoperatively in 94 and 98% of the cases [31, 40].

In case of stenoses in the ductus hepatocholedochus (e.g. pancreatic carcinoma), MRCP enables evaluation of the biliary system above the stenosis regarding possible cholangitis without the risk of residual contrast agent. The information obtained with respect to the length of the stenosis and the anatomy of the proximal biliary duct system

Table 2. Accuracy of MRCP in the diagnosis of pancreatic carcinoma

Author	n	Accuracy, %
Lopez Hanninen et al., 2002 [31]	44	95
Barish et al., 1995 [32]	30	88
Holzknecht et al., 1996 [33]	34	83
Miyazaki et al., 1996 [34]	56	83
Ueno et al., 1998 [35]	204	75 (retrospective)

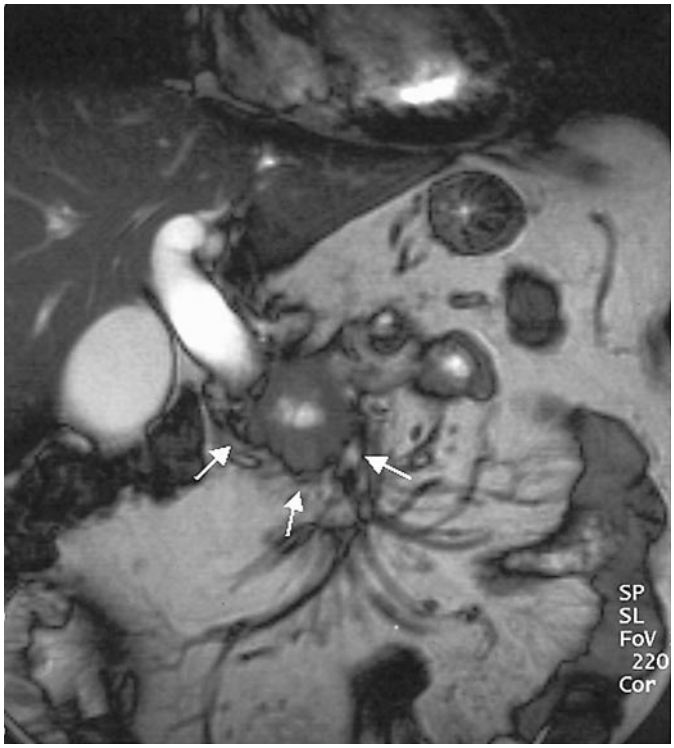

Fig. 3. T2-weighted sequence of a cancer of the pancreatic head.

Fig. 4. Characteristic endoscopic feature of IPMT (protrusion of mucin through a patulous orifice).

can be utilized to plan the therapeutic procedure for palliative care prior to intervention.

Differentiation of Malignant from Benign Lesions

It is frequently quite difficult to differentiate between inflammable and neoplastic lesions in the area of the pancreatic head. Both pathologies show a low signal in T1-weighted sequences and are associated with an obstruction in the pancreatic duct [41, 42]. A pancreatoduodenectomy performed in patients with chronic pancreatitis due to a suspected lesion in the pancreatic head increases the chances of locating a previously undetected carcinoma by at least 5% [43]. ERCP may prove helpful in these cases, since a stenosis exceeding a length of 10 mm in the pancreatic duct is indicative of pancreatic cancer [44].

Johnson and Outwater [45] retrospectively analyzed MRI images of 31 patients diagnosed with pancreatic cancer (pancreatic cancer n = 24, chronic pancreatitis n = 7) and examined with dynamic gadolinium-enhanced breath-hold spoiled gradient-echo imaging. Both chronic pancreatitis as well as pancreatic cancer showed pathological contrast agent enhancement. However, differentiation on the basis of degree and time of enhancement was not possible.

Epithelial Cystic Tumors of Exocrine Pancreas

Correct diagnosis and pre-operative evaluation of location, expansion and the malignant potential of cystic pancreatic tumors are important due to the high potential of degeneration [46] (table 4). One differentiates between intraductal papillary mucinous tumors (IPMTs), starting

Table 3. Comparison of ERCP and MRCP in the diagnosis of pancreatic carcinoma

Author	n	ERCP		MRCP + MRI	
		sensitivity, %	specificity, %	sensitivity, %	specificity, %
Diehl et al., 1999 [36]	40	94	50	91	63
Adamek et al., 2000 [37]	124	70.3	94.3	83.8	96.6

Table 4. Epithelial cystic tumors of exocrine pancreas: WHO nomenclature [47]

Benign	Transitional		Malignant
Serous cystadenoma	Transitional cystadenomas are not classified		Serous cystadenocarcinoma
Mucinous cystadenoma	Mucinous cystic tumor with dysplasia	Non-invasive mucinous cystadenocarcinoma	Mucinous cystadenocarcinoma
Intraductal papillary mucinous adenoma	Intraductal papillary mucinous tumor with dysplasia	Non-invasive intraductal papillary mucinous carcinoma	Invasive intraductal mucinous carcinoma

Table 5. IPMT (intraductal papillary mucinous tumor) of pancreas in MRCP and ERCP

Author	n	Findings
Usuki et al. 1998 [51]	11 IPMT – MRCP vs. ERCP	ERCP and MRCP are complementary: ERCP is better in visualizing main duct type and MRCP in branch duct type of IPMT
Fukukura et al. 1999 [52]	13 IPMT – MRCP vs. ERCP	MRCP might be more useful to depict the lesions and communicating duct, ERCP additionally shows papillary projections
Arakawa et al. 2000 [53]	17 IPMT – MRCP vs. histopathologic findings	Findings in MRCP are well correlated with histopathologic findings
Albert et al. 2000 [50]	3 MCN, 2 IPMT, 1 cystadenocarcinoma – MRCP vs. ERCP and histopathologic findings	More complete visualization of MCN in MRCP than in ERCP

MCN = Mucinous cystic tumor.

at the main duct of the pancreas and mucinous cystadenomas originating in the peripheral duct system [48, 49].

The diagnosis of intraductal papillary tumors is the domain of ERCP, however, the first data available indicate a comparable diagnostic potential for MRCP [50–53] (table 5). ERCP allows for the possibility of inspecting the papilla with the characteristic image of a wide papilla with mucus discharged from the pancreatic duct in 27–84% [54]. However, tumor expansion may be displayed only indirectly with ECRP. In some cases, ERCP cannot fill the entire pancreatic duct due to heavy mucous discharge. MRCP on the other hand displays the complete tumor expansion and the pancreatic duct and is therefore at times superior to ERCP as demonstrated by e.g. Sugiyma et al. [55] with a cohort of 11 patients.

As compared to IPMTs, mucinous cystic neoplasms do not communicate with the main pancreatic duct. For this reason, they are not detectable with ERCP. MRCP is therefore a valuable method for pre-operative diagnostics. For 28 patients with mucin-producing tumors, Koito et al. [56] demonstrated that MRCP is an effective diagnostic tool. As compared to ERCP, MRCP provided a significantly improved display of the dilated ducts.

Differentiation between invasive and non-invasive tumors is difficult. The accuracy of imaging systems reaches a level of about 75% [57]. Yamashita et al. [58] used diffusion-weighted MRI for characterizing cystic lesions. Based on the different viscosity of cysts, significantly lower values for diffusion capacity (ADC) were obtained in mucin-producing tumors und pseudocysts than in serous cystadenomas in a small number of cases. ADC enables differentiation between pseudocysts and mucinous tumors. In addition, the signal intensity in T1-weighted sequences may aid in the differentiation between malignant and benign mucinous cystic tumors [59]. The magnetic resonance criteria for malignancies with IPMT has been defined by Irie et al. [60]: filling defects, diffuse main pancreatic duct dilatation >15 mm in main duct type, or any main pancreatic duct dilatation in branch duct type IPMT were indicative of malignancy.

Table 6. Diagnostic accuracy of peroral pancreatoscopy and intraductal ultrasonography in differentiating benign IPMT from malignant ones according to the primary location of the tumor (n = 40) [62]

Main duct type (n = 16)		Branch type (n = 24)	
POPS		*POPS*	
Sensitivity	100%	Sensitivity	43%
Specificity	71%	Specificity	100%
Accuracy rate	88%	Accuracy rate	67%
IDUS		*IDUS*	
Sensitivity	56%	Sensitivity	77%
Specificity	71%	Specificity	100%
Accuracy rate	63%	Accuracy rate	88%

POPS = Peroral pancreatoscopy; IDUS = intraductal ultrasonography.

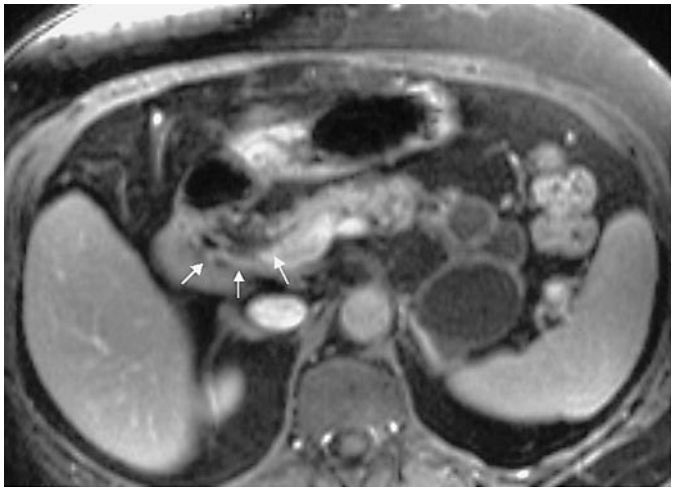

Fig. 5. IPMT (intraductal papillary mucinous tumor) of the pancreas.

Pancreatoscopy plays a role in the examination of the main pancreatic duct in patients with pancreatic tumors [61]. Hara et al. [62] retrospectively examined 60 patients with IPMTs and demonstrated the considerable value of IDUS and pancreatoscopy within the scope of ERCP in differentiating between malignant and benign lesions. A peroral pancreaticoscopy as well as an IDUS were performed in 40 patients with protruding lesions (table 6). The combination of both methods proved helpful in differentiating between malignant and benign lesions and was instrumental in developing an effective therapeutic approach.

Islet Cell Tumors

The three most commonly known islet cell tumors are insulinomas, gastrinomas, and non-functional islet cell tumors. ERCP is only able to provide indirect proof of a tumor when the pancreatic duct shows an obstruction. This is frequently indicative of the presence of a malignant lesion [63–65]. EUS shows the highest diagnostic accuracy in diagnosing small islet cell tumors [66].

To differentiate between islet cell tumors und ductal adenocarcinomas, T1- and T2-weighted sequences are required in MRI. Islet cell tumors show a higher T2 signal intensity and a more uniform hyperintense enhancement on the immediate post-gadolinium fat-suppressed T1-weighted spoiled gradient echo images and preservation of the usual T1 signal intensity of the adjacent pancreas [67–69].

Conclusions

According to the presently available data, MRCP has the potential to replace ERCP in the diagnosis of pancreatic tumors in most cases. This statement is supported by the display of the bile and pancreatic ducts comparable to ERCP, the low rate of complications and the possibility of a complete staging in a single process (work step). However, MRCP will never fully replace ERCP due to the therapy of benign and malignant pathologies of the biliopancreatic system.

Successful interpretation of MRCP images requires years of experience in diagnosing pathologies of the biliopancreatic system. Through knowledge in the area of percutaneous sonography, endoscopy, ERCP with IDUS and pancreaticoscopy, the gastroenterologist is thoroughly familiar with the anatomy and morphological changes of diseases of the pancreas. As a result, sufficient evaluation of MRCP and goal-oriented additional developments of the magnetic resonance procedure mandates a close cooperation between radiologist and gastroenterologist.

References

1 Demling L, Koch H, Classen M, Belohlavek D, Schaffner O, Schwamberger K, Stolte M: Endoscopic papillotomy and removal of gall-stones: Animal experiments and first clinical results. Dtsch Med Wochenschr 1974;99:2255–2257.
2 Kawai K, Akasaka Y, Nakajima M: Preliminary report on endoscopical papillotomy. J Kyoto Pref Univ Med 1973;82:353–355.
3 Wallner BK, Schumacher KA, Weidenmaier W, Friedrich JM: Dilated biliary tract: Evaluation with MR cholangiography with a T2-weighted contrast-enhanced fast sequence. Radiology 1991;181:805–808.
4 Adamek HE, Breer H, Layer G, Riemann JF: Magnetic resonance cholangiopancreatography. The fine art of bilio-pancreatic imaging. Pancreatology 2002;2:499–502.
5 Adamek HE, Breer H, Karschkes T, Albert J, Riemann JF: Magnetic resonance imaging in gastroenterology: Time to say good-bye to all that endoscopy? Endoscopy 2000;32:406–410.
6 Hartmann D, Riemann JF: Endoscopy and MRI. Acta Endoscopica 2002;32:797–804.
7 Albert JG, Riemann JF: ERCP and MRCP – When and why. Best Pract Res Clin Gastroenterol 2002;16:399–419.
8 Wallner BK, Schumacher KA, Weidenmaier W: Dilated biliary tract: Evaluation with MR cholangiography with a T2-weighted contrast-enhanced fast sequence. Radiology 1991;181:805–808.
9 Laubenberger J, Buchert M, Schneider B, Blum U, Hennig J, Langer M: Breath-hold projection MRCP: A new method for the examination of the bile and pancreatic ducts. Magn Reson Med 1995;33:18–23.
10 Yamashita Y, Abe Y, Tang Y, Urata J, Sumi S, Takahashi M: In vitro and clinical studies of image acquisition in breath-hold MR cholangiopancreatography: Single-shot projection technique versus multislice technique. AJR Am J Roentgenol 1997;168:1449–1454.
11 Kohler B, Maier M, Riemann JF: Endoskopie der Verdauungsorgane mit Biopsie und Zytologie; in Hahn G, Riemann JF (eds): Klinische Gastroenterologie. Stuttgart, Thieme, 1996.
12 Sherman S, Lehmann GA: ERCP- and endoscopic sphincterotomy-induced pancreatitis. Pancreas 1991;6:350–367.
13 Loperfido S, Angelini G, Benedetti G, Chilovi F, Costan F, De Berardinis F, De Bernardin M, Ederle A, Fina P, Fratton A: Major early complications from diagnostic and therapeutic ERCP: A prospective multicenter study. Gastrointestinal Endosc 1998;48:1–10.
14 Freeman ML, Nelson DB, Sherman S, Haber GB, Herman ME, Dorsher PJ, Moore JP, Fennerty MB, Ryan ME, Shaw MJ, Lande JD, Pheley AM: Complications of endoscopic biliary sphincterotomy. N Engl J Med 1996;335:909–918.
15 Goldstein HA, Kashanian FK, Blumetti RF, Holyoak WL, Hugo FP, Blumenfield DM: Safety assessment of gadopentetate dimeglumine in US clinical trials. Radiology 1990;174:17–23.
16 Flaherty JA, Hoskinson K: Emotional distress during magnetic resonance imaging. N Engl J Med 1989;320:467–468.
17 Edelman RR, Warach S: Magnetic resonance imaging. N Engl J Med 1993;328:708–716.
18 Warshaw AL, Fernandez-del Castillo C: Pancreatic carcinoma. N Engl J Med 1992;326:455–465.
19 Wagner M, Dikopoulos N, Kulli C, Friess H, Büchler MW: Standard surgical treatment in pancreatic cancer. Ann Oncol 1999;10(suppl 4):247–251.
20 Trede M, Schwall G, Saeger HD: Survival after pancreatoduodenectomy. 118 consecutive resections without an operative mortality. Ann Surg 1990;211:447–458.
21 Cameron JL, Crist DW, Sitzmann JV, Hruban RH, Boitnott JK, Seidler AJ, Coleman J: Factors influencing survival after pancreaticoduodenectomy for pancreatic cancer. Am J Surg 1991;161:120–125.
22 Yeo CJ, Cameron JL, Lillemoe KD, Sitzmann JV, Hruban RH, Goodman SN, Dooley WC, Coleman J, Pitt HA: Pancreaticoduodenectomy for cancer of the head of the pancreas: 201 patients. Ann Surg 1995;221:721–731.
23 Birk D, Fortnagel G, Formentini A, Beger HG: Small carcinoma of the pancreas. Factors of prognostic relevance. J Hepatobiliary Pancreat Surg 1998;5:450–454.
24 Gilinsky NH, Bornman PC, Girdwood AH, Marks IN: Diagnostic yield of endoscopic retrograde cholangiopancreatography in carcinoma of the pancreas. Br J Surg 1986;73:539–543.
25 Bakkevold KE, Arnesjo B, Kambestad B: Carcinoma of the pancreas and papilla of Vater: Presenting symptoms, signs, and diagnosis related to stage and tumour site. A prospective multicentre trial in 472 patients. Norwegian Pancreatic Cancer Trial. Scand J Gastroenterol 1992;27:317–325.
26 Niederau C, Grendell JH: Diagnosis of pancreatic carcinoma. Imaging techniques and tumor markers. Pancreas 1992;7:66–86.
27 Burtin P, Palazzo L, Canard JM, Person B, Oberti F, Boyer J: Diagnostic strategies for extrahepatic cholestasis of indefinite origin: Endoscopic ultrasonography or retrograde cholangiography? Results of a prospective study. Endoscopy 1997;29:349–355.
28 Rösch T, Schusdziarra V, Born P, Bautz W, Baumgartner M, Ulm K, Lorenz R, Allescher HD, Gerhardt P, Siewert JR, Classen M: Modern imaging methods versus clinical assessment in the evaluation of hospital in-patients with suspected pancreatic disease. Am J Gastroenterol 2000;95:2261–2270.
29 Furukawa T, Oohashi K, Yamao K, Naitoh Y, Hirooka Y, Taki T, Itoh A, Hayakawa S, Watanabe Y, Goto H, Hayakawa T: Intraductal ultrasonography of the pancreas: Development and clinical potential. Endoscopy 1997;29:561–569.
30 Furukawa T, Tsukamoto Y, Naitoh Y, Hirooka Y, Katoh T: Evaluation of intraductal ultrasonography in the diagnosis of pancreatic cancer. Endoscopy 1993;25:577–581.
31 Lopez Hanninen E, Amthauer H, Hosten N, Ricke J, Bohmig M, Langrehr J, Hintze R, Neuhaus P, Wiedenmann B, Rosewicz S, Felix R: Prospective evaluation of pancreatic tumors: Accuracy of MR imaging with MR cholangiopancreatography and MR angiography. Radiology 2002;224:34–41.
32 Barish MA, Yucel EK, Soto JA, Chuttani R, Ferrucci JT: MR cholangiopancreatography: Efficacy of three-dimensional turbo spin-echo technique. AJR Am J Roentgenol 1995;165:295–300.
33 Holzknecht N, Gauger J, Helmberger T, Sackmann M, Reiser M: Techniques and applications of MR pancreatography in comparison with endoscopic retrograde pancreatography. Radiologe 1996;26:427–434.
34 Miyazaki T, Yamashita Y, Tsuchigame T, Yamamoto H, Urata J, Takahashi M: MR cholangiopancreatography using HASTE (half-Fourier acquisition single-shot turbo spin-echo) sequences. AJR Am J Roentgenol 1996;166:1297–1303.
35 Ueno E, Takada Y, Yoshida I, Toda J, Sugiura T, Toki F: Pancreatic diseases: Evaluation with MR cholangiopancreatography. Pancreas 1998;16:418–426.
36 Diehl SJ, Lehmann KJ, Gaa J, Meier-Willersen HJ, Wendl K, Georgi M: The value of magnetic resonance tomography, magnetic resonance cholangiopancreatography and endoscopic retrograde cholangiopancreatography in the diagnosis of pancreatic tumors. Röfo Fortschr Geb Röntgenstr Neuen Bildgeb Verfahr 1999;170:463–469.
37 Adamek HE, Albert J, Breer H, Weitz M, Schilling D, Riemann JF: Pancreatic cancer detection with magnetic resonance cholangiopancreatography and endoscopic retrograde cholangiopancreatography: A prospective controlled study. Lancet 2000;356:190–193.
38 Ichikawa T, Haradome H, Hachiya J, Nitatori T, Ohtomo K, Kinoshita T, Araki T: Pancreatic ductal adenocarcinoma: Preoperative assessment with helical CT versus dynamic MR imaging. Radiology 1997;202:655–662.
39 Nishiharu T, Yamashita Y, Abe Y, Mitsuzaki K, Tsuchigame T, Nakayama Y, Takahashi M: Local extension of pancreatic carcinoma: Assessment with thin-section helical CT versus with breath-hold fast MR imaging – ROC analysis. Radiology 1999;212:445–452.
40 Gaa J, Wendl K, Tesdal IK, Meier-Willersen HJ, Lehmann KJ, Bohm C, Mockel R, Richter A, Trede M, Georgi M: Combined use of MRI and MR cholangiopancreatography and contrast-enhanced dual phase 3-D MR angiography in diagnosis of pancreatic tumors: Initial clinical results. Röfo Fortschr Geb Röntgenstr Neuen Bildgeb Verfahr 1999;170:528–533.

41 DelMaschio A, Vanzulli A, Sironi S, Castrucci M, Mellone R, Staudacher C, Carlucci M, Zerbi A, Parolini D, Faravelli A: Pancreatic cancer versus chronic pancreatitis: Diagnosis with CA 19-9 assessment, US, CT, and CT-guided fine-needle biopsy. Radiology 1991;178:95–99.
42 Baker ME: Pancreatic adenocarcinoma: Are there pathognomonic changes in the fat surrounding the superior mesenteric artery? Radiology 1991;180:613–614.
43 Van Gulik TM, Reeders JW, Bosma A, Moojen TM, Smits NJ, Allema JH, Rauws EA, Offerhaus GJ, Obertop H, Gouma DJ: Incidence and clinical findings of benign, inflammatory disease in patients resected for presumed pancreatic head cancer. Gastrointest Endosc 1997; 46:417–423.
44 Shemesh E, Czerniak A, Nass S, Klein E: Role of endoscopic retrograde cholangiopancreatography in differentiating pancreatic cancer coexisting with chronic pancreatitis. Cancer 1990;65:893–896.
45 Johnson PT, Outwater EK: Pancreatic carcinoma versus chronic pancreatitis: Dynamic MR imaging. Radiology 1999;212:213–218.
46 Silas AM, Morrin MM, Raptopoulos V, Keogan MT: Intraductal papillary mucinous tumors of the pancreas. AJR Am J Roentgenol 2001;176:179–185.
47 Grundmann E, Hermanek P, Wagner G: Tumorhistologieschlüssel, ed 2. Berlin, Springer, 1997, p 64.
48 Loftus EV Jr, Olivares-Pakzad BA, Batts KP, Adkins MC, Stephens DH, Sarr MG, DiMagno EP: Intraductal papillary-mucinous tumors of the pancreas: Clinicopathologic features, outcome, and nomenclature. Members of the Pancreas Clinic, and Pancreatic Surgeons of Mayo Clinic. Gastroenterology 1996;110:1909–1918.
49 Siech M, Tripp K, Schmidt-Rohlfing B, Mattfeldt T, Gorich J, Beger HG: Intraductal papillary mucinous tumor of the pancreas. Am J Surg 1999;177:117–120.
50 Albert J, Schilling D, Breer H, Jungius KP, Riemann JF, Adamek HE: Mucinous cystadenomas and intraductal papillary mucinous tumors of the pancreas in magnetic resonance cholangiopancreatography. Endoscopy 2000; 32:472–476.
51 Usuki N, Okabe Y, Miyamoto T: Intraductal mucin-producing tumor of the pancreas: Diagnosis by MR cholangiopancreatography. J Comput Assist Tomogr 1998;22:875–879.
52 Fukukura Y, Fujiyoshi F, Sasaki M, Ichinari N, Inoue H, Kajiya Y, Nakajo M: HASTE MR cholangiopancreatography in the evaluation of intraductal papillary-mucinous tumors of the pancreas. J Comput Assist Tomogr 1999;23: 301–305.
53 Arakawa A, Yamashita Y, Namimoto T, Tang Y, Tsuruta J, Kanemitsu K, Hirota M, Hiraoka T, Ogawa M, Tsuchigame T, Yoshimatsu S, Kurano R, Sagara K, Matsuo A, Shibata K, Tanimura M, Takahashi M: Intraductal papillary tumors of the pancreas. Histopathologic correlation of MR cholangiopancreatography findings. Acta Radiol 2000;41:343–347.
54 Paye F, Sauvanet A, Terris B, Ponsot P, Vilgrain V, Hammel P, Bernades P, Ruszniewski P, Belghiti J: Intraductal papillary mucinous tumors of the pancreas: Pancreatic resections guided by preoperative morphological assessment and intraoperative frozen section examination. Surgery 2000;127:536–544.
55 Sugiyama M, Atomi Y, Hachiya J: Intraductal papillary tumors of the pancreas: Evaluation with magnetic resonance cholangiopancreatography. Am J Gastroenterol 1998;93:156–159.
56 Koito K, Namieno T, Ichimura T, Yama N, Hareyama M, Morita K, Nishi M: Mucin-producing pancreatic tumors: Comparison of MR cholangiopancreatography with endoscopic retrograde cholangiopancreatography. Radiology 1998;208:231–237.
57 Cellier C, Cuillerier E, Palazzo L, Rickaert F, Flejou JF, Napoleon B, Van Gansbeke D, Bely N, Ponsot P, Partensky C, Cugnenc PH, Barbier JP, Deviere J, Cremer M: Intraductal papillary and mucinous tumors of the pancreas: Accuracy of preoperative computed tomography, endoscopic retrograde pancreatography and endoscopic ultrasonography, and long-term outcome in a large surgical series. Gastrointest Endosc 1998;47:42–49.
58 Yamashita Y, Namimoto T, Mitsuzaki K, Urata J, Tsuchigame T, Takahashi M, Ogawa M: Mucin-producing tumor of the pancreas: Diagnostic value of diffusion-weighted echo-planar MR imaging. Radiology 1998;208:605–609.
59 Nishihara K, Kawabata A, Ueno T, Miyahara M, Hamanaka Y, Suzuki T: The differential diagnosis of pancreatic cysts by MR imaging. Hepatogastroenterology 1996;43:714–720.
60 Irie H, Honda H, Aibe H, Kuroiwa T, Yoshimitsu K, Shinozaki K, Yamaguchi K, Shimada M, Masuda K: MR cholangiopancreatographic differentiation of benign and malignant intraductal mucin-producing tumors of the pancreas. AJR Am J Roentgenol 2000;174:1403–1408.
61 Riemann JF, Kohler B: Endoscopy of the pancreatic duct. Gastrointest Endosc 1993;39: 367–370.
62 Hara T, Yamaguchi T, Ishihara T, Tsuyuguchi T, Kondo F, Kato K, Asano T, Saisho H: Diagnosis and patient management of intraductal papillary-mucinous tumor of the pancreas by using peroral pancreatoscopy and intraductal ultrasonography. Gastroenterology 2002;122: 34–43.
63 Kaufman AR, Sivak MV Jr, Ferguson DR: Endoscopic retrograde cholangiopancreatography in pancreatic islet cell tumors. Gastrointest Endosc 1988;34:47–52.
64 Mao C, Howard JM: Pancreatitis associated with neuroendocrine (islet cell) tumors of the pancreas. Am J Surg 1996;171:562–564.
65 Obara T, Shudo R, Fujii T, Tanno S, Mizukami Y, Izawa T, Saitoh Y, Satou S, Kohgo Y: Pancreatic duct obstruction caused by malignant islet cell tumors of the pancreas. Gastrointest Endosc 2000;51:604–607.
66 Rösch T, Lightdale CJ, Botet JF, Boyce GA, Sivak MV Jr, Yasuda K, Heyder N, Palazzo L, Dancygier H, Schusdziarra V: Localization of pancreatic endocrine tumors by endoscopic ultrasonography. N Engl J Med 1992;326:1721–1726.
67 Martin DR, Semelka RC: MR imaging of pancreatic masses. Magn Reson Imaging Clin N Am 2000;8:787–812.
68 Semelka RC, Cumming MJ, Shoenut JP, Magro CM, Yaffe CS, Kroeker MA, Greenberg HM: Islet cell tumors: Comparison of dynamic contrast-enhanced CT and MR imaging with dynamic gadolinium enhancement and fat suppression. Radiology 1993;186:799–802.
69 Buetow PC, Parrino TV, Buck JL, Pantongrag-Brown L, Ros PR, Dachman AH, Cruess DF: Islet cell tumors of the pancreas: Pathologic-imaging correlation among size, necrosis and cysts, calcification, malignant behavior, and functional status. AJR Am J Roentgenol 1995; 165:1175–1179.

Review Article

Digestive Diseases

Dig Dis 2004;22:26–31
DOI: 10.1159/000078732

Role of Endoscopic Ultrasound in the Diagnosis of Patients with Solid Pancreatic Masses

Stefan Kahl Peter Malfertheiner

Department of Gastroenterology, Otto von Guericke University, Magdeburg, Germany

Key Words

Adenocarcinoma · Adenoma · Islet cell tumors, diagnosis · Digestive system neoplasms · Endosonography · Neoplasm staging · Pancreatic neoplasms · Pancreatitis · EUS, review of the literature · Solid pancreatic tumors, surgery · Ultrasonography, interventional

Abstract

Endoscopic ultrasound (EUS) is the most sensitive imaging procedure for the detection of small solid pancreatic masses and is accurate in determining vascular invasion of the portal venous system. Even compared to the new CT techniques, EUS provides excellent results in preoperative staging of solid pancreatic tumors. Compared to helical CT techniques, EUS is less accurate in detecting tumor involvement of the superior mesenteric artery. EUS staging and EUS-guided FNA can be performed in a single-step procedure, to establish the diagnosis of cancer. There is no known negative impact of tumor cell seeding due to EUS-guided fine needle aspiration (FNA). Without FNA, EUS and additional methods are not able to reliably distinguish between inflammatory and malignant masses.

Copyright © 2004 S. Karger AG, Basel

Introduction

Endoscopic ultrasound (EUS), initially introduced in the 1980s to improve imaging of the pancreas, has added significantly to the diagnosis of pancreatic tumors. The value of different imaging methods in the assessment of pancreatic tumors is related to the accuracy in detecting the tumor and providing information on the involvement of surrounding organs and lymph nodes. EUS provides direct visualization of the pancreas, pancreatic tumors, the common bile duct, the portal and splenic vein, the superior mesenteric vessels and adjacent lymph nodes. In comparison to other imaging modalities, EUS is able to visualize tumors of size <2 cm in diameter.

This review will focus on the ability of EUS to diagnose and stage accurately solid pancreatic masses by using three important criteria: (1) detection and imaging of the tumor; (2) determination of tumor resectability, and (3) confirmation of the diagnosis using additional techniques.

Solid masses in the pancreas mostly occur in the pancreatic head and may either be related to inflammation due to chronic pancreatitis or may be caused by a malignancy. Ductal pancreatic adenocarcinoma is the most common malignant pancreatic neoplasm, accounting for more than 95% of malignant solid pancreatic tumors. Islet cell tumors represent only a minority of those tumors. While islet cell tumors tend to clinically present

KARGER

Fax + 41 61 306 12 34
E-Mail karger@karger.ch
www.karger.com

© 2004 S. Karger AG, Basel
0257–2753/04/0221–0026$21.00/0

Accessible online at:
www.karger.com/ddi

Stefan Kahl, MD
Department of Gastroenterology, Otto von Guericke University Magdeburg
Leipziger Strasse 44, DE–39120 Magdeburg (Germany)
Tel. +49 391 6713100, Fax +49 391 6713105
E-Mail stefan.kahl@medizin.uni-magdeburg.de

earlier in the course of the disease (due to symptoms caused by tumor-related hormone production), adenocarcinomas present in nearly all cases in advanced stages when curative resection is not feasible.

Detection

Most patients are diagnosed after they start to become jaundiced. In these patients the symptoms causing masses are easily diagnosed by combining clinical examination and transcutaneous ultrasound. Only a minority of patients present without an obvious mass lesion. In comparison to other imaging modalities in these cases, EUS is superior in detection of small lesions and is able to visualize tumors of size <2 cm in diameter, when curative resection is more likely [1–4]. Sensitivity and specificity of EUS to detect pancreatic tumors in comparison to other imaging methods are reported in table 1.

Sensitivity of the advanced modern CT techniques will possibly be enhanced in comparison to EUS, but even EUS – using additional contrast medium – has now an improved sensitivity. Confirmation of this statement by larger studies is necessary.

Benign versus Malignant Mass Lesions

Once a mass lesion is detected in a patient known to suffer from chronic pancreatitis, problems arise from the difficulty to reliably distinguish between a benign mass, caused by advanced inflammation or fibrosis, and a malignant tumor. Several authors tried to identify characteristics that assist in distinguishing benign from malignant lesions. The specificity of EUS in distinguishing both types of lesions varies between 46 and 93% [3, 5].

Rösch et al. [3] and Glasbrenner et al. [5] independently proposed criteria suggestive of an inflammatory mass: inhomogeneous echo pattern, calcification, peripancreatic echo-rich stranding, cysts, etc., whereas malignant masses would invade adjacent organs, cause enlargement of adjacent lymph nodes and the mass would be with irregular outer margins. These criteria led to a remarkable specificity, but, unfortunately, the sensitivity remains low.

Newer and compared to the conventional systems more sophisticated EUS applications offer the opportunity to add Doppler and power-Doppler tools. While adenocarcinomas are mostly hypoperfused, inflammatory lesions present as hyperperfused [6]. Using these characterizations results in an enhancement of sensitivity and specificity of EUS for the differentiation of pancreatic adenocarcinoma from focal inflammatory lesions of 94 and 100%, respectively.

Table 1. Accuracy of EUS to detect pancreatic tumors in comparison to CT

Group (first author)	Year	n	EUS		CT	
			sensitivity	specificity	sensitivity	specificity
Mertz [23]	2000	35	93	75	53	25
Gress [11]	1999	81	100		74	
Midwinter [24]	1999	48	97		76	
Legmann [25]	1998	33	100	33	92	100
Muller [1]	1994	49	94	100	69	100

With respect to differentiating benign from malignant lesions (causing stenosis of the main pancreatic duct), intraductal application of the echoprobe could be an alternative. Furukawa et al. [7] examined patients with a stricture in the main pancreatic duct by a 30-MHz probe. The findings were divided into two types of lesions: an echo-rich area surrounded by an echo-poor margin was characteristic for pancreatic cancer, and a ring-like echo-lucent band surrounded by a fine reticular pattern characterized CP. Sensitivity and specificity were 100 and 92%, respectively. Unfortunately, these data had not yet been confirmed by other groups, which is mainly due to the very limited use of intraductal EUS in a restricted number of centers.

The only 100% accuracy for confirmation of malignancy with a given lesion is offered by a biopsy-guided positive histology or cytology.

Confirmation of Diagnosis

The use of EUS to obtain tissue for the diagnosis of pancreatic adenocarcinoma is a major advantage, developed and established in the past [8, 9]. The overall safety of EUS-guided fine needle aspiration (EUS-FNA) is very good and well established in several reports [9]. The complication rate is equivalent to that of an only diagnostic EUS [10].

Several studies have been published showing a consistently high accuracy for providing cytological or even histological diagnosis of pancreatic cancer by EUS-FNA. A prospective study by Gress et al. [11] reported a sensitivity and specificity to establish the diagnosis of pancreatic

adenocarcinoma by EUS-FNA of 93 and 100%, respectively.

The clinical utility of EUS-FNA was studied by Chang et al. [12]. EUS-FNA was reported to have a 95% accuracy rate for the detection of malignant pancreatic lesions and 88% accuracy rate for lymph node involvement. EUS-FNA is accompanied by an only very low complication rate [10]. In the study of O'Toole et al. [10], biopsies were taken from 345 lesions and no severe or fatal incidents were reported. Minor complications occurred in 1.6%. The risk for complications after EUS-FNA therefore appears only slightly higher than that of standard EUS alone and is even lower compared to other biopsy techniques.

In a direct comparison between three different tissue sampling techniques, EUS-FNA was proven as accurate as CT-guided biopsy technique compared to biopsies obtained by transcutaneous ultrasonography and open surgery [13]. While diagnostic accuracy is equal to other methods but the complication rate is lower, EUS-FNA should be the method of choice for obtaining tissue samples from solid pancreatic masses. In clinical routine the only limiting factor is the availability of EUS. However, treatment of patients with pancreatic disease is mostly restricted to specialized centers which offer EUS routinely to their patients, therefore EUS-FNA can be offered to the majority of patients [14–16].

The major late complication of tissue sampling in patients who will later undergo surgery is peritoneal carcinomatosis due to suspected tumor cell seeding during a diagnostic biopsy. With EUS it no longer seems to be a significant problem. In a group of 89 patients, 46 had a EUS-guided biopsy and in the remaining 43 the percutaneous route was used. In the EUS-FNA group, 1 patient developed peritoneal carcinomatosis compared with 7 in the percutaneous FNA group (2.2 vs. 16.3%; $p < 0.025$) [17].

EUS-FNA can be recommended as the method of choice for obtaining biopsies for histological confirmation, also in patients with potentially resectable pancreatic cancer. However, there is an ongoing debate about the necessity for establishing diagnosis prior to surgery. In our opinion, for presumably curative resectable lesions that will definitively undergo surgery, any preoperative histological confirmation is unnecessary. In these cases a histological confirmation will not change the current practice of the surgeon and has no impact on the patient's management.

EUS-FNA is particularly important in patients who are poor candidates for surgery or have advanced disease and therefore would not be considered for surgical resection. On the other hand, while there is no proven negative impact on a EUS-FNA on tumor seeding, a positive confirmation of malignancy in a suspected mass lesion will not automatically lead to palliative treatment.

Determination of Resectability

In patients with pancreatic adenocarcinoma, preoperative staging with reliable information concerning the T-stage is essential to avoid unnecessary surgery. Vascular invasion and lymph node involvement are the most important prognostic factors to predict failure of surgery. Data are given in table 2 regarding sensitivity, specificity and accuracy of EUS for the prediction of irresectability of pancreatic tumors [2, 11, 18–27].

Determination of resectability seems to be more difficult in larger tumors. In general, lower accuracies are obtained in larger tumors. Ahmad et al. [21] hypothesized that a peritumoral inflammation affects EUS accuracy. This hypothesis was again supported by another extended study from the same group, indicating that EUS is more effective in detecting vascular involvement in tumors <3 cm in size [28].

The criteria proposed by several authors for the prediction of vascular invasion are: (1) visualization of tumor in the lumen; (2) complete obstruction; (3) collateral vessels, and (4) irregular tumor-vessel relationship [29].

Earlier reports demonstrated superior accuracy for preoperative staging of solid pancreatic masses if done by EUS. A key study reporting on T- and N-stages by EUS in comparison with CT found EUS to be more accurate than dynamic CT in all possible tumor stages [11]. In a meta-analysis involving 357 patients from 14 studies, EUS was reported to have an overall accuracy in preoperative staging of 83% [30].

The visualization of vascular structures may be difficult with EUS in patients with large tumors and altered anatomy (possibly due to peritumoral inflammation [21]). Rösch et al. [29] described a sensitivity of only 43% but a specificity of 91% of EUS to detect venous vascular invasion. EUS is particularly accurate for the demonstration of splenoportal venous invasion but less accurate for demonstrating involvement of the superior mesenteric artery [29, 31]. A study by Brugge et al. [32] confirmed the inadequacy of EUS in the determination of superior mesenteric vein involvement but found EUS to be superior to angiography in determining portal and splenic vein invasion with tumor, with accuracies ranging from 77 to 85%.

Table 2. Accuracy of prediction of tumor resectability by EUS and CT

Group (first author)	Year	EUS				CT				Comment
		n	sensitivity	specificity	accuracy	n	sensitivity	specificity	accuracy	
Catalano [18]	2003					46	96	86	93	Multisclice CT
Huang [19]	2002					68	90.6	97.7	90.7	Multiphase CT
Tierney [20]	2001	51	100	93		51	62.5	100		Dual-phase helical CT
Ahmad [21]	2000	89			69					
Mertz [23]	2000	35	100			35	50			Single-phase helical CT
Gress [11]	1999	81			93	81			60	Axial CT
Midwinter [24]	1999	34	81	86		3	56	100		Venous involvement; dual-phase CT
Midwinter [24]	1999	34	17	67		34	50	100		Superior mesenteric artery involvement; dual-phase CT
Legmann [25]	1998	30			86	30			100	Dual-phase helical CT
Palazzo [2]	1993	64	100			64	71			Venous involvement; dual-phase helical CT
Rösch [26]	1992	46	91	97		46	36	85		Venous involvement; dual-phase helical CT

In the past, EUS offered most accurate data about the tumor T-stage, but nowadays, with the introduction of advanced and sophisticated CT-scanning methods (dynamic, multiphase, multislice helical CT), accuracy of the cross-sectional procedures has significantly improved. The volumetric data acquisition of helical CT permits computer reconstruction of the images acquired into three-dimensional volume-rendered images. The arterial and venous anatomy found in CT is equivalent to conventional angiography. Therefore, the question whether EUS still has advantages over cross-sectional procedures was again addressed.

Helical CT is an advance in CT technology that allows for more rapid acquisition of CT images. In helical CT there is continuous activation and spinning of the X-ray source and continuous movement of the tabletop leading to continuous data acquisition. With helical CT, thinner slices can be obtained in a single breath hold through reconstruction of overlapping venous system. Helical CT therefore provides consistently higher levels of circulating contrast medium, allowing more accurate assessment of the splanchnic vessels. Computer algorithms that allow three-dimensional reconstruction are also possible. Helical CT angiography has been described and may be better than axial helical CT imaging for detecting vascular invasion. This question was extensively discussed in a recently published review by Hunt and Faigel [4] in *Gastrointestinal Endoscopy.*

To date there have been four studies comparing EUS with helical CT in patients with pancreatic cancer [20, 23–25]. The data given in table 2 compare the corresponding definitions of EUS. Analyzing the overall results demonstrates that again EUS remains the most sensitive test for detecting small tumors in the pancreas [4]. Hunt and Faigel [4] summarize the results in the above-mentioned review: For determining whether the tumor is resectable, helical CT has good accuracy (83%), although EUS is somewhat better (91%). The improved accuracy of EUS is due to its greater sensitivity for detecting vascular invasion of the portal venous system.

Invasion of the portal venous system as a criterion of irresectability is questioned by some surgeons. In patients with adenocarcinoma of the pancreatic head who require venous resection during pancreaticoduodenectomy for isolated tumor extension to the superior mesenteric or portal vein, there exist data where the survival period is not different from that of patients who undergo standard pancreaticoduodenectomy [33]. These data may suggest that venous involvement is a function of tumor location rather than an indicator of aggressive tumor biology.

Under these circumstances, the advantage of EUS over helical CT staging may disappear. Again, further studies are needed, addressing this special issue to establish the value of EUS and helical CT in prediction of irresectability and their impact on clinical management.

Clinical Role of EUS in Solid Pancreatic Masses

The major clinical challenge of EUS in malignant pancreatic tumors is to identify those who may potentially undergo curative resection or vice versa to identify patients with high risk for advanced, unresectable disease. For patients who have a high suspicion of advanced disease or who are poor surgical candidates, EUS provides a less expensive staging approach. Powis and Chang [34] calculated total costs for laparotomy with approximately USD 22,000 compared to costs of a staging EUS (combined with FNA) of approximately USD 2,500, meaning that only 1 patient for every 8.8 patients staged would need to have unresectable disease by EUS to financially justify using the EUS technique. The direct comparison of EUS-FNA, CT-guided FNA and surgery revealed EUS-FNA the least costly strategy in the staging workup of patients with pancreatic head cancer [17, 34, 35].

Identifying the patient population who most likely benefit from surgery is the major advantage of EUS. Defining this patient population helps to reduce direct medical care costs in pancreatic cancer [34]. However, prospective data are lacking in this regard and will need to be addressed in the future.

To summarize: EUS is a highly sensitive imaging procedure for detecting small solid pancreatic masses and is accurate in determining vascular invasion of the portal venous system. EUS should be performed in patients with solid pancreatic masses but without distant metastasis or in patients with suspected tumors not visualized by other imaging procedures. EUS reliably predicts resectability by determining vascular involvement. Advanced CT scanning methods reach equal accuracy values to predict irresectability. EUS staging and EUS-FNA can be performed in a single, combined procedure. EUS-FNA can be considered in the majority of patients undergoing EUS to establish the diagnosis of cancer, determine histologic type, confirm lymph node histology. There is no known negative impact of tumor cell seeding due to EUS-FNA. However, for potentially resectable cancers immediate histological or cytological confirmation of malignancy is unnecessary.

Helical CT is an advance over standard CT in its ability to detect and stage pancreatic cancer. The major advantage of helical CT over standard EUS technique is related to a more accurate detection of tumor involvement of the superior mesenteric artery. Even more than 20 years after the introduction of EUS into the clinical workup of patients with pancreatic mass lesions, EUS and additional methods are still not able to reliably distinguish between inflammatory and malignant masses in some cases.

References

1 Muller MF, Meyenberger C, Bertschinger P, Schaer R, Marincek B: Pancreatic tumors: Evaluation with endoscopic US, CT, and MR imaging. Radiology 1994;190:745–751.

2 Palazzo L, Roseau G, Gayet B, Vilgrain V, Belghiti J, Fekete F, Paolaggi JA: Endoscopic ultrasonography in the diagnosis and staging of pancreatic adenocarcinoma. Results of a prospective study with comparison to ultrasonography and CT scan. Endoscopy 1993;25:143–150.

3 Rösch T, Lorenz R, Braig C, Feuerbach S, Siewert JR, Schusdziarra V, Classen M: Endoscopic ultrasound in pancreatic tumor diagnosis. Gastrointest Endosc 1991;37:347–352.

4 Hunt GC, Faigel DO: Assessment of EUS for diagnosing, staging, and determining resectability of pancreatic cancer: A review. Gastrointest Endosc 2002;55:232–237.

5 Glasbrenner B, Schwarz M, Pauls S, Preclik G, Beger HG, Adler G: Prospective comparison of endoscopic ultrasound and endoscopic retrograde cholangiopancreatography in the preoperative assessment of masses in the pancreatic head. Dig Surg 2000;17:468–474.

6 Becker D, Strobel D, Bernatik T, Hahn EG: Echo-enhanced color- and power-Doppler EUS for the discrimination between focal pancreatitis and pancreatic carcinoma. Gastrointest Endosc 2001;53:784–789.

7 Furukawa T, Tsukamoto Y, Naitoh Y, Hirooka Y, Hayakawa T: Differential diagnosis between benign and malignant localized stenosis of the main pancreatic duct by intraductal ultrasound of the pancreas. Am J Gastroenterol 1994;89:2038–2041.

8 Wiersema MJ, Kochman ML, Cramer HM, Tao LC, Wiersema LM: Endosonography-guided real-time fine-needle aspiration biopsy. Gastrointest Endosc 1994;40:700–707.

9 Wiersema MJ, Vilmann P, Giovannini M, Chang KJ, Wiersema LM: Endosonography-guided fine-needle aspiration biopsy: Diagnostic accuracy and complication assessment. Gastroenterology 1997;112:1087–1095.

10 O'Toole D, Palazzo L, Arotcarena R, Dancour A, Aubert A, Hammel P, Amaris J, Ruszniewski P: Assessment of complications of EUS-guided fine-needle aspiration. Gastrointest Endosc 2001;53:470–474.

11 Gress FG, Hawes RH, Savides TJ, Ikenberry SO, Cummings O, Kopecky K, Sherman S, Wiersema MJ, Lehman GA: Role of EUS in the preoperative staging of pancreatic cancer: A large single-center experience. Gastrointest Endosc 1999;50:786–791.

12 Chang KJ, Nguyen P, Erickson RA, Durbin TE, Katz KD: The clinical utility of endoscopic ultrasound-guided fine-needle aspiration in the diagnosis and staging of pancreatic carcinoma. Gastrointest Endosc 1997;45:387–393.

13 Mallery JS, Centeno BA, Hahn PF, Chang Y, Warshaw AL, Brugge WR: Pancreatic tissue sampling guided by EUS, CT/US, and surgery: A comparison of sensitivity and specificity. Gastrointest Endosc 2002;56:218–224.

14 Andren-Sandberg A, Neoptolemos JP: Resection for pancreatic cancer in the new millennium. Pancreatology 2002;2:431–439.

15 Saettler EB, Temple WJ: The surgeon as a prognostic factor in the management of pancreatic cancer. Surg Oncol Clin N Am 2000;9:133–142, viii.

16 Bassi C, Falconi M, Salvia R, Mascetta G, Molinari E, Pederzoli P: Management of complications after pancreaticoduodenectomy in a high volume centre: Results on 150 consecutive patients. Dig Surg 2001;18:453–457.
17 Micames C, Jowell PS, White R, Paulson E, Nelson R, Morse M, Hurwitz H, Pappas T, Tyler D, McGrath K: Lower frequency of peritoneal carcinomatosis in patients with pancreatic cancer diagnosed by EUS-guided FNA vs. percutaneous FNA. Gastrointest Endosc 2003;58: 690–695.
18 Catalano C, Laghi A, Fraioli F, Pediconi F, Napoli A, Danti M, Reitano I, Passariello R: Pancreatic carcinoma: The role of high-resolution multislice spiral CT in the diagnosis and assessment of resectability. Eur Radiol 2003; 13:149–156.
19 Huang QJ, Xu Q, Wang XN, Zhang LL: Spiral multi-phase CT in evaluating resectability of pancreatic carcinoma. Hepatobiliary Pancreat Dis Int 2002;1:614–619.
20 Tierney WM, Francis IR, Eckhauser F, Elta G, Nostrant TT, Scheiman JM: The accuracy of EUS and helical CT in the assessment of vascular invasion by peripapillary malignancy. Gastrointest Endosc 2001;53:182–188.
21 Ahmad NA, Lewis JD, Ginsberg GG, Rosato EF, Morris JB, Kochman ML: EUS in preoperative staging of pancreatic cancer. Gastrointest Endosc 2000;52:463–468.
22 Ahmad NA, Lewis JD, Siegelman ES, Rosato EF, Ginsberg GG, Kochman ML: Role of endoscopic ultrasound and magnetic resonance imaging in the preoperative staging of pancreatic adenocarcinoma. Am J Gastroenterol 2000;95:1926–1931.
23 Mertz HR, Sechopoulos P, Delbeke D, Leach SD: EUS, PET, and CT scanning for evaluation of pancreatic adenocarcinoma. Gastrointest Endosc 2000;52:367–371.
24 Midwinter MJ, Beveridge CJ, Wilsdon JB, Bennett MK, Baudouin CJ, Charnley RM: Correlation between spiral computed tomography, endoscopic ultrasonography and findings at operation in pancreatic and ampullary tumours. Br J Surg 1999;86:189–193.
25 Legmann P, Vignaux O, Dousset B, Baraza AJ, Palazzo L, Dumontier I, Coste J, Louvel A, Roseau G, Couturier D, Bonnin A: Pancreatic tumors: comparison of dual-phase helical CT and endoscopic sonography. AJR Am J Roentgenol 1998;170:1315–1322.
26 Rösch T, Braig C, Gain T, Feuerbach S, Siewert JR, Schusdziarra V, Classen M: Staging of pancreatic and ampullary carcinoma by endoscopic ultrasonography. Comparison with conventional sonography, computed tomography, and angiography. Gastroenterology 1992;102: 188–199.
27 Rösch T, Lorenz R, Braig C, Classen M: Endoscopic ultrasonography in diagnosis and staging of pancreatic and biliary tumors. Endoscopy 1992;24(suppl 1):304–308.
28 Ahmad NA, Kochman ML, Lewis JD, Kadish S, Morris JB, Rosato EF, Ginsberg GG: Endosonography is superior to angiography in the preoperative assessment of vascular involvement among patients with pancreatic carcinoma. J Clin Gastroenterol 2001;32:54–58.
29 Rösch T, Dittler HJ, Strobel K, Meining A, Schusdziarra V, Lorenz R, Allescher HD, Kassem AM, Gerhardt P, Siewert JR, Hofler H, Classen M: Endoscopic ultrasound criteria for vascular invasion in the staging of cancer of the head of the pancreas: A blind reevaluation of videotapes. Gastrointest Endosc 2000;52:469–477.
30 Rösch T: Staging of pancreatic cancer. Analysis of literature results. Gastrointest Endosc Clin N Am 1995;5:735–739.
31 Snady H, Bruckner H, Siegel J, Cooperman A, Neff R, Kiefer L: Endoscopic ultrasonographic criteria of vascular invasion by potentially resectable pancreatic tumors. Gastrointest Endosc 1994;40:326–333.
32 Brugge WR, Lee MJ, Kelsey PB, Schapiro RH, Warshaw AL: The use of EUS to diagnose malignant portal venous system invasion by pancreatic cancer. Gastrointest Endosc 1996; 43:561–567.
33 Leach SD, Lee JE, Charnsangavej C, Cleary KR, Lowy AM, Fenoglio CJ, Pisters PW, Evans DB: Survival following pancreaticoduodenectomy with resection of the superior mesenteric-portal vein confluence for adenocarcinoma of the pancreatic head. Br J Surg 1998;85:611–617.
34 Powis ME, Chang KJ: Endoscopic ultrasound in the clinical staging and management of pancreatic cancer: Its impact on cost of treatment. Cancer Control 2000;7:413–420.
35 Harewood GC, Wiersema MJ: A cost analysis of endoscopic ultrasound in the evaluation of pancreatic head adenocarcinoma. Am J Gastroenterol 2001;96:2651–2656.

Review Article

Digestive Diseases

Dig Dis 2004;22:32–38
DOI: 10.1159/000078733

Echo-Enhanced Sonography – An Increasingly Used Procedure for the Differentiation of Pancreatic Tumors

Steffen Rickes Peter Malfertheiner

Department of Gastroenterology, Hepatology and Infectiology, Otto von Guericke University, Magdeburg, Germany

Key Words
Pancreatic tumors · Differential diagnosis · Echo-enhanced sonography

Abstract
Echo-enhanced sonography is increasingly being used for differential diagnosis of pancreatic tumors. Ductal carcinomas are often hypovascularized compared with the surrounding tissue. On the other hand, neuroendocrine tumors are hypervascularized lesions. Tumors associated with pancreatitis have a different vascularization pattern depending on inflammation and necrosis. Cystadenomas frequently show many vessels along the fibrotic strands. Pancreatic tumors have a different vascularization pattern in echo-enhanced sonography. These characteristics can be used for differential diagnosis. However, histology is the standard of reference.

Copyright © 2004 S. Karger AG, Basel

Introduction

The differentiation of pancreatic tumors is difficult by imaging techniques. Histology is the standard of reference but can produce false results. Endoscopic retrograde (ERCP) and magnetic resonance cholangiopancreatography (MRCP) are the current imaging standards for differential diagnosis of pancreatic lesions [1–5]. With conventional transabdominal ultrasound, there are no characteristic signs for the differentiation of pancreatic masses and the diagnostic accuracy is <70% [6–9]. Echo-enhanced sonography is a procedure with good results in the differentiation of liver lesions [10–15]. In the following, the use of this method in differential diagnosis of pancreatic tumors will be depicted and discussed.

Ultrasound Methods and Criteria for Pancreatic Tumor Differentiation

All patients will initially be investigated by conventional sonography using a dynamic sector scanner. For echo-enhanced sonography the power Doppler mode under the conditions of 2nd Harmonic Imaging or the Pulse Inversion technique are available. Echo-enhanced power Doppler sonography starts immediately after injection of 4 g Levovist® (concentration 300 mg/ml) and lasts approximately 2 min. One focus zone with depth adapted to the area of interest and a mechanical index of 0.8–1.3 should be used. For echo-enhanced sonography with Pulse Inversion, 2.4 ml SonoVue® will be injected and the mechanical index varies between 0.1 and 0.2. As for echo-enhanced power Doppler sonography, the investigation lasted approximately 2 min.

Criteria for the differentiation of pancreatic masses by conventional and echo-enhanced sonography (table 1) have recently been published [9, 16]: (1) A ductal carcino-

KARGER

Fax + 41 61 306 12 34
E-Mail karger@karger.ch
www.karger.com

© 2004 S. Karger AG, Basel
0257–2753/04/0221–0032$21.00/0

Accessible online at:
www.karger.com/ddi

Dr. S. Rickes, Otto von Guericke University Magdeburg
Department of Gastroenterology, Hepatology and Infectiology
Leipziger Strasse 44, DE–39120 Magdeburg (Germany)
Tel. +49 391 6713100, Fax +49 391 6713105
E-Mail steffen.rickes@medizin.uni-magdeburg.de

Table 1. Criteria for pancreatic tumor differentiation with conventional ultrasound, unenhanced power Doppler sonography and echo-enhanced ultrasound [9, 16]

	B-mode sonography	Unenhanced power Doppler sonography	Echo-enhanced power Doppler sonography
Ductal carcinoma	Low-echo pattern Lobulated margins Dilated Wirsung's duct Vascular infiltration Metastases	No tumor vessels detectable	Poorly vascularized tumor Marginal tumor vessels
Pancreatitis (chronic and acute)	Low-echo pattern Lobulated margins Thrombosis Necrotic areas Dilated Wirsung's duct	Vessels rarely detectable	Vascularization depending on inflammation and necrosis
Neuroendocrine tumor	Low-echo pattern Sharply delineated round margins No dilated Wirsung's duct Vascular infiltration rare metastases	Tumor vessels rarely detectable	Highly vascularized tumor
Cystadenoma	Small cystic areas (often <3 cm) Spoke-like pattern of fibrotic strands with small calcifications No dilated Wirsung's duct	No tumor vessels detectable	Highly vascularized tumor arteries along the fibrotic strands
Cystadeno-carcinoma	Large cystic areas (often >5 cm) Solid areas No dilated Wirsung's duct Metastases	Rarely tumor vessels with chaotic pattern detectable	Poorly and chaotic vascularized solid areas
Pseudocyst	Often echo-free pattern Sharply delineated wall Features of acute and/or chronic pancreatitis Signs of bleeding and/or calcifications Bowel infiltration is possible	Rarely tumor vessels detectable in 'young cysts'	'Young cysts' (few weeks of age) show often a highly vascularized wall 'Old cysts' (few months of age) show often a poorly vascularized wall
Metastasis of a renal cell carcinoma	Low-echo pattern Lobulated margins	Tumor vessels rarely detectable	Highly vascularized tumor
Lymphoma	Low-echo pattern Sharply delineated round margins No dilated Wirsung's duct	No tumor vessels detectable	Differently vascularized tumor masses

ma presents at B-mode ultrasound with low-echo pattern and lobulated margins. Wirsung's duct is dilated (fig. 1a). At echo-enhanced sonography, the lesion is poorly vascularized in most cases (fig. 1b). (2) In contrast to adenocarcinomas, neuroendocrine tumors and metastases of renal cell carcinomas show sharply delineated margins, and Wirsung's duct is usually not dilated (fig. 2a). A hypervascularization after injection of an echo-enhancer is a characteristic sign of these masses (fig. 2b). (3) In particular, the differential diagnosis of adenocarcinomas and pancreatitis-associated masses is notoriously problematic, since both tumors can appear as low-echo and lobulated lesions with dilatation of Wirsung's duct. The vascularization of pancreatitis-associated tumors depends on inflammation and necrosis. (4) Cystic pancreatic neoplasms are rare. While cystadenomas are characterized by small cystic areas and highly vascularized fibrotic strands (fig. 3), cystadenocarcinomas consist of large cysts and poorly vascularized solid areas (fig. 4). Pseudocysts show an echo-free pattern and a sharply delineated wall (fig. 5a). At the pancreas, features of chronic inflammation (calcifications and dilated Wirsung's duct) can be found. After

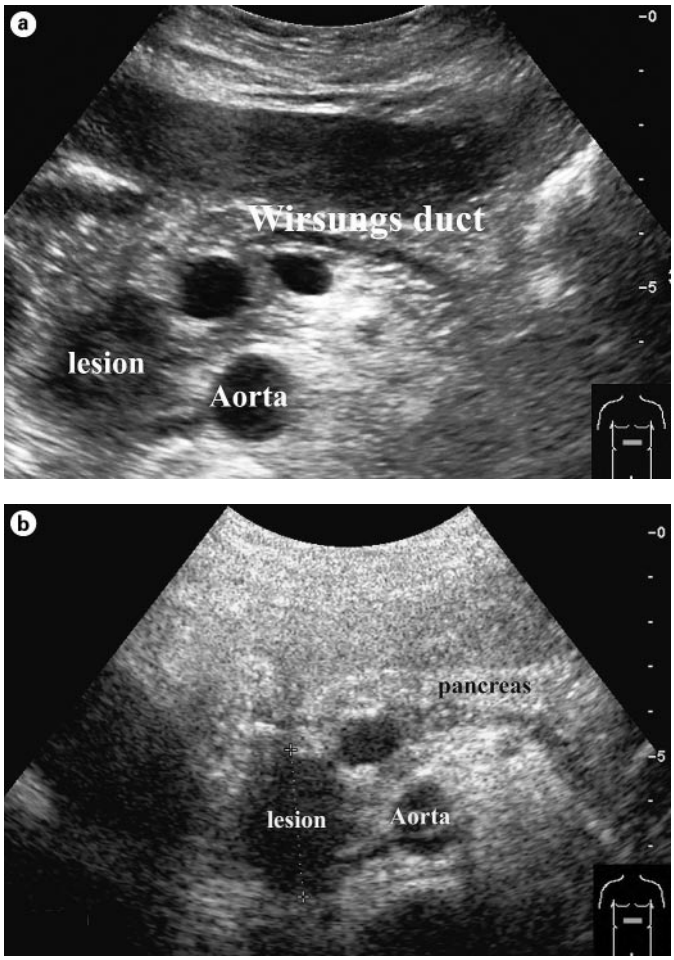

Fig. 1. Ductal pancreatic carcinoma at conventional (**a**) and echo-enhanced sonography (**b**). **a** Low-echo tumor with lobulated margins and dilatation of Wirsung's duct. **b** Poorly vascularized lesion.

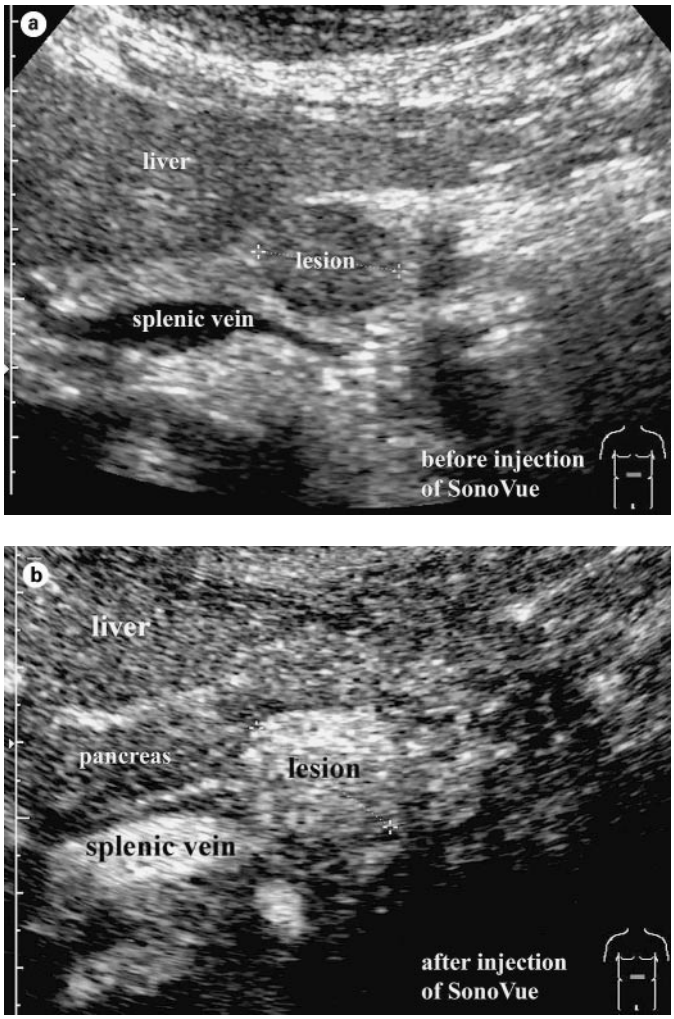

Fig. 2. Pancreatic metastasis of a renal cell carcinoma at conventional (**a**) and echo-enhanced sonography (**b**). **a** Low-echo mass with sharply delineated margins without dilatation of Wirsung's duct. **b** Highly vascularized lesion.

injection of an echo-enhancer the wall of the pseudocysts is highly ('young cyst', fig. 5b) or poorly vascularized ('old cysts').

Results of Echo-Enhanced Sonography in the Differentiation of Pancreatic Tumors

Table 2 presents the results of several studies in the differentiation of pancreatic lesions with echo-enhanced sonography.

In a study published in 2002 [17], only 57% of the adenocarcinomas were correctly classified by conventional and unenhanced ultrasound. However, with echo-enhanced sonography, 87% of the masses could be differentiated ($p = 0.0001$). Two carcinomas were interpreted erroneously as lesions associated with pancreatitis.

From the pancreatitis-associated masses, 85% were diagnosed correctly by echo-enhanced sonography. Four tumors were classified falsely as ductal carcinomas. All of them showed necrotic tissue at histology.

Another study showed good results of echo-enhanced ultrasound in the differentiation of neuroendocrine pancreatic tumors [18]. Table 2 demonstrates that a sensitivity of 94% and a specificity of 96% were achieved with this procedure. Other reports have confirmed these good results [19]. On the other hand, it was shown that the overall sensitivity of somatostatin receptor scintigraphy in the

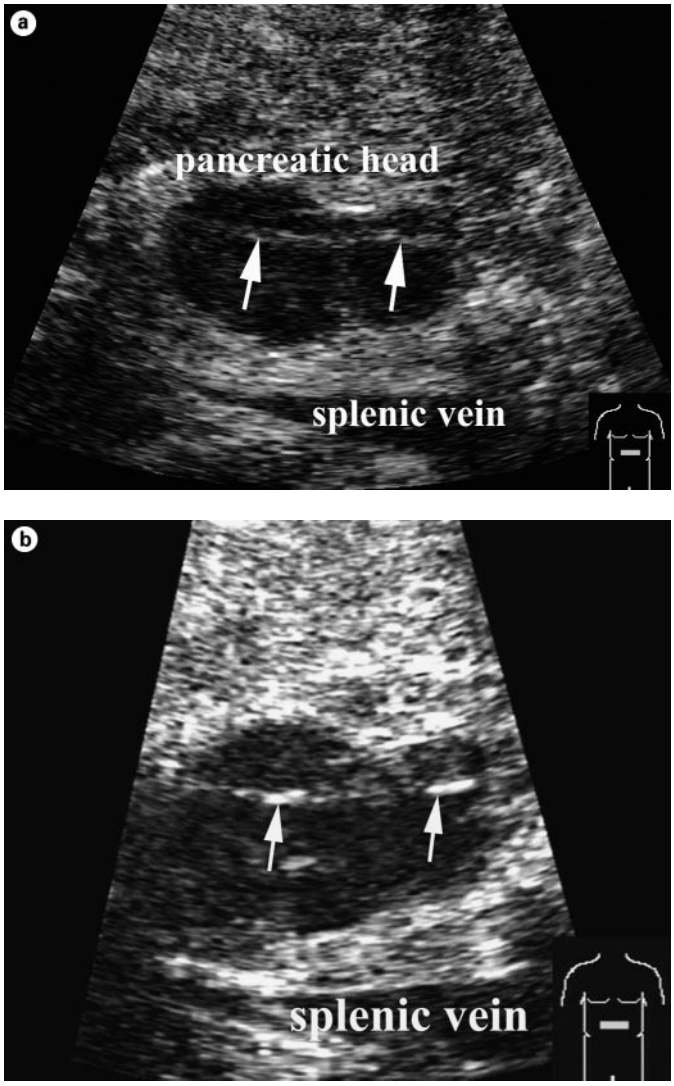

Fig. 3. Cystadenoma at conventional (**a**) and echo-enhanced sonography (**b**). **a** Tumor (diameter 25 mm) with small cystic areas and thin fibrotic strands (arrows). **b** Highly vascularized tumor arteries along the fibrotic strands.

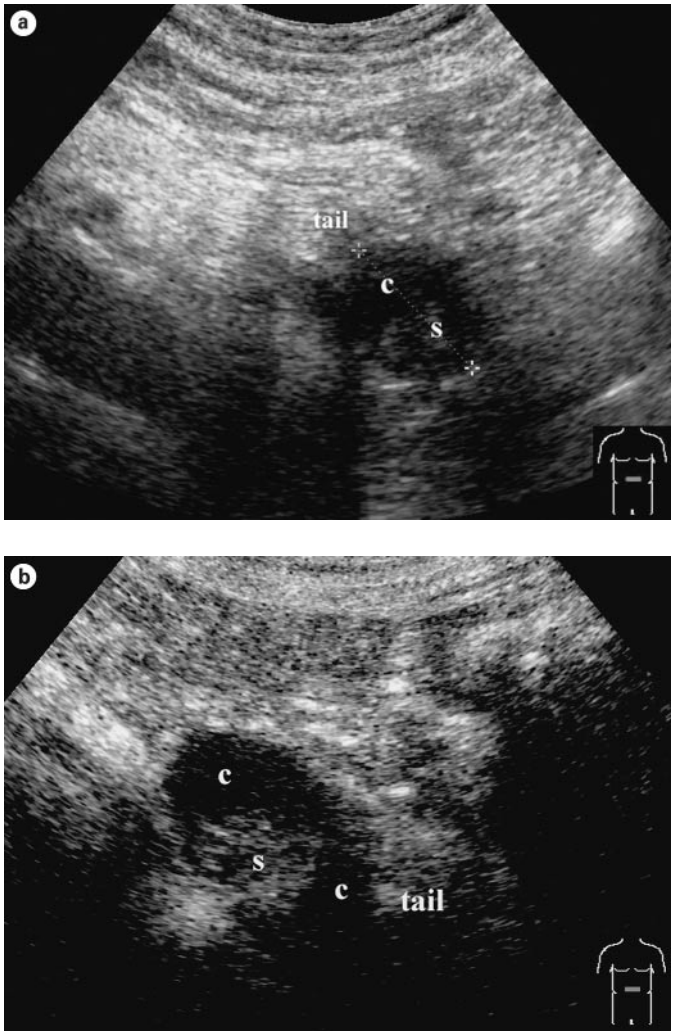

Fig. 4. Cystadenocarcinoma at conventional (**a**) and echo-enhanced sonography (**b**). **a** Tumor (diameter 70 mm) with cystic (c) and solid (s) areas. **b** Poorly vascularized solid areas.

differential diagnosis of neuroendocrine pancreatic tumors is less than 55% [18]. Furthermore, a recently published study showed that with echo-enhanced sonography, cystic neoplasms can be differentiated well from pseudocysts [20]. However, one cystadenoma was misdiagnosed as a cystadenocarcinoma, and vice versa. The morphological variability of these cystic lesions at conventional ultrasound and the difficulties in the evaluation of the vascularization of cystic masses seem to be responsible for the false results.

Discussion

There is no ideal diagnostic procedure for the differentiation of pancreatic tumors. Histology is the standard of reference but can produce false results. ERCP is the standard for diagnostic imaging, but is burdened with the risk of complications, the most important being pancreatitis [21, 22]. MRCP has a similar sensitivity and specificity for detecting pancreatic cancer or chronic pancreatitis to ERCP [1–5]. However, this procedure is expensive, time-consuming, and available only in large medical centers.

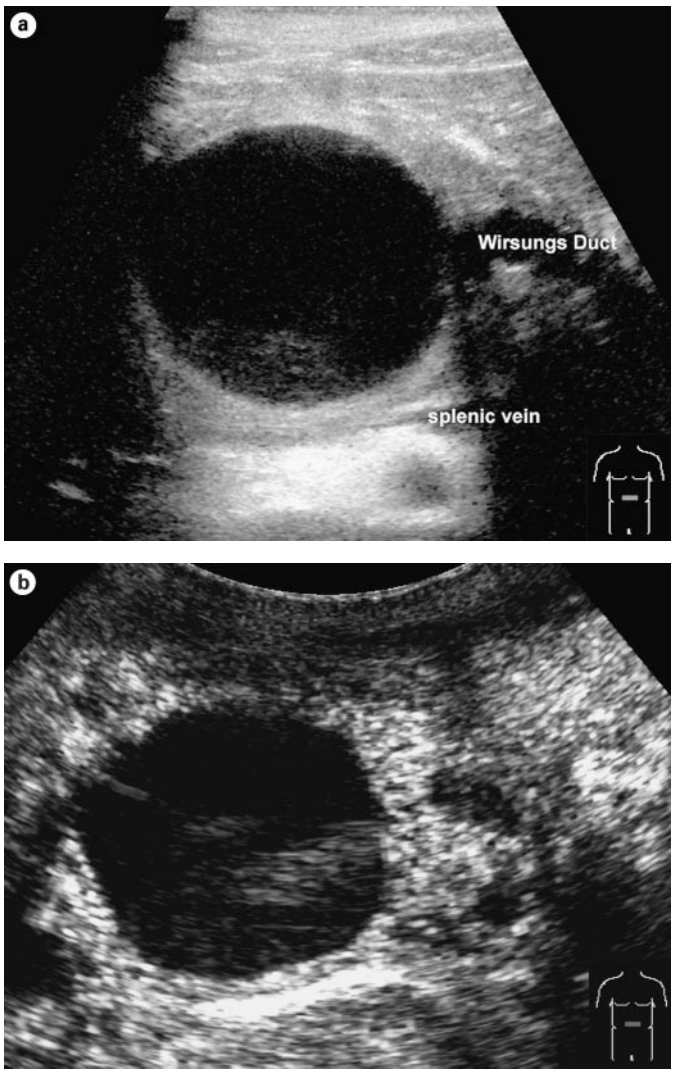

Fig. 5. Pseudocyst at conventional (**a**) and echo-enhanced sonography (**b**). **a** Lesion with an echo-free pattern and a sharply delineated wall. Wirsung's duct is dilated. **b** Highly vascularized wall.

Computed tomography and endoscopic ultrasonography are unable to differentiate pancreatic tumors satisfactorily but may be the best methods to stage for resectability and detect metastases [23–25].

There are no characteristic signs for the different pancreatic lesions in conventional transabdominal ultrasound. In particular, the differentiation of ductal carcinoma from chronic pancreatitis is notoriously problematic [9, 16].

Some years ago, the angiographic vascularization pattern was reported to be helpful for the differentiation of pancreatic tumors [26–28]. Whereas ductal carcinomas are characterized by their hypovascularization, neuroendocrine tumors were found to be hypervascularized. However, the diagnostic accuracy of angiography is low because it is impossible to investigate the macroscopic tumor features.

Unenhanced power Doppler sonography allows the investigation of the vascularization pattern of tumors by ultrasound as well. For instance, there are good results in the differentiation of hepatocellular carcinomas with this method [13, 29]. In the differential diagnosis of pancreatic masses, no diagnostic advantage of this method was observed in comparison to conventional ultrasound. This might be explained by the low sensitivity of unenhanced power Doppler sonography for detecting low blood flow velocity or small vessels, and the existence of multiple tissue artifacts [9, 10].

The sensitivity of power Doppler sonography can be increased by echo-enhancers, for example Levovist®. This preparation consists of microbubbles of air which enhance the Doppler signal at 20–30 dB [10, 30, 31]. With echo-enhanced power Doppler sonography, however, the signal intensity from flowing blood is much lower compared to that of moving solid structures, such as tissue

Table 2. Results of echo-enhanced sonography in the differential diagnosis of pancreatic tumors

Lesion	Study (ref. No.)	Sensitivity %	Specificity %	PPV %	NPV %
Adenocarcinoma	17	87	94	89	93
Pancreatitis	17	85	99	97	94
Neuroendocrine tumor	18, 19	94	96	76	99
Cystic tumor	20	95–100	92–100	95–100	92–100

movements. 2nd Harmonic Imaging was developed to overcome these difficulties. This method is based on the property of microbubbles to resonate and emit harmonic waves in an ultrasound field with a frequency of 1–5 MHz. If the harmonic frequency is to be detected at twice the transmitted frequency, the procedure is called 2nd Harmonic Imaging. Tissue particles have fewer 2nd harmonic waves than microbubbles, so the signals of echo-enhancers are more distinguishable [10].

Recently, the new contrast agent Sonovue® is being used more frequently for echo-enhanced sonography. Furthermore, 2nd Harmonic Imaging was replaced partially by the Pulse Inversion Imaging technique. There are remarks that with this new procedure more favorable results can be achieved than with 2nd Harmonic Imaging. With 2nd Harmonic Imaging it is impossible to separate the transmitted and received harmonic signal completely because of limited bandwidth. However, Pulse Inversion Imaging avoids these bandwidth limitations by using characteristics specific to microbubble vibrations to subtract rather than filter out the fundamental. Because this imaging transmits two reciprocal pulses, leading to subtract fundamental signals, it can allow the use of broader transmit and receive bandwidths for improved resolution and can provide increased sensitivity to contrast [32]. However, comparative results of large prospective studies are missing.

Characteristic signs of pancreatic tumors at echo-enhanced sonography have been published [9, 16]. Similar to their angiographic features, ductal carcinomas and solid areas of cystadenocarcinomas were found to be hypovascularized. In contrast, neuroendocrine tumors and solid parts of cystadenomas are mostly hypervascularized. Pancreatitis-associated masses show different patterns of vascularization depending on inflammation, fibrotic scars, and the extent of necrosis [9, 16].

The results of the studies of table 2 demonstrate that, with the combination of echo-enhanced sonography and 2nd Harmonic or Pulse Inversion Imaging, a higher percentage of ductal carcinomas, pancreatitis-associated masses, and neuroendocrine and cystic tumors can be classified correctly. However, conventional ultrasound, unenhanced and echo-enhanced sonography must not be used as separate imaging techniques. Conventional ultrasound is the basic sonographic method, and a tumor differentiation is hardly possible with echo-enhanced ultrasound alone. Echo-enhanced sonography offers more diagnostic criteria than conventional ultrasound alone. Therefore, all sonographic procedures should be combined.

In comparison with reported results of ERCP and MRCP [1], echo-enhanced sonography has a similar accuracy in diagnosing pancreatic carcinoma. With respect to the differentiation of pancreatitis-associated tumors, the sensitivity of echo-enhanced power Doppler sonography seems to be slightly lower, while the specificity is somewhat higher compared to ERCP and MRCP [1]. Necroses and fibroses are major problems for the differential diagnosis of ductal carcinomas and pancreatitis-associated masses. Since both tissues are not vascularized, necrotic pancreatitis may be interpreted falsely as ductal carcinoma. On the other hand, it is possible to find inflammation in the surrounding tissue of an adenocarcinoma leading to the suspicion of a pancreatitis.

Echo-enhanced sonography displayed above all a high sensitivity and specificity in the differentiation of neuroendocrine tumors. Whereas endoscopic ultrasonography is of great value for localizing neuroendocrine pancreatic tumors [33], echo-enhanced sonography could become the new standard of reference for their differential diagnosis by imaging procedures. However, there are reports on false results of echo-enhanced sonography due to by hypervascularized metastases of a renal cell carcinoma. A hypervascularization of metastases from renal cell carcinomas had also been observed in angiographic studies [34, 35]. This phenomenon is based on a well-vascularized stroma.

Cystic pancreatic masses are often associated with multiple artifacts at sonography. Although it is difficult to investigate the vascularization pattern of the solid tumor parts, the present results demonstrate the higher diagnostic value of echo-enhanced sonography compared to conventional or unenhanced ultrasound [36]. However, MRCP seems to be more successful in the differentiation of cystic pancreatic tumors [37, 38].

The successful treatment of pancreatic tumors requires a highly sensitive and specific diagnostic procedure. Echo-enhanced sonography is a powerful tool that may satisfy this requirement. However, histology is the standard of reference for the differentiation of pancreatic tumors.

References

1 Adamek HE, Albert J, Breer H, Weitz M, Schilling D, Riemann JF: Pancreatic cancer detection with magnetic resonance cholangiopancreatography and endoscopic retrograde cholangiopancreatography: A prospective controlled study. Lancet 2000;356:190–193.
2 Sugiyama M, Atomi Y, Hachiya J: Intraductal papillary tumours of the pancreas. Evaluation with magnetic resonance cholangiopancreatography. Am J Gastroenterol 1998;93:156–159.
3 Hintze RE, Adler A, Veltzke H, et al: Clinical significance of magnetic resonance cholangiopancreatography compared to endoscopic retrograde cholangiopancreatography. Endoscopy 1997;29:182–187.
4 Adamek HE, Weitz M, Breer H, Jakobs R, Schilling D, Riemann JF: Value of magnetic-resonance cholangiopancreatography after unsuccessful endoscopic retrograde cholangiopancreatography. Endoscopy 1997;29:741–744.
5 Soto JA, Barish MA, Yucel EK, Siegenberg D, Ferrucci JT, Chuttani R: Magnetic resonance cholangiography: Comparison with endoscopic retrograde cholangiopancreatography. Gastroenterology 1996;110:589–597.
6 Karlson BM, Ekbom A, Lindgren PG, et al: Abdominal US for diagnosis of pancreatic tumour: Prospective cohort analysis. Radiology 1999;213:107–111.
7 Palazzo L, Roseau G, Gayet B, et al: Endoscopic ultrasonography in the diagnosis and staging of pancreatic adenocarcinoma. Endoscopy 1993;25:143–150.
8 Rösch T, Lorenz R, Braig C, Feuerbach S, Siewert JR, Classen M: Endoscopic ultrasound in the diagnosis of pancreatic tumours. Dtsch Med Wochenschr 1990;115:1339–1347.
9 Rickes S, Unkrodt K, Ocran K, et al: Evaluation of Doppler sonographic criteria for the differentiation of pancreatic tumours. Ultraschall Med 2000;20:253–258.
10 Wermke W, Gassmann B: Tumour Diagnostics of the Liver with Echo Enhancers. Berlin, Springer, 1998.
11 Tanaka S, Kitamra T, Fujita M, Yoshioka F: Value of contrast-enhanced color Doppler sonography in diagnosing hepatocellular carcinoma with special attention to the 'color-filled pattern'. J Clin Ultrasound 1998;26:207–212.
12 Rickes S, Ocran K, Schulze S, Wermke W: Evaluation of Doppler sonographic criteria for the differentiation of hepatocellular carcinomas and regenerative nodules in patients with liver cirrhosis. Ultraschall Med 2002;23:83–90.
13 Rickes S, Schulze S, Neye H, Ocran KW, Wermke W: Improved diagnosing of small hepatocellular carcinomas by echo-enhanced power Doppler sonography in patients with cirrhosis. Eur J Gastroenterol Hepatol 2003;15:893–900.
14 Strobel D, Hoefer A, Martus P, Hahn EG, Becker D: Dynamic contrast-enhanced power Doppler sonography improves the differential diagnosis of liver lesions. Int J Colorectal Dis 2001;16:247–256.
15 Beissert M, Delorme S, Mutze S, et al: Comparison of B-mode and conventional colour/power Doppler ultrasound, contrast-enhanced Doppler ultrasound and spiral CT in the diagnosis of focal lesions of the liver: Results of a multicentre study. Ultraschall Med 2002;23:245–250.
16 Rickes S, Flath B, Unkrodt K, et al: Pancreatic metastases of renal cell carcinomas – evaluation of the contrast behaviour at echo-enhanced power Doppler sonography in comparison to primary pancreatic tumours. Z Gastroenterol 2001;39:571–578.
17 Rickes S, Unkrodt K, Neye H, Ocran KW, Wermke W: Differentiation of pancreatic tumours by conventional ultrasound, unenhanced and echo-enhanced power Doppler sonography. Scand J Gastroenterol 2002;37:1313–1320.
18 Rickes S, Unkrodt K, Ocran K, Neye H, Wermke W: Differentiation of neuroendocrine tumours from other pancreatic lesions by echo-enhanced power Doppler sonography and somatostatin receptor scintigraphy. Pancreas 2003;26:76–81.
19 Ding H, Kudo M, Onda H, Nomura H, Haji S: Sonographic diagnosis of pancreatic islet cell tumor: Value of intermittent harmonic imaging. J Clin Ultrasound 2001;29:411–416.
20 Rickes S, Wermke W: Differentiation of cystic pancreatic neoplasms and pseudocysts by conventional and echo-enhanced ultrasound. J Gastroenterol Hepatol (in press).
21 Loperfido A, Angelini G, Benedetti G, et al: Major early complications from diagnostic and therapeutic ERCP: A prospective multicenter study. Gastrointest Endosc 1998;48:1–10.
22 Bilbao MK, Dotter CT, Lee TG, Katon RM: Complications of endoscopic retrograde cholangiopancreatography. Gastroenterology 1976;70:314–320.
23 Diehl SJ, Lehmann KJ, Sadick M, Lachmann R, Georgi M: Pancreatic cancer: Value of dual-phase helical CT in assessing resectability. Radiology 1998;206:373–378.
24 Legman P, Vignans O, Dousser B, et al: Pancreatic tumours: Comparison of dual-phase helical CT and endoscopic sonography. Am J Radiol 1998;170:1315–1322.
25 Rösch T, Braig C, Gain T, et al: Staging of pancreatic and ampullary carcinoma by endoscopic ultrasound. Gastroenterology 1992;102:188–199.
26 Goldstein HM, Neiman HL, Bookstein JJ: Angiography evaluation of pancreatic disease. A further appraisal. Radiology 1974;112:275–282.
27 Reuter SR, Redman HC, Bookstein JJ: Differential diagnosis of carcinoma of the pancreas. Radiology 1970;96:93–99.
28 Appleton GV, Bathurst NC, Virjee J, Cooper MJ, Williamson RC: The value of angiography in the surgical management of pancreatic disease. Ann R Coll Surg Engl 1989;71:92–96.
29 Koito K, Namieno T, Morita K: Differential diagnosis of small hepatocellular carcinoma and adenomatous hyperplasia with power Doppler sonography. AJR 1998;170:157–161.
30 Calliada F, Campani R, Bottinelli O, Bozzini A, Sommaruga MG: Ultrasound contrast agents. Basic principles. Eur J Radiol 1998;27:157–160.
31 Correas JM, Hélénon O, Pourcelot L, Moreau JF: Ultrasound contrast agents. Examples of blood pool agents. Acta Radiologica 1997;38:101–112.
32 Kim AY, Choi BI, Kim TK, Kim KW, Lee JY, Han JK: Comparison of contrast-enhanced fundamental imaging, second-harmonic imaging, and pulse-inversion harmonic imaging. Invest Radiol 2001;36:582–588.
33 Rösch T, Lightdale CJ, Botet JF, et al: Localisation of pancreatic endocrine tumours by endoscopic ultrasonography. N Engl J Med 1992;326:1721–1726.
34 Hirota T, Tomida T, Iwasa M, Takahashi K, Kaneda M, Tamaki H: Solitary pancreatic metastasis occurring eight years after nephrectomy for renal cell carcinoma: A case report and review of the literature. Int J Pancreatol 1996;19:145–153.
35 Thompson LDR, Heffess CS: Renal cell carcinoma to the pancreas in surgical pathology material. A clinopathological study of 21 cases with a review of the literature. Cancer 2000;89:1076–1088.
36 Rickes S, Unkrodt K, Neye H, Ocran K, Lochs H, Wermke W: Differential diagnosis of frequent pancreatic tumours with echo-enhanced power Doppler sonography – Presentation of case reports. Z Gastroenterol 2002;40:235–240.
37 Ueno E, Takada Y, Yoshida I, Toda J, Sugiura T, Toki F: Pancreatic diseases: Evaluation with MR cholangiopancreatography. Pancreas 1998;16:418–426.
38 Koito K, Namieno T, Ichimura T, et al: Mucin-producing tumour of the pancreas: Comparison of MR cholangiopancreatography with ER cholangiopancreatography. Radiology 1998;208:231–237.

Review Article

Digestive Diseases

Dig Dis 2004;22:39–55
DOI: 10.1159/000078734

CT Scan and MRI in the Differentiation of Liver Tumors

Masatoshi Hori Takamichi Murakami Tonsok Kim Kaname Tomoda Hironobu Nakamura

Department of Radiology, Osaka University Graduate School of Medicine, Suita City, Osaka, Japan

Key Words
Liver neoplasms, CT · Liver neoplasms, MR · Liver neoplasms, diagnosis · Liver, diseases

Abstract
Computed tomography (CT) and magnetic resonance imaging (MRI) are useful for detection and characterization of liver tumors, and widely used in clinical practice. By using dynamic CT and MRI with extracellular contrast material or MRI with liver-specific contrast material, we can investigate the morphological, hemodynamical and functional nature of focal hepatic lesions. Tumors often show characteristic findings on CT and MRI. Thus, we can correctly establish a diagnosis of liver tumors based on those findings. In this article, we describe the role of CT scan and MRI in the differentiation of liver tumors as well as presenting some typical CT and MR images.

Copyright © 2004 S. Karger AG, Basel

Introduction

Both computed tomography (CT) and magnetic resonance imaging (MRI) are useful for detection and characterization of liver tumors, and widely used in clinical practice. Especially, dynamic CT and MRI with extracellular contrast material improve differential diagnosis in the characterization of liver tumors and detection sensitivity of hypervascular tumors such as hepatocellular carcinoma (HCC) [1–5]. To perform a dynamic study, it is necessary to use a CT unit which can make a helical scan, or a MR system with fast imaging technique that can obtain more than 15 slices within a single breathhold. For the detection of liver tumors, there is no significant difference in sensitivity between dynamic CT and dynamic MRI with advanced fast imaging techniques [6, 7]. Generally, CT shows greater temporal and spatial resolution than MRI. However, there are some advantages in using MRI, as follows: (1) it shows better soft tissue contrast than CT; (2) it is possible to image many times sequentially because there is no limitation of X-ray tube heating or exposure dose, and (3) side effects of contrast media for MRI are relatively less. Moreover, tissue-specific contrast medium, such as superparamagnetic iron oxide (SPIO) is available only on MRI. Therefore, both imaging techniques are widely used for diagnosis of liver tumors. In this paper, we would like to present a role of CT scan and MRI in the differentiation of liver tumors.

Techniques

CT with Intravenous Injection of Contrast Medium

Dynamic helical CT with intravenous bolus injection of contrast medium improves differential diagnosis in the characterization of liver tumors and detection sensitivity of hypervascular tumors. Thus, dynamic CT is important

KARGER
Fax + 41 61 306 12 34
E-Mail karger@karger.ch
www.karger.com

© 2004 S. Karger AG, Basel
0257–2753/04/0221–0039$21.00/0

Accessible online at:
www.karger.com/ddi

Masatoshi Hori, MD, PhD
Department of Radiology
Osaka University Graduate School of Medicine
D1, 2-2, Yamadaoka, Suita City, Osaka 565-0871 (Japan)
Tel. +81 6 6879 3434, Fax +81 6 6879 3439, E-Mail mhori@radiol.med.osaka-u.ac.jp

and indispensable technique for diagnosis of liver tumors. For the liver, precontrast, arterial, portal venous, and equilibrium phase CT images are obtained. By combining some of those different phase images, appropriate CT scan protocols should be made depending on the aims of the examinations.

Many radiologists have initiated arterial phase imaging with a scan delay of 20–30 s [3, 5, 8, 9] after initiation of the intravenous contrast bolus injection, using a contrast agent volume of 100–150 ml or 2 ml/kg BW to compensate patient's size, and an injection rate of 3–5 ml/s. However, the optimal timing of the arterial phase is influenced by numerous variables, such as the patient's size and cardiovascular status.

To determine the optimal delay time to start with, a test bolus injection technique or an automatic bolus tracking technique should be employed. With the test injection technique, the scanning time delay is determined using a test bolus (15–20 ml) of contrast medium through a catheter placed in the antecubital vein followed by a series of single-level CT scans at low dose [10]. The time to peak arterial enhancement from initiation of contrast medium is used for determining the delay time of arterial phase scanning. If an automatic bolus tracking technique is available, it is also useful to adjust the timing of arterial phase CT scan [11].

By using multi-detector row helical CT (MDCT) scanner, we can obtain multiple CT data sets with each rotation of the X-ray tube and can scan through large anatomic areas more than 10 times faster compared to single-detector row helical CT scanners. This system enables us to scan through the entire liver in 10 s or less with thinner slice thickness than single-detector row system. Thus, two separate hepatic arterial phase images can be obtained with a MDCT scanner. Those images are referred to as the early arterial phase images and the late arterial phase images, respectively [10]. The early arterial phase imaging should be performed during maximal arterial enhancement. CT hepatic angiographic images can be made using those images [12]. The late arterial phase imaging should be done during a phase of maximal enhancement of hypervascular tumors without significant hepatic parenchymal enhancement. The interval between the onset of the early arterial phase and that of the late arterial phase is about 10–15 s. The late arterial phase images usually show better detection sensitivity for hypervascular liver tumors than the early arterial phase images [10].

Portal venous phase CT images are usually obtained 60–70 s after the initiation of contrast medium injection, and almost 3 min later the equilibrium phase images are obtained [13]. Theoretically, the portal venous phase is considered to be optimal for detecting hypovascular metastatic liver tumors because contrast between the tumor and the liver parenchyma should be greatest in the portal venous phase [14]. In addition, the portal venous phase is usually optimal for additional characterization of liver tumors and demonstration of vascular anatomy and pathology. We believe that portal venous phase imaging should be performed routinely in any CT evaluation for known or suspected primary or metastatic liver tumors [3, 5, 8, 15]. For the detection of hypervascular HCC, the equilibrium phase images have superior sensitivity to the portal venous phase images because some HCC nodules become isoattenuated compared to surrounding liver parenchyma during the portal venous phase [16].

Angiographically Assisted CT

Both CT arterial portography (CTAP) and CT hepatic arteriography (CTHA) are CT techniques with angiographic assistance. Although CTAP and CTHA are more invasive than helical dynamic CT or dynamic MRI with intravenous injection of contrast material, these angiographically assisted CT techniques are reportedly more sensitive for detection of liver tumors [9, 17, 18]. In addition, findings on CTAP or CTHA can sometimes help characterize the hepatic focal lesions [19, 20], because CTAP and CTHA have the ability to show subtly altered vascularity in lesions, which is not satisfactorily shown with CT or MRI with intravenous injection of contrast materials. For both CTAP and CTHA, a catheter is placed in adequate artery with Seldinger's approach through the femoral artery. For CTAP, the tip is placed in the superior mesenteric artery or the splenic artery. The exact protocol of CTAP or CTHA would depend on CT scanner's performance [21].

MRI with Intravenous Injection of Extracellular Contrast Medium

As precontrast imaging, T2-weighted fast spin echo images and T1-weighted gradient echo images with both in-phase and opposed-phase echo are usually obtained. For dynamic MRI with extracellular gadolinium chelate contrast medium, two-dimensional Fourier transformation (2DFT) opposed-phase gradient echo sequence or 3DFT gradient echo sequence with fat saturation technique is usually employed [6, 7], because the MR signal of the liver parenchyma predominantly from lipid decreases in the opposed-phase or fat saturation images and the arterial enhancement of the hepatic tumor is expected to be seen clearly. Precontrast, arterial phase, portal venous phase, and equilibrium phase images are obtained after

intravenous contrast material injection. To determine the scanning delay of arterial phase imaging, a test bolus injection technique or an automatic bolus tracking technique should be employed. Portal venous phase imaging and equilibrium phase imaging are performed 60 and 120–180 s, respectively, after the start of injection of the contrast medium.

MRI with Liver-Specific Contrast Medium

The liver-specific contrast media such as SPIO, which is absorbed into the reticuloendothelial system [22], and hepatobiliary contrast media, which are absorbed into the liver cells and excreted into the bile [23–26], can contrast a tumor with a surrounding part, by being absorbed in the liver parenchyma which has normal liver cell function, but not in the tumor which has no liver cell function. They improve the sensitivity of MRI for the detection of liver tumors by contrast enhancement. In addition, it may be possible to differentiate between benign and malignant tumors by evaluating residual reticuloendothelial or hepatocellular function of the tumor.

T2-weighted fast spin echo and T2*-weighted gradient echo sequences are usually employed for SPIO-enhanced MRI. On SPIO-enhanced MRI, a tumor is visualized as an area with a higher signal than the surrounding liver parenchyma, without decreasing signal reflecting decreased uptake of SPIO due to decreased reticuloendothelial function in the tumor.

On the contrary, hepatobiliary contrast agents, such as Gd-EOB-DTPA, Gd-BOPTA, and Mn-DPDP, enhance normal liver parenchyma on T1-weighted gradient echo images where the contrast medium is absorbed. A tumor without hepatocellular function is usually visualized as an area with low intensity compared with the surrounding liver parenchyma. Because some hepatobiliary contrast agents can be injected bolusly, a dynamic study can be performed with the hepatobiliary contrast media to evaluate the hemodynamics of each lesion and improve detection of the tumor.

Differential Diagnosis of Liver Tumors

Malignant Tumors

Primary Liver Tumor

Hepatocellular Carcinoma and Dysplastic Nodules

Most HCCs develop in cirrhotic livers, especially those associated with hepatitis B or C virus. Typically, HCCs have fibrous capsules and show mosaic-like cleavage plane consisting of nodes, which are different in the degree of differentiation and tissue structure, divided by fibrous septa. In these nodes, there may be metamorphosis (fatty metamorphosis, clear cell formation), necrosis, or hemorrhage. The tumor usually has a little interstitial component. HCC can appear on CT scan or MRI as solitary mass, a dominant mass with daughter lesions, or a diffusely infiltrating neoplasm. It may be multifocal.

Hemodynamically, almost all moderately or poorly differentiated HCCs are hypervascular [20], but for well-differentiated ones, only around one third of tumors show hypervascularity, and many of them appear as hypovascular lesions [20]. Hypervascular HCC appears as an enhanced lesion in comparison with surrounding liver parenchyma on arterial phase images by dynamic CT or MRI with intravenous injection of extracellular contrast medium. But in the equilibrium phase, the contrast medium washes out rapidly and shows relatively low density on dynamic CT (fig. 1) and relatively low signal intensity on dynamic MRI (fig. 2a–d). On CTAP, hypervascular HCC appears as a portal perfusion defect (fig. 3a), and it appears as a hyperdense nodular area sometimes encompassing fibrous capsules or has a mosaic appearance on CTHA (fig. 3b).

On T1-weighted MRI, HCC may be hypo-, iso-, or hyperintense relative to hepatic parenchyma. About 90% of T2-weighted MRI consists of hyperintensity signals (fig. 2e, f), which seem to reflect dilated intratumoral blood sinuses (peliotic change), pseudoductal tissue, or fatty metamorphosis. For well-differentiated tumors, T2-weighted images often show low or equivalent intensity signals.

Fibrous capsule is observed as a low-attenuation area within the surrounding tumor on unenhanced CT, and it is not enhanced on arterial phase images. It is often visualized as a high-attenuation area surrounding the tumor during the portal venous and the equilibrium phases. On T1-weighted MRI, fibrous capsule is visualized as low-signal areas, and it is observed as enhanced areas during the portal venous and the equilibrium phase on dynamic MRI (fig. 2c, d). The fibrous septum is also well visualized as a mosaic image during the delayed phase. Fatty metamorphosis is observed as a low-attenuation area on CT and high-intensity area on T1-weighted MRI.

On SPIO-enhanced MRI, many of moderately or poorly differentiated HCCs are visualized as areas with a higher signal than the surrounding liver parenchyma on T2- or T2*-weighted images (fig. 2g), reflecting decreased uptake of SPIO due to decreased Kupffer cells in the tumor. However, many of well-differentiated HCCs show isoin-

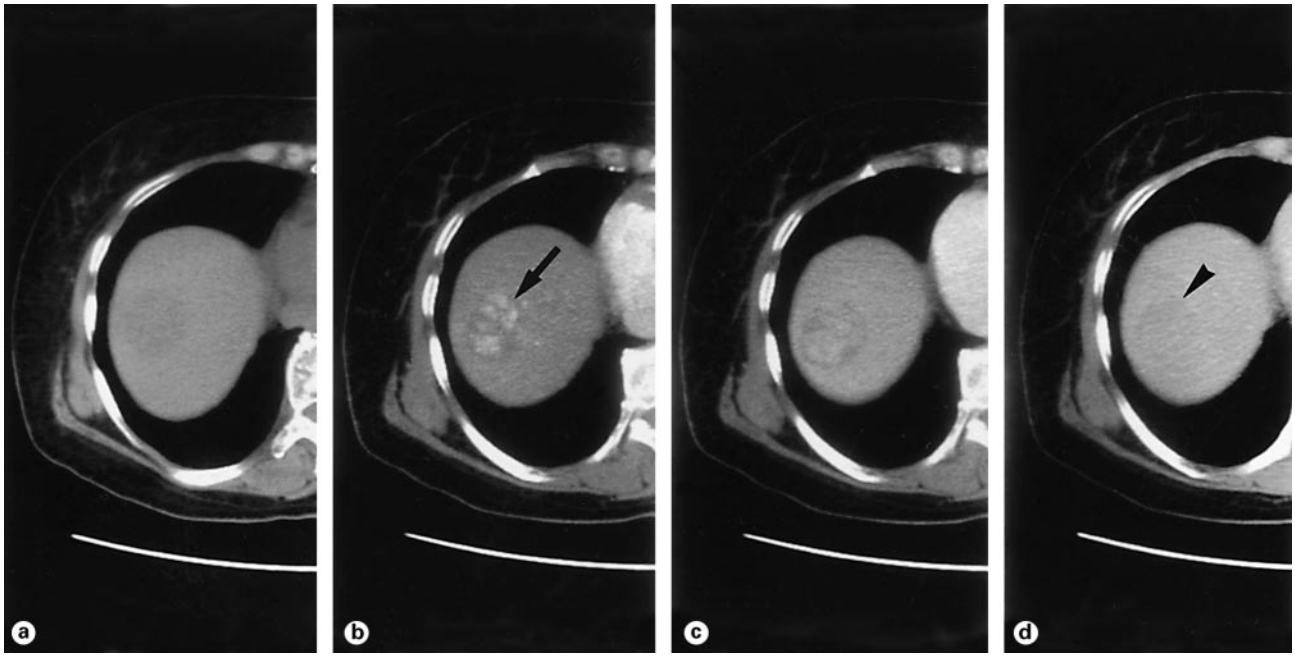

Fig. 1. HCC in a 64-year-old woman. Unenhanced (**a**), arterial phase (**b**), portal venous phase (**c**), and equilibrium phase (**d**) images of dynamic helical CT with intravenous contrast medium injection show a hypervascular tumor. The tumor is enhanced during the arterial phase in comparison with the surrounding hepatic parenchyma (arrow). In the equilibrium phase, the tumor shows washout of contrast material and hypoattenuation compared with the surrounding hepatic parenchyma (arrowhead).

tensity, reflecting preserved Kupffer cell functions in the tumor. Thus, SPIO-enhanced MRI is useful for estimation of histological grading in HCCs [27].

Dysplastic nodule refers to a nodular region of hepatocytes ≥ 1 mm in diameter with dysplasia but without definite histologic features of malignancy. Those nodules are divided into low- and high-grade ones. Dysplastic nodules in cirrhotic liver are thought to be premalignant. It is believed that the risk of developing HCC is higher in patients with those nodules. Dysplastic nodules have variable arterial and portal blood supplies. Most of them show isodense on CTAP and CTHA especially for low-grade ones [20], thus they are also difficult to visualize on dynamic CT or dynamic MRI. Some of the dysplastic nodules show hypodense on CTAP and CTHA [20], but there are some dysplastic nodules that show hypervascularity [20, 28]. On SPIO-enhanced MRI, almost all of the dysplastic nodules show isointensity, reflecting Kupffer cell functions in the nodule [27]. Consequently, distinguishing dysplastic nodules from well-differentiated HCCs is sometimes difficult even with dynamic CT, angiographically assisted CT, dynamic MRI, or MRI with liver-specific contrast medium, because there is considerable overlap in those imaging appearances.

Dysplastic nodules with foci of HCC are sometimes observed and they are clearly malignant lesions. Doubling times of less than 3 months for the HCC focus have been reported [29]. The focus may demonstrate enhancement on CTHA (fig. 3b) or on the arterial phase images of dynamic CT and MRI (fig. 3d), and high intensity on T2-weighted MRI.

Hepatoblastoma

Most patients are under 3 years of age and it is more frequently found in boys than girls. On unenhanced CT, hepatoblastoma shows lower attenuation than the surrounding hepatic tissue. It often shows a segmented structure due to calcification and septal formation, which is relatively characteristic. On MRI, it shows a low signal on T1-weighted images and a high signal on T2-weighted images [30]. Hepatoblastoma is usually hypervascular.

Cholangiocarcinoma

Histologically, cholangiocarcinoma is usually an adenocarcinoma, with various degrees of mucin production. It often contains a stromal fibrous component, and if located in the liver margin, it forms a cancer navel similar to that seen in metastatic hepatic cancer. It does not form

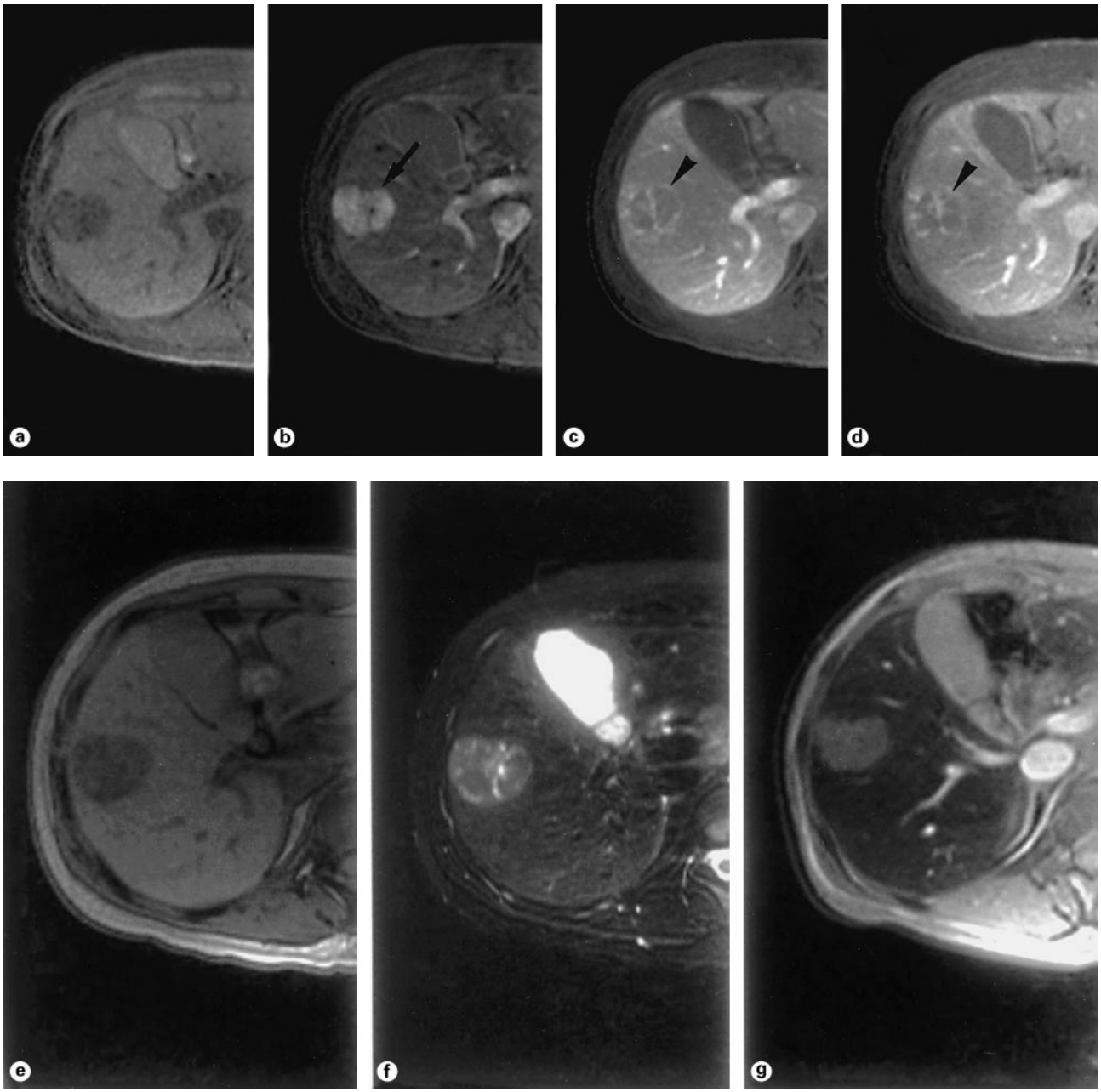

Fig. 2. HCC in a 36-year-old woman. Unenhanced (**a**), arterial phase (**b**), portal venous phase (**c**), and equilibrium phase (**d**) images of dynamic MRI (3D gradient echo, 4.7/1/20) with intravenous Gd contrast medium injection show a hypervascular tumor. The tumor is enhanced during the arterial phase in comparison with the surrounding hepatic parenchyma (arrow). On the portal venous and the equilibrium phase images, the tumor shows washout of contrast material and hypointensity compared with the surrounding hepatic parenchyma. Fibrous capsule is observed as a hyperintensity area surrounding the tumor during the portal venous and the equilibrium phase images (arrowheads). The tumor shows hypointensity on T1-weighted MRI (2D gradient echo, 190/2.3/90) (**e**) and hyperintensity on T2-weighted MRI (FSE, 8000/89) (**f**). On SPIO-enhanced T2*-weighted MRI (gradient echo, 150/9.7/60) (**g**), the tumor is visualized as area with a higher signal than the surrounding liver parenchyma due to decreased uptake of SPIO in the tumor.

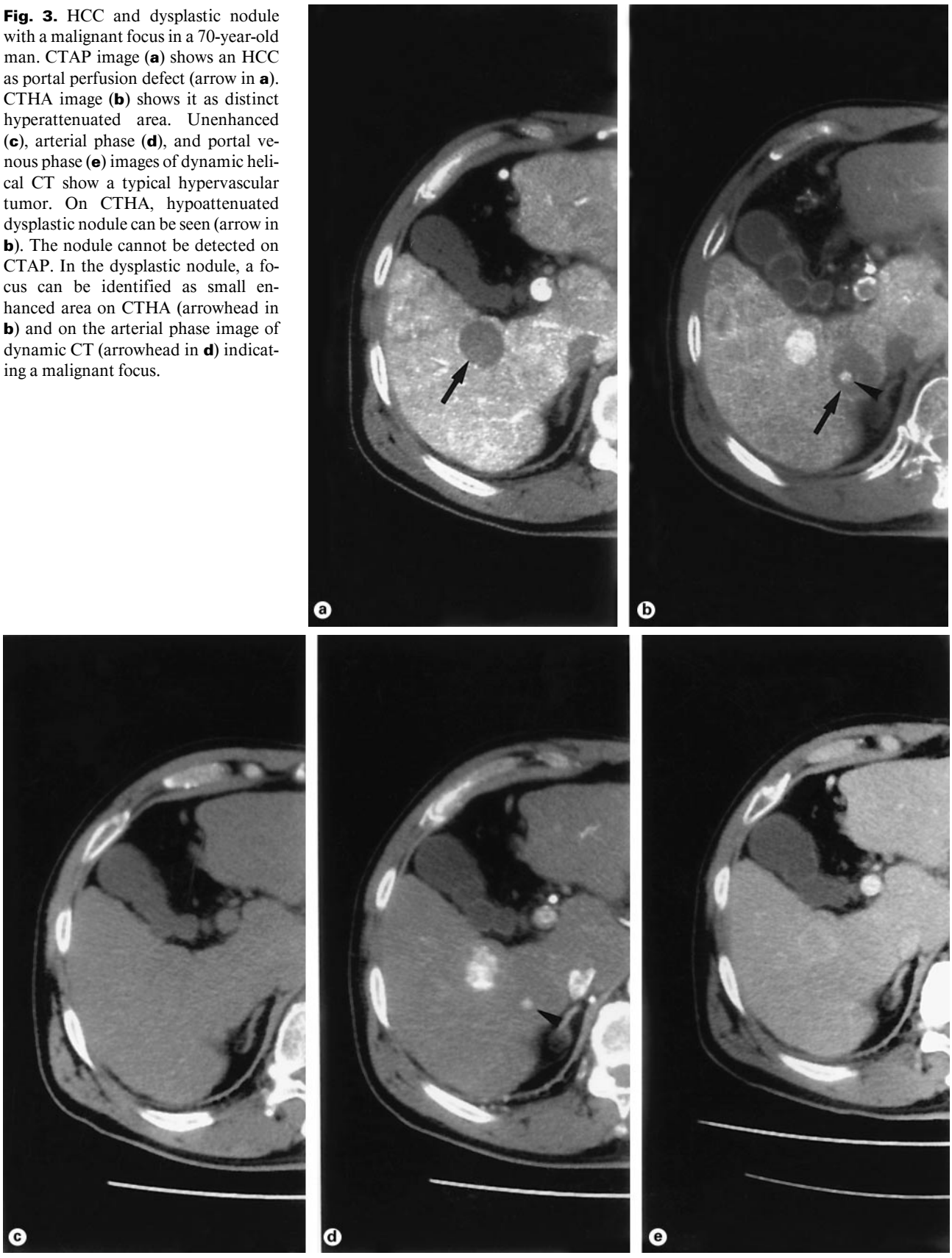

Fig. 3. HCC and dysplastic nodule with a malignant focus in a 70-year-old man. CTAP image (**a**) shows an HCC as portal perfusion defect (arrow in **a**). CTHA image (**b**) shows it as distinct hyperattenuated area. Unenhanced (**c**), arterial phase (**d**), and portal venous phase (**e**) images of dynamic helical CT show a typical hypervascular tumor. On CTHA, hypoattenuated dysplastic nodule can be seen (arrow in **b**). The nodule cannot be detected on CTAP. In the dysplastic nodule, a focus can be identified as small enhanced area on CTHA (arrowhead in **b**) and on the arterial phase image of dynamic CT (arrowhead in **d**) indicating a malignant focus.

a fibrous capsule or septum as regularly as HCC. Infiltration into Glisson's capsule and lymph node metastasis are relatively characteristic of cholangiocarcinoma and more frequently found than in HCC.

On unenhanced CT, cholangiocarcinoma is visualized in the low attenuation. The tumor border becomes obscure and irregular as the tumor grows. On dynamic CT, it is hardly enhanced at all during the arterial phase, but the fibrous stroma in the center is enhanced relatively to the surrounding tissue during the delayed phase [31]. Atrophy of the liver parenchyma can be seen in the peripheral region due to tumor infiltration into the bile ducts and the portal vein. Dilatation of the peripheral bile duct is important as a secondary finding and can be observed clearly on CT (fig. 4a–c).

On MRI, cholangiocarcinoma often shows a low signal on T1-weighted images and a high signal on T2-weighted images. In the latter, high signal areas correspond to mucin production, necrosis, and fibrosis. Dilated intrahepatic bile ducts are visualized as high-signal luminal structures on T2-weighted images (fig. 4d–h).

In graphical observation, the tumor-forming type is similar to metastatic hepatic cancer originating in the gastrointestinal tract, and requires further examination of the primary focus and diagnosis by exclusion of the other parts of the gastrointestinal tract.

Combined or Mixed Hepatocellular and Cholangiocarcinoma

These are combinations of hepatocellular and cholangiocarcinoma mixed in various ratios, and often show the graphical characteristics of the two types.

Biliary Cystadenocarcinoma and Biliary Cystadenoma

These often occur in middle-aged women. In most cases, they are monostotic and multilocular with the lumen surrounded by glandular cells. Papillary growth of epithelium to the lumen is also observed. Rarely, they can be monolocular and multiple. On CT, calcification may be found in the stroma. On MRI, they show a low signal on T1-weighted image and a high signal on T2-weighted image. Although it is not easy to differentiate biliary cystadenoma from biliary cystadenocarcinoma, cystadenocarcinoma is more likely to show papillary projection, mural nodule, and coarse calcification [32] (fig. 5).

Other Primary Malignant Tumors

There are some other primary malignant liver tumors. Those include hepatic angiosarcoma, fibrolamellar carcinoma, epithelioid hemangioendothelioma, undifferentiated (embryonal) sarcoma, and lymphoma.

Metastatic Liver Tumor

In most cases, these arise by hematogenous metastasis from a gastrointestinal adenocarcinoma. Most tumor cells are located within the tumor margin and are often divided by fibrous tissue with metamorphosis and necrosis inside. On unenhanced CT, it often shows low attenuation, but sometimes isoattenuation. Calcification is relatively characteristic to metastatic liver tumor from colon cancer (fig. 6a). Most metastases are hypovascular and appear hypoattenuating relative to liver parenchyma on portal venous phase CT images (fig. 6). On arterial phase images, the tumor margin may be enhanced in the form of a ring (fig. 7a–c). On MRI, it is usually visualized as low intensity on T1-weighted images and high intensity on T2-weighted images (fig. 7d, e), and the central metamorphic necrosis is visualized as higher intensity. Dynamic MRI shows similar imaging patterns to dynamic CT (fig. 7f–h).

For hypervascular metastatic tumors, lesions are often more easily identified on arterial phase CT or MRI. Such tumors include renal cell carcinoma, thyroid carcinoma, adrenal tumors, breast carcinoma, neuroendocrine tumors (pancreatic islet and gastrointestinal), melanoma, and sarcomas.

(For fig. 4 see next page.)

Fig. 4. Cholangiocarcinoma in a 54-year-old man. Unenhanced (**a**), arterial phase (**b**), and portal venous phase (**c**) images of dynamic helical CT with intravenous contrast medium injection show a hypovascular tumor. On unenhanced CT, the low-attenuation tumor is seen in the left lobe (arrow). The tumor shows an irregular contour. On dynamic CT, it is hardly enhanced at all during the arterial phase. Intrahepatic bile duct of the left lobe shows dilatation due to tumor infiltration into the bile ducts (arrowhead in **c**). The tumor shows a low signal on T1-weighted MRI (2D gradient echo, 4.8/1.1/90) (**d**) and a high signal on T2-weighted MRI (SSFSE, TE = 96) (**e**). Dilated intrahepatic bile ducts are visualized as high-signal luminal structures on T2-weighted image (arrowhead in **e**). Unenhanced (**f**), arterial phase (**g**), and portal venous phase (**h**) images of dynamic MRI (3D gradient echo, 4.8/1.1/30) with intravenous Gd contrast medium injection show similar imaging patterns to dynamic CT. However, the tissue contrast resolution of MRI is superior to those of CT.

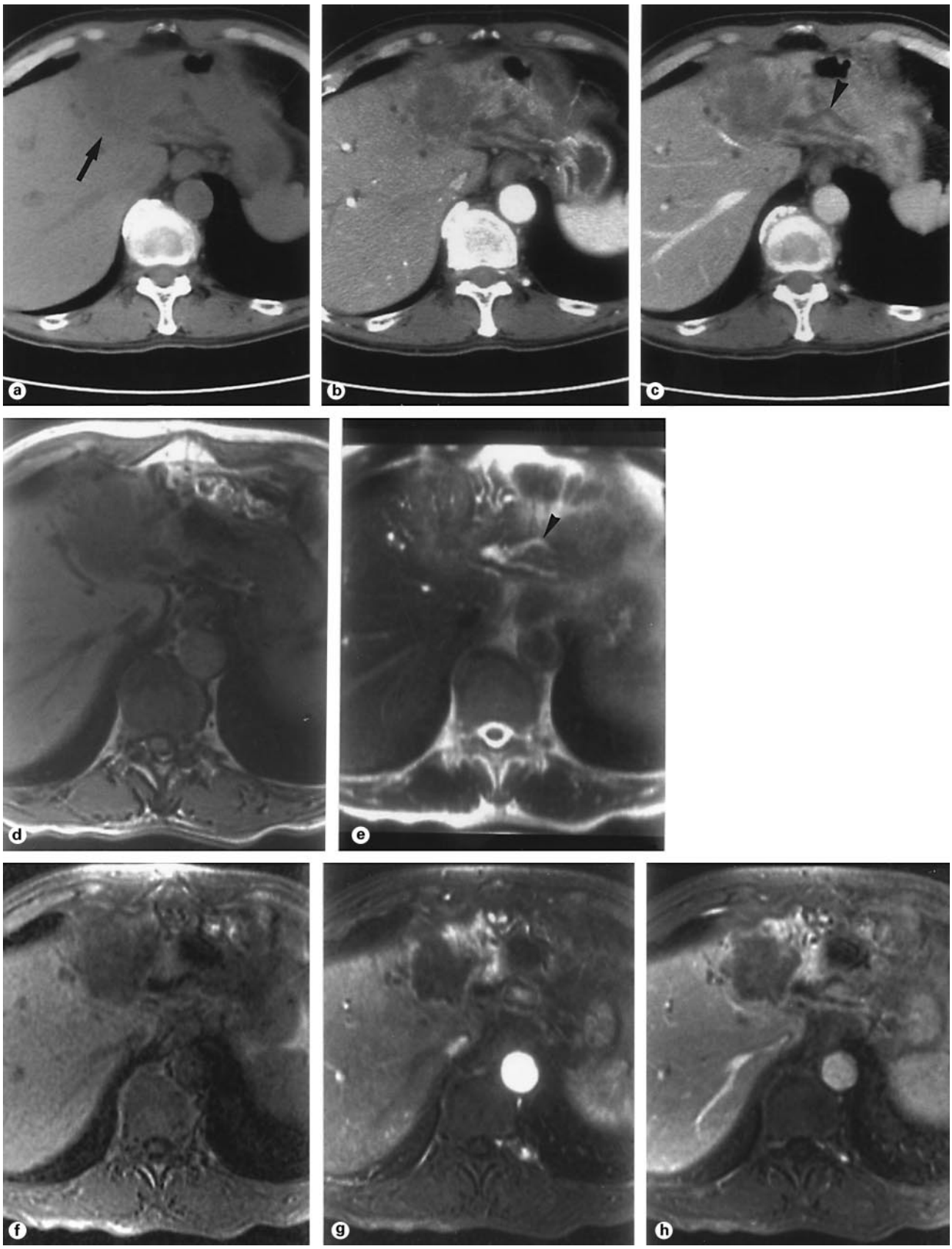

4

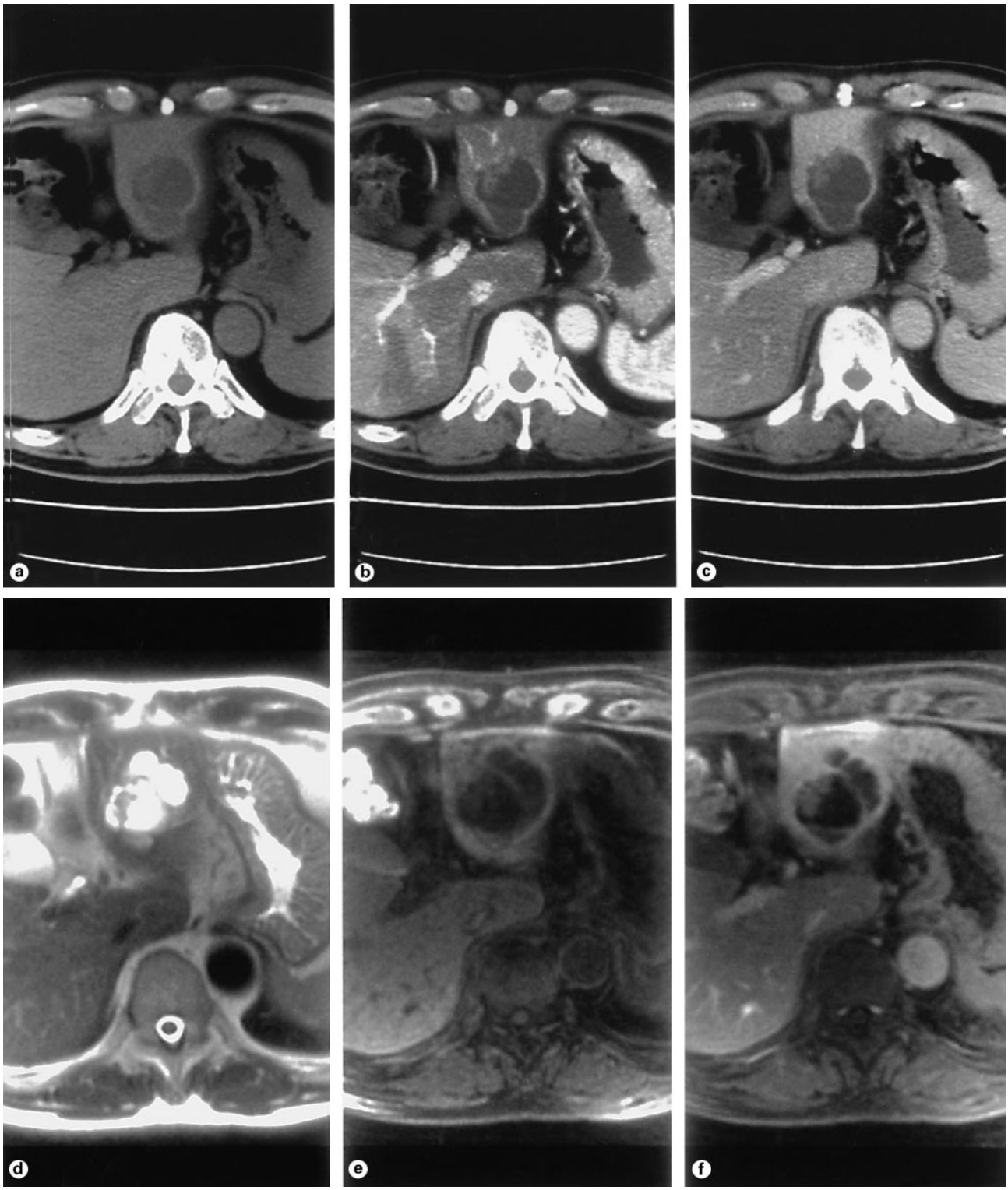

Fig. 5. Biliary cystadenocarcinoma in a 64-year-old man. Unenhanced (**a**), arterial phase (**b**), and portal venous phase (**c**) images of dynamic helical CT show a multilocular cystic mass with enhanced papillary projection in the left lobe of the liver. The tumor shows a high signal on T2-weighted MRI (HASTE, TE = 64) (**d**) and a low signal on T1-weighted image (gradient echo, 4.4/1.8/20) (**e**). Septa and papillary projection are enhanced on contrast-enhanced T1-weighted image (**f**).

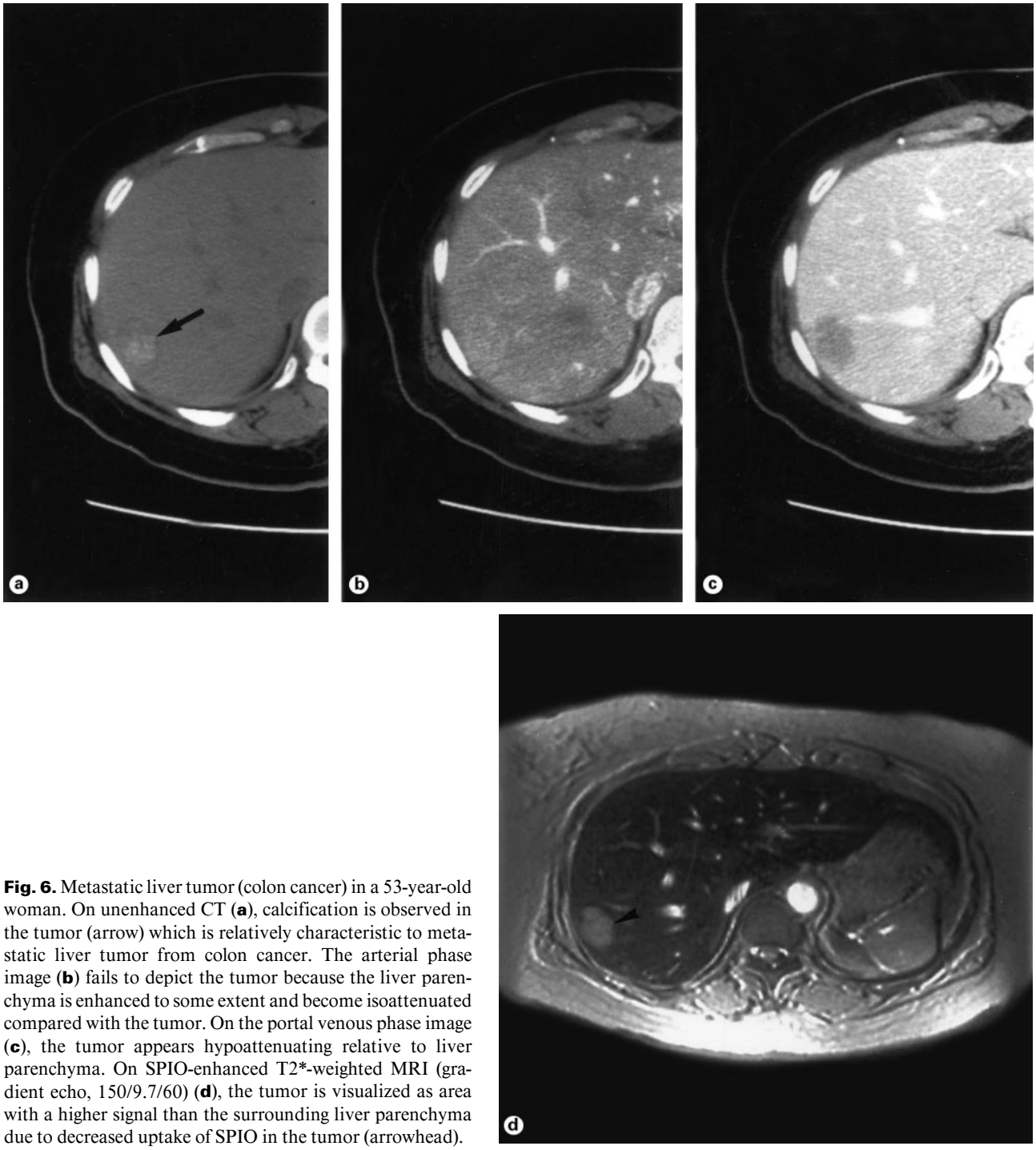

Fig. 6. Metastatic liver tumor (colon cancer) in a 53-year-old woman. On unenhanced CT (**a**), calcification is observed in the tumor (arrow) which is relatively characteristic to metastatic liver tumor from colon cancer. The arterial phase image (**b**) fails to depict the tumor because the liver parenchyma is enhanced to some extent and become isoattenuated compared with the tumor. On the portal venous phase image (**c**), the tumor appears hypoattenuating relative to liver parenchyma. On SPIO-enhanced T2*-weighted MRI (gradient echo, 150/9.7/60) (**d**), the tumor is visualized as area with a higher signal than the surrounding liver parenchyma due to decreased uptake of SPIO in the tumor (arrowhead).

Fig. 7. Metastatic liver tumor (rectal cancer) in a 53-year-old woman. On unenhanced CT (**a**), the tumor shows low attenuation (arrow). On the arterial phase CT (**b**), the tumor margin is enhanced in the form of a ring (arrowhead). On the portal venous phase CT (**c**), the tumor appears hypoattenuating relative to liver parenchyma. The tumor is visualized as low intensity on T1-weighted MRI (2D gradient echo, 150/1.8/90) (**d**) and high intensity on T2-weighted MRI (FSE, 5000/76) (**e**). Unenhanced (**f**), arterial phase (**g**), and portal venous phase (**h**) images of dynamic MRI (3D gradient echo, 4.8/1.1/30) show similar peripheral ring-like enhancement pattern to dynamic CT.

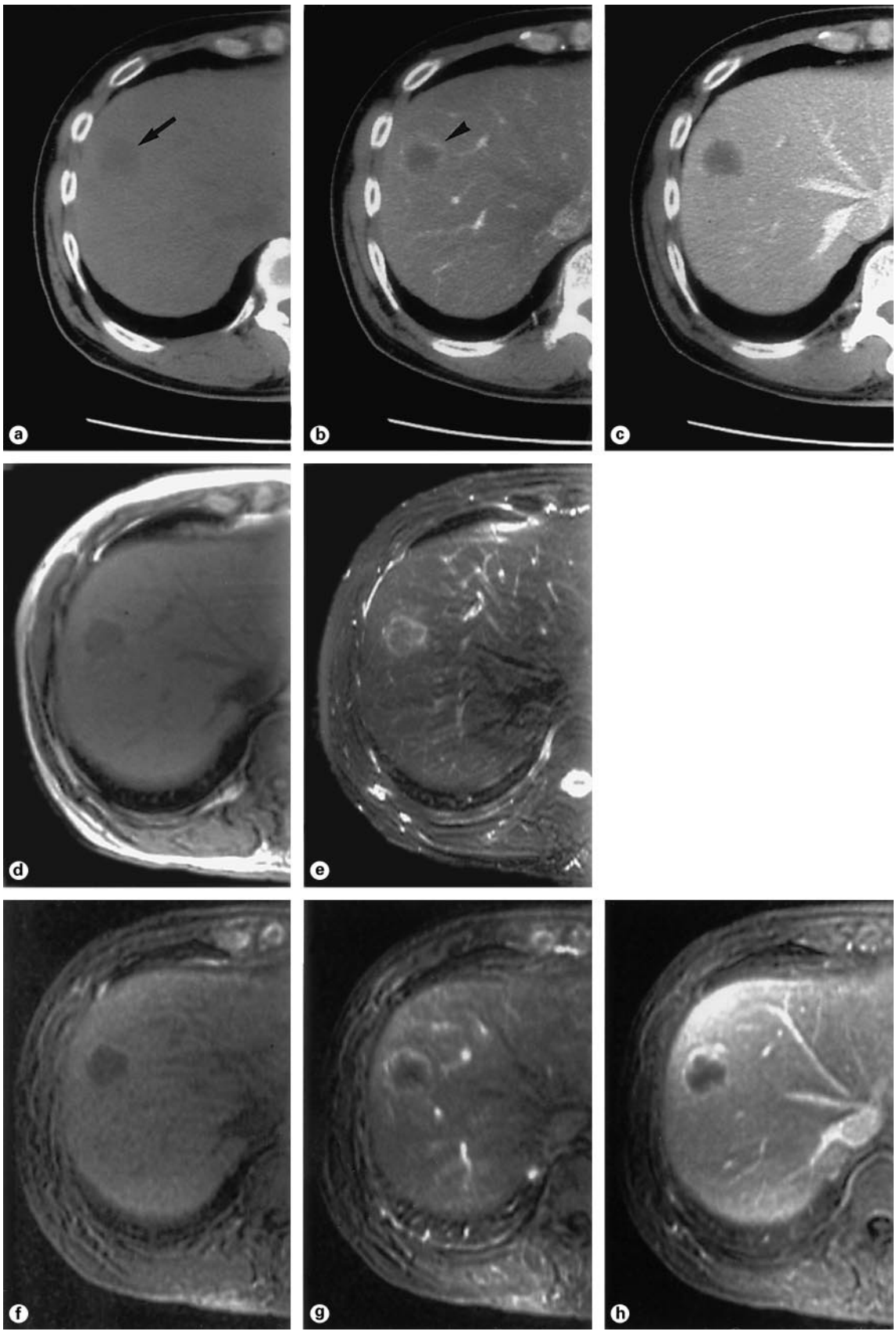

7

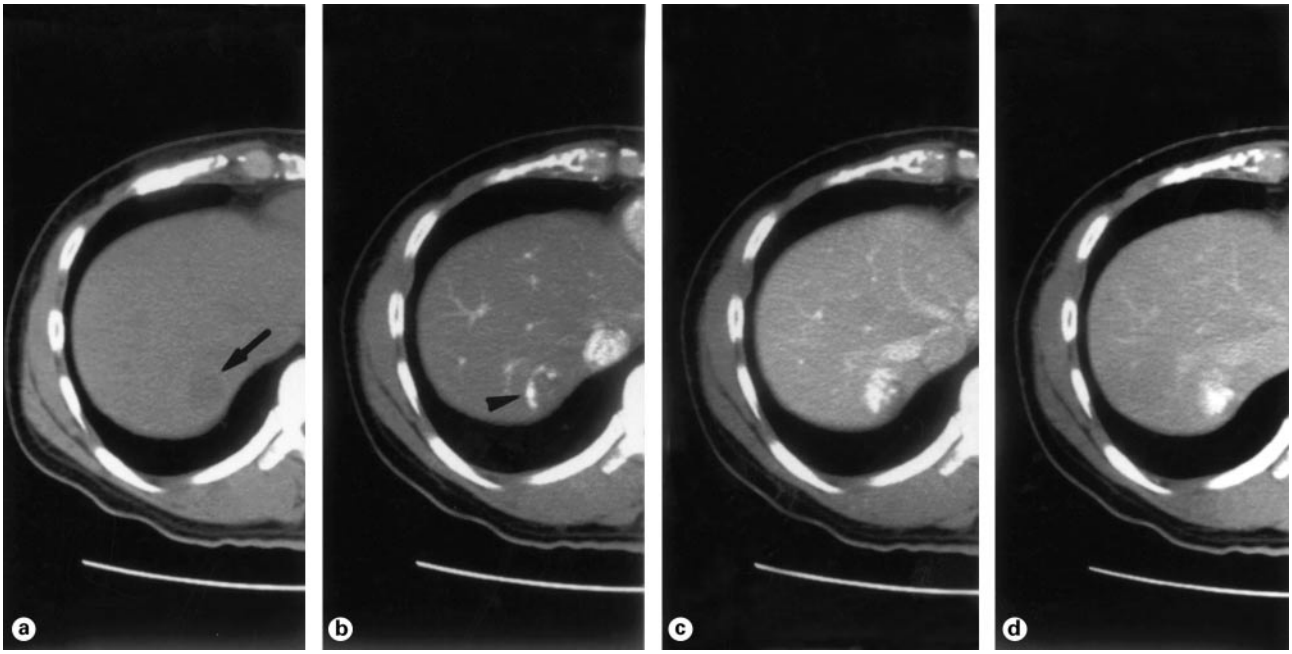

Fig. 8. Cavernous hemangioma in a 33-year-old man. On unenhanced CT (**a**), the tumor is visualized as an area of low attenuation showing equivalent absorption to the blood (arrow). On dynamic CT, the tumor margin is densely enhanced (arrowhead) in the arterial phase (**b**) (peripheral globular enhancement) and the enhancement expands toward the inside with time on the portal venous (**c**) and equilibrium phases (**d**) (filling-in phenomenon).

Metastatic liver tumors usually do not take up liver-specific contrast material. On SPIO-enhanced MRI, metastatic tumors are usually visualized as areas with a higher signal than the surrounding liver parenchyma on T2- or T2*-weighted images (fig. 6d).

Benign Tumors

Cavernous Hemangioma

This is one of the most commonly encountered benign hepatic tumors. It consists of vessels dilated to various degrees with fibrous connective tissue around each vascular lumen. Large tumors may show secondary changes such as metamorphosis, necrosis, hemorrhage, intravascular thrombogenesis, and calcification. On unenhanced CT, it is usually visualized as an area of low attenuation showing equivalent absorption to the blood. The form is irregular and can be circular. Large tumors often show an irregular low attenuation range inside, due to metamorphosis and necrosis. On dynamic CT, the tumor margin is densely enhanced in the arterial phase (peripheral globular enhancement) and the enhancement expands toward the inside with time on the portal venous and the equilibrium phases (filling-in phenomenon) (fig. 8). On the delayed phase images, the tumor is visualized with iso- or high attenuation relatively to the surrounding hepatic tissue due to pooling of the contrast medium. Metamorphosis, necrosis, and thrombosis are not enhanced.

On MRI, it is usually visualized as low intensity on T1-weighted images and strong high intensity on T2-weighted images (fig. 9a, b). Signal intensity becomes various as the secondary changes occur. Dynamic MRI shows similar imaging patterns to dynamic CT (fig. 9b–e).

A small cavernous hemangioma, with a diameter of ≤ 1 cm, is often enhanced densely and homogeneously in the arterial phase of dynamic CT or dynamic MRI, showing images like those of HCC, but if the dense enhancement lasts to the later phase, and low intensity and strong high intensity are observed on T1- and T2-weighted MRI respectively, it suggests hemangioma. Hemangioma with well-developed metamorphosis or fibrosis fails to show typical images.

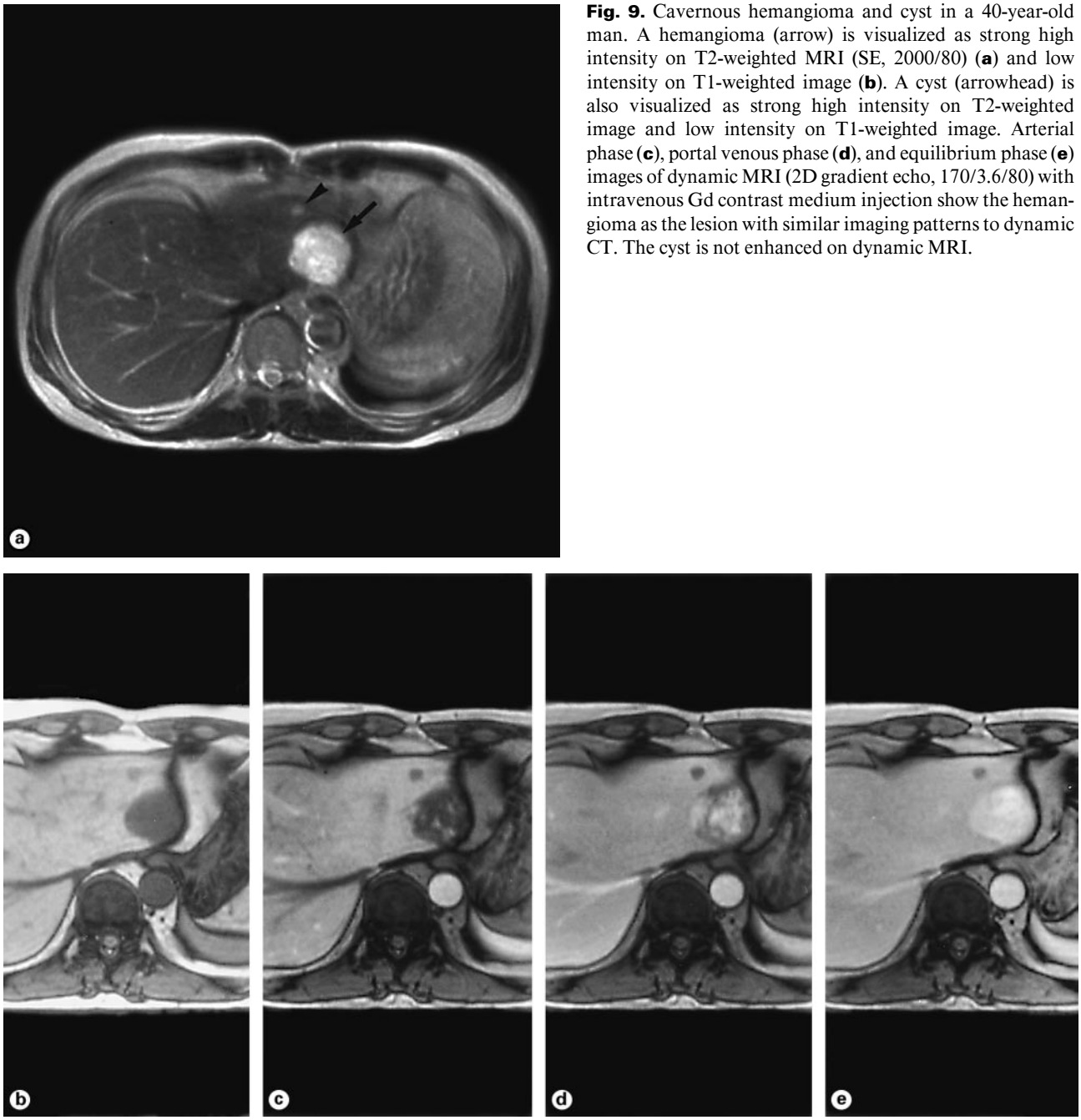

Fig. 9. Cavernous hemangioma and cyst in a 40-year-old man. A hemangioma (arrow) is visualized as strong high intensity on T2-weighted MRI (SE, 2000/80) (**a**) and low intensity on T1-weighted image (**b**). A cyst (arrowhead) is also visualized as strong high intensity on T2-weighted image and low intensity on T1-weighted image. Arterial phase (**c**), portal venous phase (**d**), and equilibrium phase (**e**) images of dynamic MRI (2D gradient echo, 170/3.6/80) with intravenous Gd contrast medium injection show the hemangioma as the lesion with similar imaging patterns to dynamic CT. The cyst is not enhanced on dynamic MRI.

Hepatic Adenoma

This occurs in a non-cirrhotic liver, particularly in the right lobe. The border with the surrounding hepatic tissue is obvious, and though it has no capsule, the surrounding liver parenchyma may become a pseudocapsule. Intratumoral hemorrhage is often found.

On unenhanced CT, it is usually visualized as low attenuation. Small tumors are homogeneous, but they become heterogeneous inside due to hemorrhage and necrosis as they grow. The tumor is densely enhanced on the arterial phase images but it changes to iso- or low attenuation on the later phase images [33]. On MRI, the

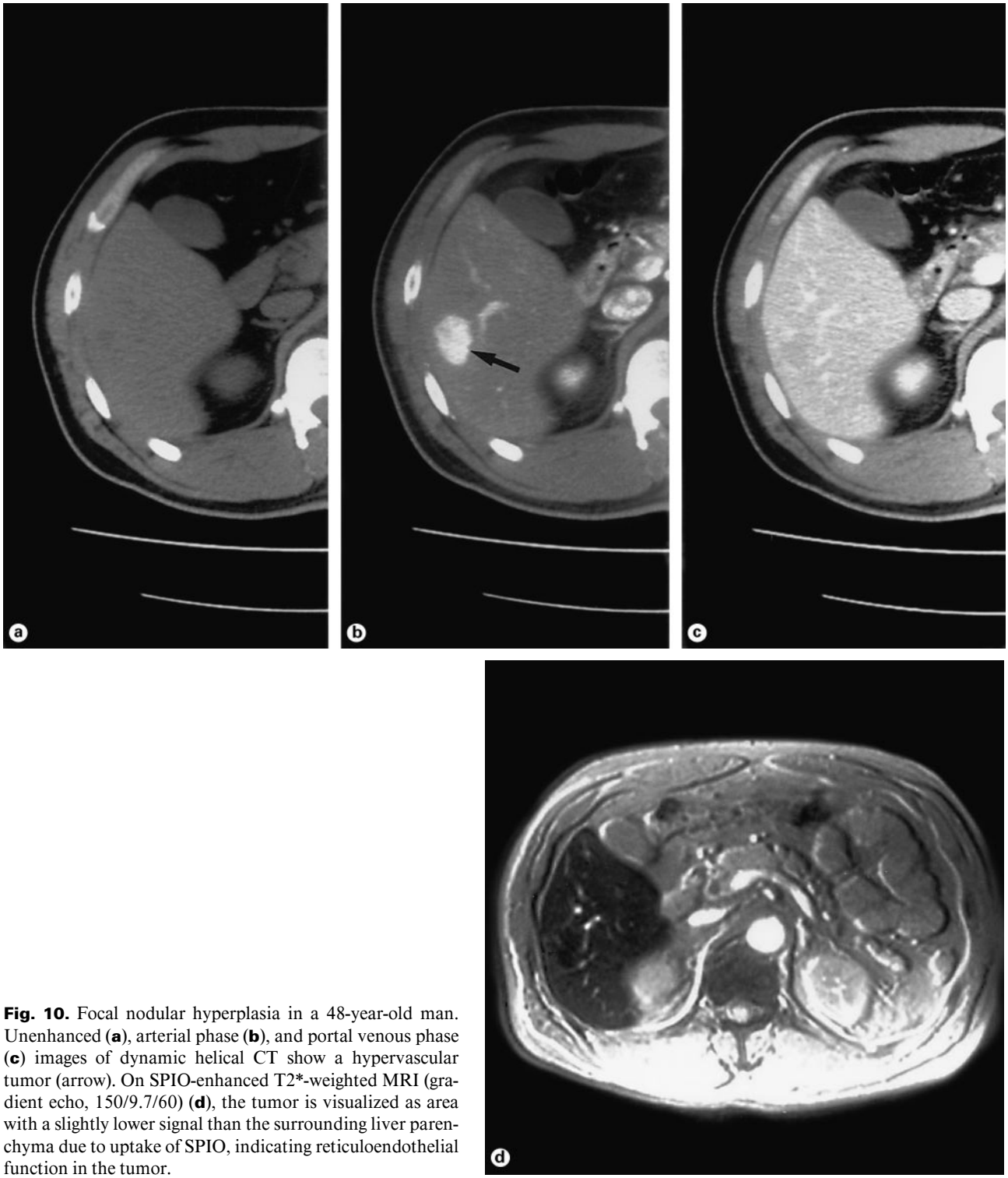

Fig. 10. Focal nodular hyperplasia in a 48-year-old man. Unenhanced (**a**), arterial phase (**b**), and portal venous phase (**c**) images of dynamic helical CT show a hypervascular tumor (arrow). On SPIO-enhanced T2*-weighted MRI (gradient echo, 150/9.7/60) (**d**), the tumor is visualized as area with a slightly lower signal than the surrounding liver parenchyma due to uptake of SPIO, indicating reticuloendothelial function in the tumor.

internal signal is often heterogeneous, with high intensity on T1-weighted images reflecting fat and hemorrhage. The uptake of liver-specific contrast material, such as SPIO and hepatobiliary contrast media, in adenomas may be seen [26, 34].

Focal Nodular Hyperplasia

It is often observed in the non-cirrhotic liver of women in their 20–40s. Usually it has an obvious border but without capsule formation. The tumor consists of hepatic cells, sinusoids and some Kupffer cells. Typically, it has a central scar consisting of fibrous connective tissue in the center and this extends to the surrounding area in a spoke-wheel pattern. The connective tissue has arteries and bile ducts, but no portal vein. Usually, it does not show metamorphosis, necrosis, or hemorrhage.

On unenhanced CT, it is visualized as iso- or low attenuation and the scar appears as low attenuation. It is densely enhanced on the arterial phase CT (fig. 10a–c) and the central scar can be observed with arteries. On MRI, it is often visualized as low or isointensity on T1-weighted images and high intensity on T2-weighted images. The central scar shows low intensity on T1-weighted images and high intensity on T2-weighted images [35]. The uptake of liver-specific contrast material, such as SPIO and hepatobiliary contrast media, may be seen [26, 34, 36] (fig. 10d).

Fatty Tumors of the Liver

Benign fatty tumors of the liver include lipoma, angiomyolipoma, myelolipoma, and angiomyelolipoma. The imaging diagnosis of fatty tumors is based on the identification of fat within the mass. Fatty components are visualized as high echo on US, low attenuation on CT, and high intensity on T1- and T2-weighted MRI. The appearance on CT and MRI depends on the amount of fat present. Angiomyolipoma is usually hypervascular and is sometimes difficult to differentiate from HCC accompanied by fatty metamorphosis.

Mesenchymal Hamartoma

This is a rare disease observed usually in infants under 2 years of age. It may be found in adults. It mainly consists of loose connective tissue and includes bile ducts and hepatic cells. On CT, it is visualized as a cystic tumor with septal structure, but if it has a lot of stromal components it may be seen as a solid tumor containing cysts.

Biliary Hamartoma (Bile Duct Hamartoma, von Meyenburg Complex)

This is a hamartomatous node with a diameter of ≤ 1 cm within fibrous connective tissue in which large and small bile duct-like cystic vessels proliferate. It may be diffused over the whole liver. It is asymptomatic and often detected incidentally. On CT and MRI, it shows images of cysts, but they may not be visualized if the node is small.

Non-Tumorous Lesions

Simple Cysts

On CT, they are not enhanced and shown as low attenuation with a CT value close to that of water. On MRI, they are visualized as low intensity on T1-weighted images and high intensity on T2-weighted images (fig. 9a, b). They show no enhancement after intravenous contrast material administration (fig. 9b–e).

Ciliated Hepatic Foregut Cyst

This is a ciliated cyst formed by residual epithelium of the foregut. It has a fibrous capsule with an internal surface covered with ciliated epithelium and is histologically the same as a bronchial cyst. The fluid content contains fatty components and various proteins as well as some calcium components. It may show higher internal CT value than a simple cyst and is visualized as higher attenuation than the liver. On MRI, though it may be difficult to differentiate from solid lesions, it is visualized as high intensity on T2-weighted images and proved to be a cystic lesion [37].

Inflammatory Pseudotumor

This is a localized inflammatory lesion accompanied with infiltration of plasmacytes and lymphocytes, fibroblasts, and hyperplasia of collagenous fiber. It is often visualized as low attenuation on CT and is heterogeneously enhanced on contrast-enhanced CT. The tumor border is irregular in most cases.

Focal Fatty Change

This puts no pressure on the surrounding area, and large lesions have normal vasculature inside. On unenhanced CT, they are often observed with slightly low attenuation and may show similar findings to multiple metastatic foci. The uptake of liver-specific contrast material is usually seen.

Abscesses

Hepatic abscesses include bacterial liver abscess (pyogenic abscess), amebic liver abscess, and hepatic candidiasis. Bacterial liver abscess and amebic liver abscess show similar radiological images each other, and it is often difficult to differentiate one from the other. It can either be solitary or multiple, and mono- or multilocular in various forms, such as circle, false circle, and other irregular forms. It shows relatively rapid metamorphosis with time. On unenhanced CT, an abscess cavity is visualized by heterogeneous low attenuation. In the liver parenchyma around the abscess cavity, there may be a certain range of low attenuation with an obscure border reflecting inflammation and edema. On contrast-enhanced CT, an abscess cavity is not enhanced. Inflammation of the liver parenchyma around the abscess is relatively well enhanced. On MRI, an abscess cavity is visualized as low intensity on T1-weighted images and high intensity on T2-weighted images. The liver parenchyma around the abscess often shows high intensity on T2-weighted images corresponding to edematous changes. On contrast-enhanced MRI, the wall of the abscess is strongly enhanced, and inflammation and edema of the surrounding liver show enhancement than the most of the liver parenchyma [38].

Hepatic candidiasis is usually found in patients with immune depression. It often appears as multiple lesions, sometimes with diffuse microabscesses. On CT, it is often observed in multiple low-attenuation ranges and can be visualized clearly on contrast-enhanced CT. On MRI, it is visualized as high-intensity area on T2-weighted images.

Parasitic Diseases

Parasitic diseases, such as *Echinococcosis (E. granulosus* and *E. multilocularis)* and *Schistosomiasis japonica*, can also show focal hepatic lesions [39, 40].

Conclusion

CT and MRI can reveal the morphological, hemodynamical and functional nature of focal hepatic lesions. Because tumors often show characteristic findings on CT and MRI, we can correctly establish a diagnosis of liver tumors. They are useful diagnostic techniques in the differentiation of liver tumors.

References

1 Murakami T, Mitani T, Nakamura H, Hori S, Marukawa T, Nakanishi K, Nishikawa M, Kuroda C, Kozuka T: Differentiation between hepatoma and hemangioma with inversion-recovery snapshot FLASH MRI and Gd-DTPA. J Comput Assist Tomogr 1992;16:198–205.

2 Ito K, Choji T, Nakada T, Nakanishi T, Kurokawa F, Okita K: Multislice dynamic MRI of hepatic tumors. J Comput Assist Tomogr 1993; 17:390–396.

3 Kihara Y, Tamura S, Yuki Y, Kakitsubata S, Sugimura H, Kakitsubata Y, Watanabe K: Optimal timing for delineation of hepatocellular carcinoma in dynamic CT. J Comput Assist Tomogr 1993;17:719–722.

4 Nakamura H, Murakami T, Ishida T, Tsuda K, Hashimoto T, Nakanishi K, Mitani T, Tomoda K, Hori S, Kozuka T: 3DFT-FISP MRI with gadopentetate dimeglumine in differential diagnosis of small liver tumors. J Comput Assist Tomogr 1994;18:49–54.

5 Murakami T, Kim T, Oi H, Nakamura H, Igarashi H, Matsushita M, Okamura J, Kozuka T: Detectability of hypervascular hepatocellular carcinoma by arterial phase images of MR and spiral CT. Acta Radiol 1995;36:372–376.

6 Noguchi Y, Murakami T, Kim T, Hori M, Osuga K, Kawata S, Okada A, Sugiura T, Tomoda K, Narumi Y, Nakamura H: Detection of hypervascular hepatocellular carcinoma by dynamic magnetic resonance imaging with double-echo chemical shift in-phase and opposed-phase gradient echo technique: Comparison with dynamic helical computed tomography imaging with double arterial phase. J Comput Assist Tomogr 2002;26:981–987.

7 Noguchi Y, Murakami T, Kim T, Hori M, Osuga K, Kawata S, Kumano S, Okada A, Sugiura T, Nakamura H: Detection of hepatocellular carcinoma: Comparison of dynamic MR imaging with dynamic double arterial phase helical CT. AJR Am J Roentgenol 2003;180:455–460.

8 Ohashi I, Hanafusa K, Yoshida T: Small hepatocellular carcinomas: Two-phase dynamic incremental CT in detection and evaluation. Radiology 1993;161:851–855.

9 Hori M, Murakami T, Oi H, Kim T, Takahashi S, Matsushita M, Tomoda K, Narumi Y, Kadowaki K, Nakamura H: Sensitivity in detection of hypervascular hepatocellular carcinoma by helical CT with intra-arterial injection of contrast medium, and by helical CT and MR imaging with intravenous injection of contrast medium. Acta Radiol 1998;39:144–151.

10 Murakami T, Kim T, Takamura M, Hori M, Takahashi S, Federle MP, Tsuda K, Osuga K, Kawata S, Nakamura H, Kudo M: Hypervascular hepatocellular carcinoma: Detection with double arterial phase multi-detector row helical CT. Radiology 2001;218:763–767.

11 Kim T, Murakami T, Hori M, Takamura M, Takahashi S, Okada A, Kawata S, Cruz M, Federle MP, Nakamura H: Small hypervascular hepatocellular carcinoma revealed by double arterial phase CT performed with single breath-hold scanning and automatic bolus tracking. AJR Am J Roentgenol 2002;178:899–904.

12 Takahashi S, Murakami T, Takamura M, Kim T, Hori M, Narumi Y, Nakamura H, Kudo M: Multi-detector row helical CT angiography of hepatic vessels: Depiction with dual-arterial phase acquisition during single breath hold. Radiology 2002;222:81–88.

13 Mitsuzaki K, Yamashita Y, Ogata I, Nishiharu T, Urata J, Takahashi M: Multiple-phase helical CT of the liver for detecting small hepatomas in patients with liver cirrhosis: Contrast-injection protocol and optimal timing. AJR Am J Roentgenol 1996;167:753–757.

14 Baron RL: Understanding and optimizing use of contrast material for CT of the liver. AJR Am J Roentgenol 1994;163:323–331.

15 Baron RL, Oliver JH 3rd, Dodd GD 3rd, Nalesnik M, Holbert BL, Carr B: Hepatocellular carcinoma: Evaluation with biphasic, contrast-enhanced, helical CT. Radiology 1996;199: 505–511.
16 Kim T, Murakami T, Takahashi S, Tsuda K, Tomoda K, Narumi Y, Oi H, Sakon M, Nakamura H: Optimal phases of dynamic CT for detecting hepatocellular carcinoma: Evaluation of unenhanced and triple-phase images. Abdom Imaging 1999;24:473–480.
17 Soyer P, Levesque M, Elias D, Zeitoun G, Roche A: Preoperative assessment of resectability of hepatic metastases from colonic carcinoma: CT portography vs. sonography and dynamic CT. AJR Am J Roentgenol 1992;159: 741–744.
18 Kanematsu M, Oliver JH 3rd, Carr B, Baron RL: Hepatocellular carcinoma: The role of helical biphasic contrast-enhanced CT versus CT during arterial portography. Radiology 1997; 205:75–80.
19 Ueda K, Matsui O, Kawamori Y, Kadoya M, Yoshikawa J, Gabata T, Nonomura A, Takashima T: Differentiation of hypervascular hepatic pseudolesions from hepatocellular carcinoma: Value of single-level dynamic CT during hepatic arteriography. J Comput Assist Tomogr 1998;22:703–708.
20 Hayashi M, Matsui O, Ueda K, Kawamori Y, Kadoya M, Yoshikawa J, Gabata T, Takashima T, Nonomura A, Nakanuma Y: Correlation between the blood supply and grade of malignancy of hepatocellular nodules associated with liver cirrhosis: Evaluation by CT during intraarterial injection of contrast medium. AJR Am J Roentgenol 1999;172:969–976.
21 Hori M, Murakami T, Kim T, Nakamura H: Diagnosis of hepatic neoplasms using CT arterial portography and CT hepatic arteriography. Tech Vasc Interv Radiol 2002;5:164–169.
22 Stark DD, Weissleder R, Elizondo G, Hahn PF, Saini S, Todd LE, Wittenberg J, Ferrucci JT: Superparamagnetic iron oxide: Clinical application as a contrast agent for MR imaging of the liver. Radiology 1988;168:297–301.
23 Hamm B, Staks T, Muhler A, Bollow M, Taupitz M, Frenzel T, Wolf KJ, Weinmann HJ, Lange L: Phase I clinical evaluation of Gd-EOB-DTPA as a hepatobiliary MR contrast agent: Safety, pharmacokinetics, and MR imaging. Radiology 1995;195:785–792.
24 Caudana R, Morana G, Pirovano GP, Nicoli N, Portuese A, Spinazzi A, Di Rito R, Pistolesi GF: Focal malignant hepatic lesions: MR imaging enhanced with gadolinium benzyloxypropionictetra-acetate – Preliminary results of phase II clinical application. Radiology 1996; 198:513–520.
25 Lim KO, Stark DD, Leese PT, Pfefferbaum A, Rocklage SM, Quay SC: Hepatobiliary MR imaging: First human experience with MnDPDP. Radiology 1991;178:79–82.
26 King LJ, Burkill GJ, Scurr ED, Vlavianos P, Murray-Lyons I, Healy JC: MnDPDP enhanced magnetic resonance imaging of focal liver lesions. Clin Radiol 2002;57:1047–1057.
27 Imai Y, Murakami T, Yoshida S, Nishikawa M, Ohsawa M, Tokunaga K, Murata M, Shibata K, Zushi S, Kurokawa M, Yonezawa T, Kawata S, Takamura M, Nagano H, Sakon M, Monden M, Wakasa K, Nakamura H: Superparamagnetic iron oxide-enhanced magnetic resonance images of hepatocellular carcinoma: Correlation with histological grading. Hepatology 2000;32:205–212.
28 Lim JH, Cho JM, Kim EY, Park CK: Dysplastic nodules in liver cirrhosis: Evaluation of hemodynamics with CT during arterial portography and CT hepatic arteriography. Radiology 2000;214:869–874.
29 Sadek AG, Mitchell DG, Siegelman ES, Outwater EK, Matteucci T, Hann HW: Early hepatocellular carcinoma that develops within macroregenerative nodules: Growth rate depicted at serial MR imaging. Radiology 1995;195: 753–756.
30 Dachman AH, Pakter RL, Ros PR, Fishman EK, Goodman ZD, Lichtenstein JE: Hepatoblastoma: Radiologic-pathologic correlation in 50 cases. Radiology 1987;164:15–19.
31 Lacomis JM, Baron RL, Oliver JH 3rd, Nalesnik MA, Federle MP: Cholangiocarcinoma: Delayed CT contrast enhancement patterns. Radiology 1997;203:98–104.
32 Murphy BJ, Casillas J, Ros PR, Morillo G, Albores-Saavedra J, Rolfes DB: The CT appearance of cystic masses of the liver. Radiographics 1989;9:307–322.
33 Arrive L, Flejou JF, Vilgrain V, Belghiti J, Najmark D, Zins M, Menu Y, Tubiana JM, Nahum H: Hepatic adenoma: MR findings in 51 pathologically proved lesions. Radiology 1994; 193:507–512.
34 Vogl TL, Hammerstingl R, Schwarz W, Mack MG, Muller PK, Pegios W, Keck H, Eibl-Eibesfeldt A, Hoelzl J, Woessmer B, Bergman C, Felix R: Superparamagnetic iron oxide-enhanced versus gadolinium-enhanced MR imaging for differential diagnosis of focal liver lesions. Radiology 1996;198:881–887.
35 Lee MJ, Saini S, Hamm B, Taupitz M, Hahn PF, Seneterre E, Ferrucci JT: Focal nodular hyperplasia of the liver: MR findings in 35 proved cases. AJR Am J Roentgenol 1991;156: 317–320.
36 Kacl GM, Hagspiel KD, Marincek B: Focal nodular hyperplasia of the liver: Serial MRI with Gd-DOTA, superparamagnetic iron oxide, and Gd-EOB-DTPA. Abdom Imaging 1997;22:264–267.
37 Kadoya M, Matsui O, Nakanuma Y, Yoshikawa J, Arai K, Takashima T, Amano M, Kimura M: Ciliated hepatic foregut cyst: Radiologic features. Radiology 1990;175:475–477.
38 Mendez RJ, Schiebler ML, Outwater EK, Kressel HY: Hepatic abscesses: MR imaging findings. Radiology 1994;190:431–436.
39 De Diego Choliz J, Lecumberri Olaverri FJ, Franquet Casas T, Ostiz Zubieta S: Computed tomography in hepatic echinococcosis. AJR Am J Roentgenol 1982;139:699–702.
40 Araki T, Hayakawa K, Okada J, Hayashi S, Uchiyama G, Yamada K: Hepatic *Schistosomiasis japonica* identified by CT. Radiology 1985;157:757–760.

Review Article

Digestive Diseases

Dig Dis 2004;22:56–62
DOI: 10.1159/000078735

Imaging of Inflammatory Bowel Disease: CT and MR

Michael Zalis Ajay K. Singh

Department of Abdominal Imaging and Interventional Radiology, Massachusetts General Hospital, Boston, Mass., USA

Key Words
Inflammatory bowel disease · CT · MRI · Cross-sectional imaging

Abstract
Cross-sectional imaging has come to play a central role in the imaging of the abdomen. Concurrent to this, the role of CT and MRI in the imaging of inflammatory bowel disease has also increased in importance. These modalities offer numerous advantages over more traditonal methods of radiologic diagnosis, and provide essential information not only for initial diagnosis, but for management, follow-up and detection of potential complications. On the horizon are several derivative techniques involving CT and MRI, potentially in combination with PET imaging; these may further improve the specificity and sensitivity of imaging modalities for diagnosis of inflammatory bowel disease.

Copyright © 2004 S. Karger AG, Basel

Introduction

Diagnostic imaging plays a major role in the diagnosis of primary disease, recurrence and detection of complications related to inflammatory bowel disease. Imaging defines the extent of disease, presence or absence of associated bowel obstruction and presence of active mucosal disease. The extent of the bowel disease has important management implications, including the need for surgical intervention. Cross-sectional imaging can detect pathological findings outside the bowel loops, such as fistulas and abscesses, which are not generally visualized by endoscopy. The diagnostic modalities available to the clinicians includes barium studies, CT, MR, ultrasound, FDG-PET and ^{99m}Tc-WBC scintigraphy. In this article, we will review uses of CT and MRI for evaluation of inflammatory bowel disease.

Crohn's disease and ulcerative colitis have been traditionally imaged using barium studies, however with the increased use of CT and MR imaging for abdominal pain, these conditions are more and more commonly seen on axial imaging of the abdomen (fig. 1). Though barium studies permit the diagnosis of active mucosal disease, they are able to reliably image only the intraluminal aspect of the bowel loops. Moreover, superimposition of

KARGER

Fax + 41 61 306 12 34
E-Mail karger@karger.ch
www.karger.com

© 2004 S. Karger AG, Basel
0257–2753/04/0221–0056$21.00/0

Accessible online at:
www.karger.com/ddi

M. Zalis, MD
Department of Abdominal Imaging and Interventional Radiology
Massachusetts General Hospital
Fruit Street, Boston, MA 02114 (USA)
Fax +1 617 726 4891, E-Mail mzalis@partners.org

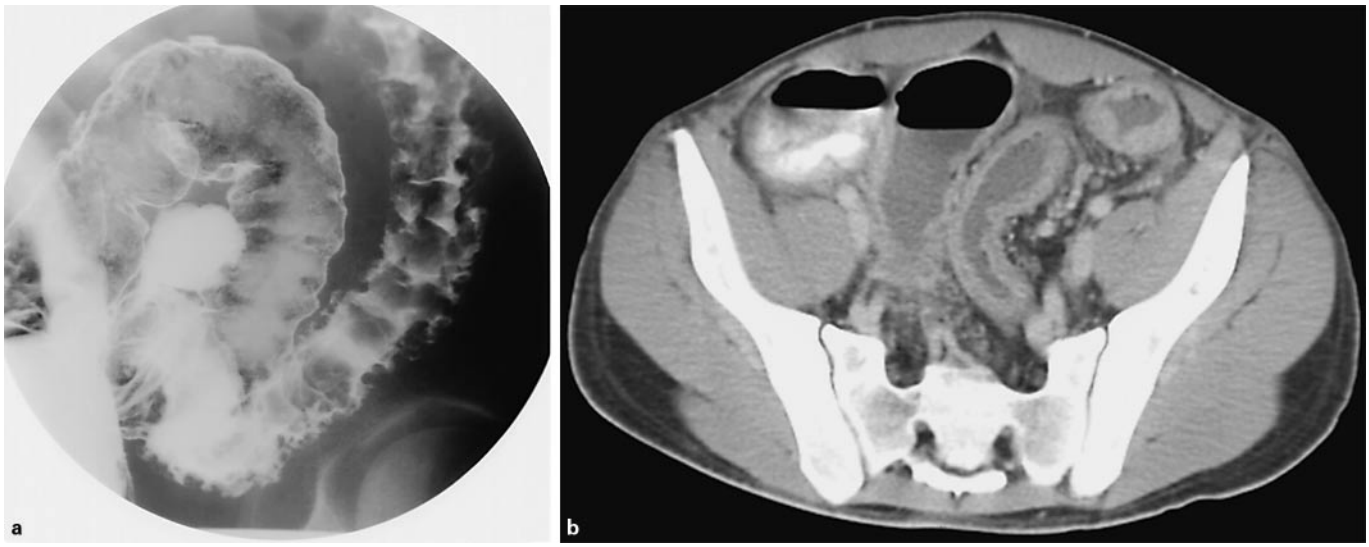

Fig. 1. A 23-year-old male with ulcerative colitis. **a** Barium enema shows multiple collar button ulcers (arrowheads) in the distal sigmoid colon. **b** Contrast-enhanced CT shows sigmoid colonic wall thickening and prominent vessels (arrowheads) in the sigmoid mesocolon.

bowel loops may make the diagnosis of Crohn's disease difficult.

The CT imaging of inflammatory bowel disease has the advantage of detection of extraluminal disease, such as abscesses, phlegmon, small amounts of free air, and associated pathologies such as liver and renal disease (fig. 2). In addition, the patients prefer multidetector CT to barium studies because of the long duration of barium studies and poor tolerance to oral barium [1].

CT Imaging

The CT findings of Crohn's disease includes intense mucosal enhancement, bowel wall thickening, stranding of mesenteric fat, large pericolic/perienteric vasculature and mural stratification (fig. 3, 4) [2–9]. The presence of multilayered wall stratification or two-layer stratification with strong mucosal enhancement and low-density prominence of submucosa have been associated with the presence of active inflammatory activity in 91 and 100% cases of Crohn's disease, respectively [10]. The presence of submucosal fat deposition and bowel wall thickening without enhancement or mural stratification typically is due to inactive disease. The thickening of small bowel wall is most commonly observed in the terminal ileum and ileocecal valve. This has been associated with 90% cases of Crohn's disease.

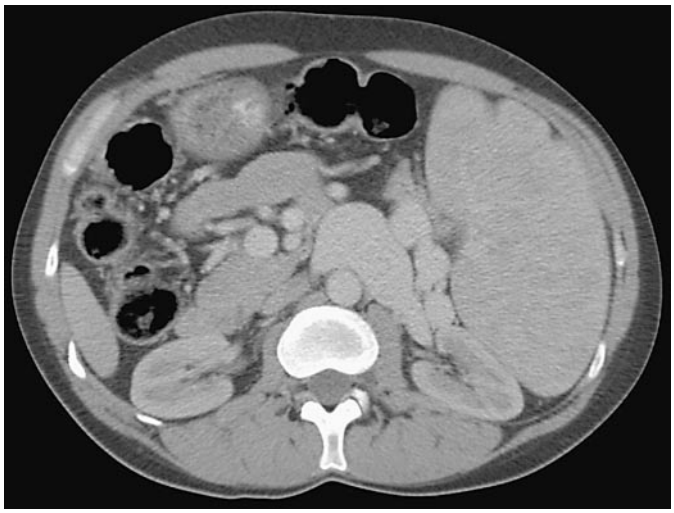

Fig. 2. Sclerosing cholangitis and portal hypertension in a 35-year-old patient with ulcerative colitis. Non-contrast axial image in the midabdomen demonstrates marked splenomegaly and a large splenorenal shunt (curved arrow). There are multiple collaterals seen near the splenic hilum.

Tortuosity and dilatation of vasa recta in the small bowel mesentery is a feature of active Crohn's disease and has been described as the comb sign on CT [9]. The presence of prominent vasculature around the small bowel or large bowel is seen in 81% of patients with active Crohn's

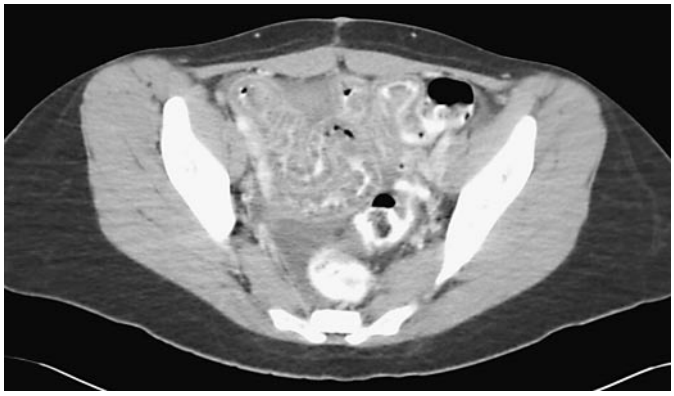

Fig. 3. Crohn's disease in a 17-year-old male. The contrast-enhanced axial CT reveals diffuse ileal wall edema and mural stratification. Free fluid is also seen in the pelvis.

Fig. 5. Crohn's colitis and stricture in a 25-year-old female. There is a concentric stricture of the sigmoid colonic wall (arrow) seen on the contrast-enhanced CT. This was biopsied and demonstrated to be benign in histology.

Fig. 4. Crohn's colitis in a 41-year-old male. Contrast-enhanced CT shows descending colon and sigmoid colon wall thickening with bowel wall stratification.

Fig. 6. Crohn's colitis involving descending colon, with localized perforation, necessitating a lateral abdominal wall. The contrast-enhanced axial CT images demonstrate thickening of the descending colonic wall. There is leakage of bowel contrast and air (arrow) from the bowel lumen into the left paracolic gutter and extension of inflammatory process into adjacent abdominal wall musculature. Incidental note is made of horseshoe kidney.

disease. In contrast, none of the patients with inactive disease had this CT finding [11].

Though stratification with deposition of fat within the submucosal layer of bowel wall is considered a relatively reliable marker for inflammatory bowel disease, this finding can be seen in obese patients in the absence of bowel wall inflammation [12]. Fibrofatty proliferation in the small bowel mesentery is also called creeping fat, and is visible on CT as loss of sharp interface between bowel and mesentery.

Overall, CT is superior to barium examinations in the detection of enterocutaneous and enterovesical fistulas. Barium examination is considered superior to CT in the detection of enteroenteric and enterocolic fistulas [13]. CT is also able to identify clinically unsuspected cases of inflammatory bowel disease by documenting the presence

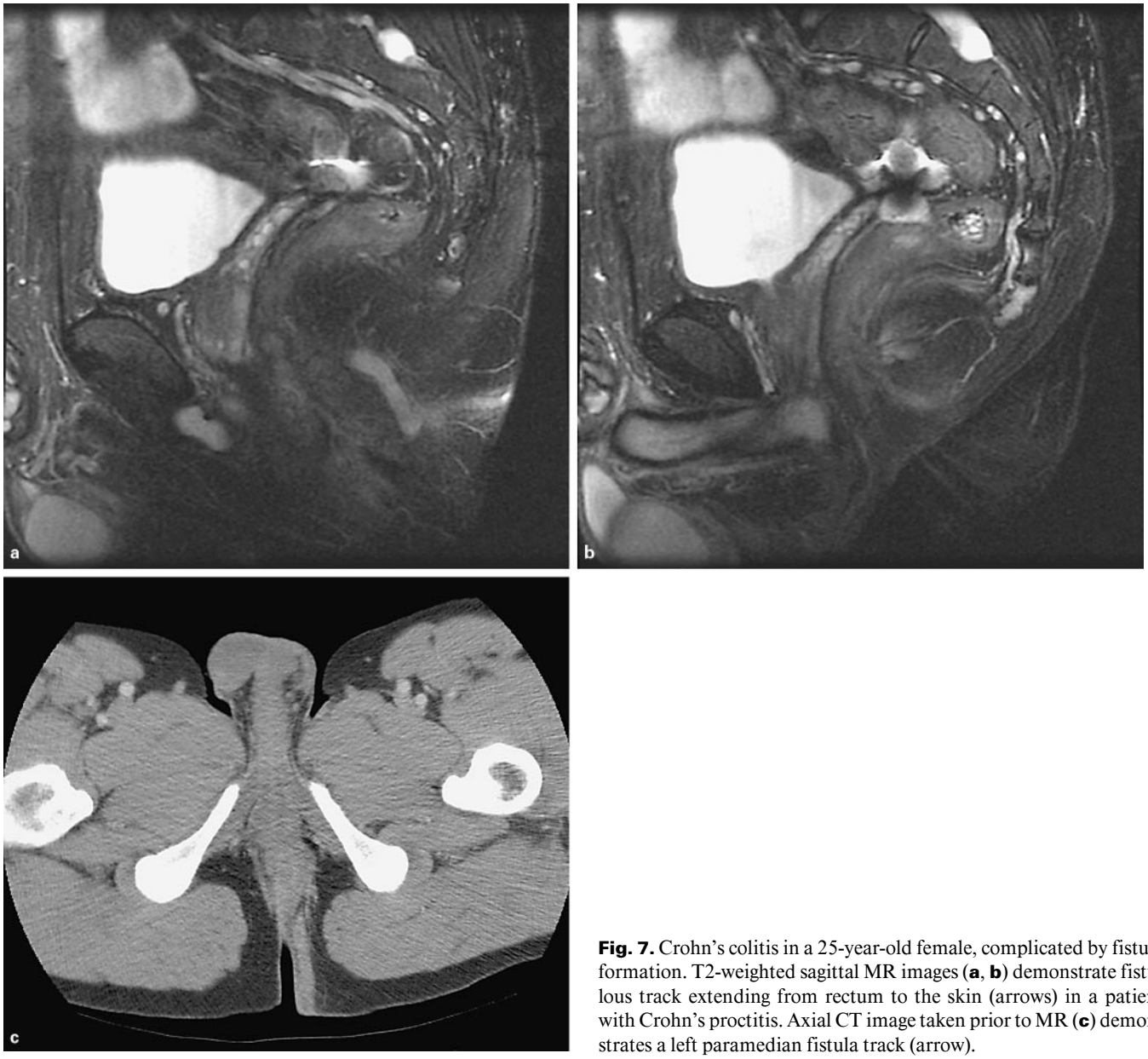

Fig. 7. Crohn's colitis in a 25-year-old female, complicated by fistula formation. T2-weighted sagittal MR images (**a**, **b**) demonstrate fistulous track extending from rectum to the skin (arrows) in a patient with Crohn's proctitis. Axial CT image taken prior to MR (**c**) demonstrates a left paramedian fistula track (arrow).

of bowel wall thickening, fat distribution abnormality around the bowel loops, and ascites [14].

CT imaging of early mucosal involvement in ulcerative colitis does not show any abnormality but more advanced disease is manifested as mural thickening, luminal narrowing, mucosal thickening, mural stratification and widening of presacral space. In contrast to Crohn's disease, there is contiguous involvement of the colon in ulcerative colitis.

The complications of inflammatory bowel disease include fistulas, sinuses, abscesses, phlegmons, strictures, bowel wall perforation and neoplastic transformation (fig. 5, 6). Cross-sectional imaging modalities such as CT and ultrasound can reliably detect the presence of intra-abdominal abscess with the accuracy ranging from 87 to 92% [15]. The accuracy is slightly higher for CT than ultrasound because of higher false-positive results with ultrasound studies. A phlegmon is seen as an ill-defined inflammatory mass in the abdomen which when inadequately treated, may liquefy into an abscess.

Fig. 8. Colonic pseudopolyp in a 22-year-old female with Crohn's disease. **a**, **b** Contrast-enhanced axial and coronal images from CT colonography demonstrate polypoid lesion (arrows) arising from descending colonic wall, consistent with pseudopolyp.

It is not unusual to see small lymph nodes in the small bowel mesentery, in a patient with inflammatory bowel disease. However, the presence of large lymph nodes should raise the suspicion of lymphoma and adenocarcinoma.

MR Imaging

Though MRI of the abdomen has the advantage of no radiation to the patient, multiplanar imaging capability, excellent soft tissue contrast and minimal contrast adverse effects, its role in the imaging of inflammatory bowel disease has been limited because of higher cost, motion artifact from peristalsis/respiration, high signal intensity of intra-abdominal fat and relatively longer imaging times compared to CT. Like CT, MR has the advantage of detection of extraintestinal manifestations of inflammatory bowel disease such as fistulae or abscesses (fig. 7).

More recently, advancements in MRI have included shorter imaging sequences and the introduction of MR enteroclysis and MR virtual colonoscopy, using endoluminal coils for high resolution. The optimized MRI technique requires a combined method of enteroclysis and MRI for optimal evaluation of the small bowel. The motion artifacts are minimized by using a combination of breath hold, pharmacologic paralysis and short imaging sequences such as gradient recalled echo and turbo spin echo sequences. In patients with Crohn's disease, gadolinium-enhanced fat-suppressed spoiled gradient recalled echo MRI better depicts the extent and severity of intestinal disease, when compared with single-shot fast spin echo imaging [16].

MR enteroclysis has been shown to detect most relevant findings in patients with inflammatory bowel disease with an accuracy superior to that of enteroclysis [17]. MR allows detection of mural enhancement, wall thickening and extramural complications in patients with Crohn's disease. MR also allows detection of perianal inflammation and fistula in patients with Crohn's disease.

The assessment of ulcerative colitis is more difficult because of lesser degree of bowel wall thickening from the mucosal disease in contrast to transmural involvement seen with Crohn's disease. The MR findings of ulcerative colitis include loss of haustral markings, contiguous colonic wall thickening and hyperenhancement. MR is similar to endoscopy in its ability to distinguish between ulcerative colitis from Crohn's disease [18]. Recent studies have shown that multidetector spiral CT enteroclysis has higher sensitivity than MR enteroclysis for the detection of bowel wall thickening (88.9 vs. 60%), bowel wall enhancement (78.6 vs. 55.5%) and lymphadenopathy (63.8 vs. 14.3%) [19].

Advances in Imaging

The new technical advancements in imaging of small bowel Crohn's disease includes non-invasive CT enterography using peroral water or methylcellulose injected through a nasojejunal tube and MR enteroclysis. CT and MR enteroclysis are a combination of enteroclysis and CT for the detection of small bowel disease.

CT enteroclysis has proved highly accurate in the detection of Crohn's disease, particularly in patients without previous surgery [20]. The accuracy of CT enterography in the detection of active Crohn's disease ranges from 80 to 88% [21]. In the study by Wold et al. [21], CT enterography was superior to fluoroscopic small bowel examination in the detection of abscesses, phlegmons, fistulas and sinus tracts.

In the CT imaging of Crohn's disease, Mucofalk® has been introduced as an alternate negative oral contrast material for distention of bowel loops and evaluating extramucosal manifestations of the disease [22, 23]. Mucofalk® is a bulk-forming low-density laxative, derived from seed shells of *Plantago ovata*. The initial studies using Mucofalk® have provided excellent results.

CT colonography is another new imaging tool, useful in the evaluation of inflammatory bowel disease. Crohn's disease can reveal bowel wall thickening, air-filled sinus tracts, loss of haustrations, pseudopolyps, deep ulcers and segments of luminal narrowing in the area where colonoscopy failed to pass (fig. 8) [24]. In a distended colonic loop, a wall thickening >5 mm indicates inflammatory bowel disease [25].

FDG-PET is a non-invasive tool for simultaneous detection of inflamed areas in the small bowel as well as the large bowel [26]. When compared to MRI and immunoscintigraphy, FDG-PET was found to have a high specificity in the detection of inflamed areas in patients with Crohn's disease. Its role in imaging of inflammatory bowel disease is still experimental.

Conclusion

Of the cross-sectional imaging modalities, CT in particular plays a crucial role in the diagnosis and management of patients with inflammatory bowel disease, especially when complications are suspected. It is a complementary imaging modality to endoscopy. MR enteroclysis is a promising imaging tool that needs further studies to define its role.

References

1 Jamieson DH, Shipman PJ, Israel DM, Jacobson K: Comparison of multidetector CT and barium studies of the small bowel: Inflammatory bowel disease in children. AJR 2003;180: 1211–1216.

2 Goldberg HI, Gore RM, Margulis AR, Moss AA, Baker EL: Computed tomography in the evaluation of Crohn's disease. AJR 1983;140: 277–282.

3 Megibow AJ: Computed tomography of the gastrointestinal tract: Techniques and principles of interpretation; in Gore RM, Levine MS, Laufer I (eds): Gastrointestinal Radiology. Philadelphia, Saunders 2000, pp 77–85.

4 Frager DH, Goldman M, Beneventano TC: Computed tomography and Crohn's disease. J Comput Assist Tomogr 1983;7:819–824.

5 Berliner L, Redmond P, Purow E, Megna D, Sottile V: Computed tomography and Crohn's disease: Effect in patient management. Am J Gastroenterol 1982;77:548–553.

6 Gore RM, Marn CS, Kirby DF, Vogelzang RL, Neiman HL: CT findings in ulcerative, granulomatous and indeterminate colitis. AJR 1984; 143:279–284.

7 Mako EK, Mester AR, Tarjan A, Karlinger K, Toth G: Enteroclysis and spiral CT examination in diagnoses of an evaluation of small bowel Crohn's disease. Eur J Radiol 2000;35:168–175.

8 Del Campo L, Arribas I, Valbuena M, Mate J, Moreno-Otero R: Spiral CT findings in active and remission phases in patients with Crohn's disease. J Comput Assist Tomogr 2001;25: 792–797.

9 Meyers MA, McGuire PV: Spiral CT demonstration of hypervascularity and Crohn's disease: 'Vascular jejunization of the ileum' or the 'comb sign'. Abdom Imaging 1995;20:327–332.

10 Choi D, Jin Lee S, Ah Cho Y, Lim HK, Hoon Kim S, Jae Lee W, et al: Bowel wall thickening in patients with Crohn's disease: CT patterns and correlation with inflammatory activity. Clin Radiol 2003;58:68–74.

11 Lee SS, Ha HK, Yang SK, Kim AY, Kim TK, Kim PN, et al: CT of prominent pericolic or perienteric vasculature in patients with Crohn's disease: Correlation with clinical disease activity and findings on barium studies. AJR 2000;179:1029–1036.

12 Harisinghani MG, Wittenberg J, Lee W, Chen S, Guitierrez AL, Mueller PR: Bowel wall fat halo sign in patients with intestinal disease. AJR 2003;181:781–784.

13 Orel SG, Rubesin SE, Jones B, Fishman EK, Bayless TM, Siegelman SS: Computed tomography versus barium studies in the acutely symptomatic patient with Crohn's disease. J Comput Assist Tomogr 1987;11:1009–1016.

14 Markose G, Ng CS, Freeman AH: The impact of helical computed tomography on the diagnoses of unsuspected inflammatory bowel disease in the large bowel. Eur Radiol 2003;13: 107–113.

15 Maconi G, Sampietro GM, Parente F, Pompili G, Russo A, Cristaldi M, et al: Contrast radiology, computed tomography and ultrasonography in detecting internal fistulas and intra-abdominal abscesses in Crohn's disease: A prospective comparative study. Am J Gastroenterol 2003;98:1545–1555.

16 Low RN, Sebrechts CP, Politoske DA, Bannett MT, Flores S, Snyder RJ: Crohn disease with endoscopic correlation: Single-shot fast spin-echo and gadolinium-enhanced fat-suppressed spoiled gradient-echo MR imaging. Radiology 2002;222:652–660.

17 Reiber A, Wruk D, Potthast S, Nussle K, Reinshagen M, Adler G, et al: Diagnostic imaging and Crohn's disease: Comparison of magnetic resonance imaging and conventional imaging methods. Int J Colorectal Dis 2000;15: 176–181.
18 Shoenut JP, Semelka RC, Magro CM, Silverman R, Yaffe CS, Micflikier AB: Comparison of magnetic resonance imaging and endoscopy in distinguishing the type and severity of inflammatory bowel disease. J Clin Gastroenterol 1994;19:31–35.
19 Schmidt S, Lepori D, Meuwly JY, Duvoisin B, Meuli R, Michetti P, et al: Prospective comparison of MR enteroclysis with multi detector spiral-CT enteroclysis: Intraobserver agreement and sensitivity by means of 'sign-by-sign' correlation. Eur Radiol 2003;13:1303–1311.
20 Hassan C, Cerro P, Zullo A, Spina C, Morini S: Computed tomography and enteroclysis in comparison with ileoscopy in patients with Crohn's disease. Int J Colorectal Dis 2003;18: 121–125.
21 Wold PB, Fletcher JG, Johnson CD, Sandborn WJ: Assessment of small bowel Crohn's disease: Noninvasive peroral CT enterography compared with other imaging methods and endoscopy – Feasibility study. Radiology 2003; 229:275–281.
22 Doerfler OC, Ruppert-Kohlmayr AJ, Reittner P, Hinterleitner T, Petritsch W, Szolar DH: Helical CT of the small bowel with an alternative oral contrast material in patients with Crohn disease. Abdom Imaging 2003;28:313–318.
23 Reittner P, Goritschnig T, Petritsch W, Doerfler O, Preidler KW, Hinterleitner T, Szolar DH: Multiplanar spiral CT enterography in patients with Crohn's disease using a negative oral contrast material: Initial results of noninvasive imaging approach. Eur Radiol 2002;12: 2253–2257.
24 Tarjan Z, Zagoni T, Gyorke T, Mester A, Karlinger K, Mako EK: Spiral CT colonography in inflammatory bowel disease. Eur J Radiol 2000;35:193–198.
25 Rottgen R, Schroder RJ, Lorenz M, Herbal A, Fischbach F, Herzog H, et al: CT-colonography with the 16-slice CT for the diagnostic evaluation of colorectal neoplasms and inflammatory colon disease. Röfo Fortschr Geb Röntgenstr Neuen Bildgeb Verfahr 2003;175:1384–1391.
26 Neurath MF, Vehling D, Schunk K, Holtman M, Brockmann H, Helisc A, et al: Noninvasive assessment of Crohn's disease: A comparison of ^{18}F-fluorodeoxyglucose positron emission tomography, hydromagnetic resonance imaging and granulocyte scintigraphy with labeled antibodies. Am J Gastroenterol 2002;97:1978–1985.

Review Article

Digestive Diseases

Dig Dis 2004;22:63–66
DOI: 10.1159/000078736

Doppler Sonography in the Diagnosis of Inflammatory Bowel Disease

Antonio Di Sabatino Elia Armellini Gino Roberto Corazza

Gastroenterology Unit, IRCCS Policlinico S. Matteo, University of Pavia, Pavia, Italy

Key Words
Crohn's disease · Doppler sonography · Intramural vascularity · Levovist · Ulcerative colitis

Abstract
Over the past few years, thanks to its ability to reveal neovascularization and inflammatory hyperemia, Doppler sonography has proved to be a valuable method for the assessment of disease activity in inflammatory bowel disease. Hypervascularization has been detected by Doppler imaging both in splanchnic vessels, in terms of flow volume and velocity, or resistance and pulsatility index on spectral analysis, and in small vessels of the affected bowel wall in terms of vessel density. In particular, power Doppler has been shown to be a highly sensitive method for evaluating the presence of flow in vessels that are poorly imaged by conventional color Doppler, and in detecting internal fistulas complicating Crohn's disease. Recently, the use of ultrasound contrast agents, such as Levovist, has been shown to improve the image quality of color Doppler by increasing the backscattered echoes from the desired regions, thus making it possible to better monitor the response to treatment and discriminate between active inflammatory and fibrotic bowel wall thickness in Crohn's disease. Additionally, Levovist-enhanced power Doppler sonography has proved to be highly sensitive and specific in the detection of inflammatory abdominal masses associated with Crohn's disease. In clinical practice, used in combination with second harmonic imaging and new generations of stable contrast agents, Doppler sonography appears to be a non-invasive and effective diagnostic tool in the diagnosis and follow-up of Crohn's disease and ulcerative colitis.

Copyright © 2004 S. Karger AG, Basel

The increasing use of Doppler sonography in inflammatory bowel disease in recent years is the result of the need to assess disease activity, a parameter undetectable with just grey scale ultrasonography [1], in order to monitor the response to treatment, to foresee impending relapses, and to make a better choice between medical treatment and surgical resection. The assessment of disease activity with Doppler imaging postulates that the vascular and microvascular changes affecting the inflamed bowel segment, i.e. vasculitis, neovascularization and dilatation of feeding arteries and draining veins [2–4], results in an increased blood flow within either the thickened wall or splanchnic vessels. Indeed, a significantly higher superior mesenteric artery and portal vein flow was reported in patients with Crohn's disease and ulcerative colitis in comparison to control subjects [5–7].

As shown in the table 1, several studies have been published since van Oostayen et al. [8] first showed that disease activity in Crohn's disease could be assessed by measuring the superior mesenteric artery flow, and different Doppler parameters, such as flow volume and velocity, resistance and pulsatility index, have been used to monitor disease activity in inflammatory bowel disease [9–11].

KARGER

Fax + 41 61 306 12 34
E-Mail karger@karger.ch
www.karger.com

© 2004 S. Karger AG, Basel
0257–2753/04/0221–0063$21.00/0

Accessible online at:
www.karger.com/ddi

Prof. Gino Roberto Corazza
Unità Operativa di Gastroenterologia, IRCCS Policlinico San Matteo, Università di Pavia
Piazzale Golgi 5
IT–27100 Pavia (Italy)
Tel. +39 0382 502974, Fax +39 0382 502618, E-Mail gr.corazza@smatteo.pv.it

Table 1. Doppler sonography in the diagnosis of inflammatory bowel disease

Group (first author)	Year	Disease	Patients	Doppler detection	Contrast agent	Parameters	Conclusions
Van Oostayen [8]	1994	CD	20	SMA flow	None	Flow volume, ml/min	Useful to monitor disease activity
Van Oostayen [9]	1998	CD	31	SMA flow	None	Flow volume, ml/min	Useful to monitor disease activity
Maconi [11]	1998	CD	79	SMA flow, PV flow	None	Flow velocity, cm/s; flow volume, ml/min, RI	Of little value in the diagnostic work-up of patients
Ludwig [10]	1999	UC	76	SMA flow, IMA flow	None	Flow velocity, cm/s; PI	Useful to monitor disease activity
Spalinger [12]	2000	CD	92	Flow within bowel wall	None	Subjective color signal intensity	Useful to monitor disease activity
Ruess [13]		CD, UC	17	Flow within bowel wall	None	Subjective color signal intensity, RI	Useful to monitor disease activity
Esteban [14]	2001	CD	79	Flow within bowel wall	None	RI	Useful to monitor disease activity
Di Sabatino [16]	2002	CD	31	Flow within bowel wall	Levovist	Audio-Doppler signal intensity, dB	Useful to distinguish inflammatory and fibrotic thickening
Maconi [23]	2002	CD	45	Flow within fistula wall	None	Subjective color signal intensity, RI	Useful to assess internal fistulas
Esteban [22]	2003	CD	28	Flow within inflammatory masses	Levovist	Subjective color signal intensity	Useful to distinguish phlegmons and abscesses

CD = Crohn's disease; dB = decibels; IMA = inferior mesenteric artery; PV = portal vein; PI = pulsatility index; RI = resistance index; SMA = superior mesenteric artery; UC = ulcerative colitis.

However, the results that emerged from these studies are somewhat conflicting. While it has been reported higher flow volumes of the superior mesenteric artery in active than in quiescent patients in Crohn's disease [9], and a significant correlation between flow velocity of the inferior mesenteric artery and clinical activity in ulcerative colitis [10], conversely Maconi et al. [11] showed that although a hyperdynamic splanchnic circulation exists in Crohn's disease it does not reflect the clinical activity, suggesting that this technique is of little value in the diagnostic work-up of Crohn's disease patients.

Recently, direct Doppler analysis of the affected bowel segment, whether color or power, has been employed to estimate the intramural vascularity in Crohn's disease [12–14]. Spalinger et al. [12], who quantified the vessel density within the thickened wall by the number of color signals per square centimeter, showed that increased intramural flow and bowel thickness >5 mm reflected clinical activity in patients with Crohn's disease. Similar results were obtained both in Crohn's disease and ulcerative colitis by Ruess et al. [13], who reported that intramural vascularity, as depicted by color and power Doppler sonography and graded on a scale from 1 to 4, correlated with laboratory and clinical parameters of disease activity. Having observed comparable levels of intramural flow in active and inactive Crohn's disease patients with color Doppler sonography, Esteban et al. [14] performed a spectral analysis of the larger arterial vessels with measurement of the resistance index, which was found to be significantly lower in the gut wall vessels of Crohn's disease patients with active disease than that obtained in the inactive patients. Although these studies are affected by the subjective or semiquantitative nature of the criteria chosen to evaluate the intensity of intramural vascularity, they indicate power Doppler sonography, however, as a highly sensitive method for evaluating the presence of flow in vessels that are poorly imaged by conventional color Doppler. In particular, the advantages of power Doppler analysis are represented by its reduced noise, angle independence and lack of aliasing, as shown in focal lesions of the gastrointestinal tract [15].

One stratagem used to improve the accuracy of color Doppler sonography in detecting the intramural blood flow in the terminal ileum in Crohn's disease was the use of Levovist, a galactose-based sonographic contrast agent, which has a well-documented role in Doppler enhancement, increasing the signal intensity from blood vessels by 10–25 dB [17, 18]. Microbubbles interact with an ultrasound beam and resonate, producing harmonic signals. This agent is particularly useful in the detection of small

vessel flow, especially in those areas in which Doppler sensitivity limits performance, including intracranial and deep abdominal Doppler examinations, in which the signal-to noise ratio determines detectability [19]. By measuring the harmonic microbubble enhancement as an increase in audio Doppler signal intensity, it has been shown that Levovist is particularly effective in Crohn's disease patients having an intramural bowel flow not consistent enough to make it possible to separate the background noise from the Doppler signals by basal acoustic emission mode. This technique has proved useful in Crohn's disease for its ability to assess disease activity, to monitor the response to treatment, and to discriminate between active inflammatory and fibrotic bowel wall thickness [16]. This last aspect is very important because fibrosis, which may lead to stenosis and is less responsive to steroid treatment, more frequently needs surgical therapy, unlike active inflammatory bowel wall thickness which is a candidate for medical therapy [20]. Additionally, it has been suggested that an increased intramural flow after Levovist injection may represent a predictive factor of impending relapse in patients with quiescent Crohn's disease and may make it possible to distinguish between inactive disease and the absence of Crohn's disease [16]. Interestingly, as lower levels of ileoterminal flow have been found after ileocolonic resection for Crohn's disease [21], Levovist-enhanced color Doppler mode could prove particularly useful in the follow-up of patients with previous intestinal resection.

Esteban et al. [22] combined the use of power Doppler analysis with Levovist injection in the assessment of inflammatory abdominal masses associated with Crohn's disease. The authors demonstrated a higher sensitivity and specificity of Levovist-enhanced power Doppler for the detection of small inflammatory masses and for the differential diagnosis of phlegmons and abscesses, particularly in those lesions <2 cm in diameter, when compared with computed tomography. This aspect together with the absence of radiation dose to the patient and the safety profile of Levovist make it possible to carry out repeated examinations during the follow-up and, thus, to accurately assess the response to treatment.

Recently, power Doppler has been shown to provide a new means of studying vascularization within the fistula wall, thus enhancing the performance of grey scale ultrasonography in detecting internal fistulas complicating Crohn's disease. In those cases in which it was possible to document arterial or venous flow within the fistula wall, a spectral analysis of intralesional blood flow was performed. The resulting resistance index turned out to be reproducible and to correlate with the biochemical and clinical activity of Crohn's disease [23].

While the recent development of Doppler imaging shows promise for the future in the diagnosis of Crohn's disease, being a simple, cost-effective, non-invasive technique, further studies are nevertheless required to better clarify its role in detecting piercing vessels, in quantifying time perfusion and neoangiogenesis within the bowel or fistula wall and abdominal masses, and in monitoring the therapeutic effect of agents shown to be efficacious in Crohn's disease, such as infliximab [24] or thalidomide [25], both known to have a potential activity in inhibiting angiogenesis [26, 27]. The production of new sonographic techniques, such as superharmonic imaging, which has been shown to be more sensitive to contrast by increasing the signal from contrast and suppressing that from tissue [28], together with the availability of new generations of stable contrast agents, such as SonoVue [29], certainly offer a new and more sensitive way of detecting small bowel microvessels in Crohn's disease in the near future.

References

1 Maconi G, Parente F, Bollani S, Cesana B, Bianchi Porro G: Abdominal ultrasound in the assessment of extent and activity of Crohn's disease: Clinical significance and implication of bowel wall thickening. Am J Gastroenterol 1996;91:1604–1609.

2 Wakefield AJ, Sankey EA, Dhillon AP, Sawyerr AM, More L, Sim R, Pittilo RM, Rowles PM, Hudson M, Lewis AA: Granulomatous vasculitis in Crohn's disease. Gastroenterology 1991;100:1279–1287.

3 Brahme F, Lindstrom C: A comparative radiographic and pathological study of intestinal vasoarchitecture in Crohn's disease and ulcerative colitis. Gut 1970;11:928–940.

4 Eriksson U, Fagerberg S, Krausse U, Olding L: Angiographic studies in Crohn's disease and ulcerative colitis. Am J Roentgenol Radium Ther Nucl Med 1970;110:385–392.

5 Bolondi L, Gaiani S, Brignola C, Campieri M, Rigamonti A, Zironi G, Gionchetti P, Belloli C, Miglioli M, Barbara L: Changes in splanchnic hemodynamics in inflammatory bowel disease. Scand J Gastroenterol 1992;27:501–507.

6 Maconi G, Imbesi V, Bianchi Porro G: Doppler ultrasound measurement of intestinal blood flow in inflammatory bowel disease. Scand J Gastroenterol 1996;31:590–593.

7 Mirk P, Palazzoni G, Gimondo P: Doppler sonography of hemodynamic changes of the inferior mesenteric artery in inflammatory bowel disease: Preliminary data. AJR 1999; 173:381–387.

8 Van Oostayen JA, Wasser MNJM, van Hogezand RA, Griffioen G, de Roos A: Activity of Crohn's disease assessed by measurement of superior mesenteric artery flow with Doppler US. Radiology 1994;193:551–554.

9 Van Oostayen JA, Wasser MNJM, Griffioen G, van Hogezand RA, Lamers CBHW, de Roos A: Diagnosis of Crohn's ileitis and monitoring of disease activity: Value of Doppler ultrasound of superior mesenteric artery flow. Am J Gastroenterol 1998;93:88–91.

10 Ludwig D, Wiener S, Brüning A, Schwarting K, Jantschek, Fellermann K, Stahl M, Stange EF: Mesenteric blood flow is related to disease activity and risk of relapse in ulcerative colitis: A prospective follow-up study. Gut 1999;45: 546–552.
11 Maconi G, Parente F, Bollani S, Imbesi V, Ardizzone S, Russo A, Bianchi Porro G: Factors affecting splanchnic haemodynamics in Crohn's disease: A prospective controlled study using Doppler ultrasound. Gut 1998;43:645–650.
12 Spalinger J, Patriquin H, Miron MC, Marx G, Herzog D, Dubois J, Dubinsky M, Seidman EG: Doppler US in patients with Crohn's disease: Vessel density in the diseased bowel reflects disease activity. Radiology 2000;217: 787–791.
13 Ruess L, Nussbaum Blask AR, Bulas DI, Mohan P, Bader A, Latimer JS, Kerzner B: Inflammatory bowel disease in children and young adults: correlation of sonographic and clinical parameters during treatment. AJR 2000;175: 79–84.
14 Esteban JM, Maldonado L, Sanchiz V, Minguez M, Benages A: Activity of Crohn's disease assessed by colour Doppler ultrasound analysis of the affected loops. Eur Radiol 2001;11: 1423–1428.
15 Clautice-Engle T, Jeffrey RB Jr, Li KC, Barth RA: Power Doppler imaging of focal lesion of the gastrointestinal tract: Comparison with conventional color Doppler imaging. J Ultrasound Med 1996;15:63–66.
16 Di Sabatino A, Fulle I, Ciccocioppo R, Ricevuti L, Tinozzi FP, Tinozzi S, Campani R, Corazza GR: Doppler enhancement after intravenous Levovist injection in Crohn's disease. Inflamm Bowel Dis 2002;8:251–257.
17 Schlief R: Galactose-based echo-enhancing agents; in Goldberg BB (ed): Ultrasound Contrast Agents. London, Dunitz, 1997, pp 75–82.
18 Blomley MJK, Cosgrove DO: Microbubble echo-enhancers: A new direction for ultrasound? Lancet 1997;349:1855–1856.
19 Goldberg BB, Liu JB, Burns PN, Merton DA, Forsberg F: Galactose-based intravenous sonographic contrast agent: Experimental studies. J Ultrasound Med 1993;12:463–470.
20 Kornbluth A, Salomon P, Sachar DB: Crohn's disease; in Sleisenger MH, Fordtran JS (eds): Gastrointestinal Disease: Pathophysiology, Diagnosis and Management. Philadelphia, Saunders, 1993, pp 1270–1304.
21 Angerson WJ, Allison MC, Baxter JN, Russell RI: Neoterminal ileal blood flow after ileocolonic resection for Crohn's disease. Gut 1993; 34:1531–1534.
22 Esteban JM, Aleixandre A, Hurtado MJ, Maldonado L, Mora FJ, Nogues E: Contrast-enhanced power Doppler ultrasound in the diagnosis and follow-up of inflammatory abdominal masses in Crohn's disease. Eur J Gastroenterol Hepatol 2003;15:253–259.
23 Maconi G, Sampietro GM, Russo A, Bollani S, Cristaldi M, Parente F, Dottorini F, Bianchi Porro G: The vascularity of internal fistulae in Crohn's disease: An in vivo power Doppler ultrasonography assessment. Gut 2002;50: 496–500.
24 Sandborn WJ, Hanauer SB: Infliximab in the treatment of Crohn's disease: A user's guide for clinicians. Am J Gastroenterol 2002;97:2962–2972.
25 Fishman SJ, Feins NR, D'Amato RJ, Folkman J: Thalidomide therapy for Crohn's disease. Gastroenterology 2000;119:596.
26 Di Sabatino A, Ciccocioppo R, Cinque B, Benazzato L, Morera R, Cifone MG, Sturniolo GC, Corazza GR: Serum basic fibroblast growth factor and vascular endothelial growth factor in Crohn's disease patients treated with infliximab. Dig Liver Dis 2002;34:A87.
27 D'Amato RJ, Loughnan MS, Flynn E, Folkman J: Thalidomide is an inhibitor of angiogenesis. Proc Natl Acad Sci USA 1994;91: 4082–4085.
28 Bouakaz A, Krenning BJ, Vletter WB, ten Cate FJ, De Jong N: Contrast superharmonic imaging: A feasibility study. Ultrasound Med Biol 2003;29:547–553.
29 Schneider M: SonoVue, a new ultrasound contrast agent. Eur Radiol 1999;9(suppl 3):347–348.

Original Article

Digestive Diseases

Dig Dis 2004;22:67–72
DOI: 10.1159/000078737

Accepted: March 5, 2004

Evaluation of Criteria for the Activity of Crohn's Disease by Power Doppler Sonography

Holger Neye[a] Winfried Voderholzer[a] Steffen Rickes[b] Jutta Weber[a]
Wolfram Wermke[a] Herbert Lochs[a]

[a]Department of Gastroenterology, Hepatology and Endocrinology, University Hospital Charité (Campus Mitte), Berlin, and [b]Department of Gastroenterology, Hepatology and Infectiology, Otto von Guericke University, Magdeburg, Germany

Key Words
Power Doppler sonography · Crohn's disease · Ileocolonoscopy · Disease activity · Prospective study · Diagnostic criteria, evaluation

Abstract
Background/Aim: In recent years, power Doppler sonography has been proposed as a method to assess disease activity in patients with Crohn's disease. The aim of this prospective study was to evaluate diagnostic criteria for power Doppler sonography by blinded comparison with ileocolonoscopy. ***Methods:*** Twenty-two patients with confirmed Crohn's disease were prospectively investigated with B-mode and power Doppler sonography (HDI 5000, Philips Ultrasound) as well as ileocolonoscopy. Sonography was performed within 3 days before endoscopy. All procedures were performed by experienced examiners who were blinded to the clinical data and other results. Defined ultrasound parameters (bowel wall thickness, vascularization pattern) were used to determine a sonographic score of the activity. The degree of activity was scored from 1 (none) to 4 (high) by both ultrasound and ileocolonoscopy (pattern, extent of typical lesions). For each patient all segments of the colon and the terminal ileum were evaluated by both ultrasound and endoscopy. The weighted κ test was used (StatXact software) for statistical analysis. ***Results:*** In total, 126 bowel segments were evaluated by both ultrasound and endoscopy. The study showed a high concordance of power Doppler sonography and ileocolonoscopy (weighted κ by region: sigmoid colon: 0.81; transverse colon: 0.78; ascending colon: 0.75; cecum: 0.84; terminal ileum: 0.82). Highest concordance was found in the descending colon (weighted κ: 0.91; 95% CI: 0.83–0.98). ***Conclusions:*** Combination of B-mode and power Doppler sonography has a high accuracy in the determination of disease activity in Crohn's disease when compared to ileocolonoscopy. The diagnostic criteria established in this study can be useful for the evaluation of inflammatory bowel diseases by ultrasound.

Copyright © 2004 S. Karger AG, Basel

KARGER
Fax + 41 61 306 12 34
E-Mail karger@karger.ch
www.karger.com

© 2004 S. Karger AG, Basel
0257–2753/04/0221–0067$21.00/0

Accessible online at:
www.karger.com/ddi

Holger Neye
Department of Gastroenterology, Hepatology and Endocrinology
University Hospital Charité (Campus Mitte)
DE–10098 Berlin (Germany)
Tel. +49 30 450 514 102, Fax +49 30 450 514 923, E-Mail holger.neye@charite.de

Introduction

Crohn's disease is characterized by episodes of recurrent inflammation alternating with periods of disease inactivity. Assessment of the extent and activity of the disease is essential in patients with Crohn's disease in order to determine the therapeutic strategy and prognosis. Currently, endoscopy is the preferred technique for assessing the activity of the disease in the colon and the terminal ileum, but this is invasive. Since patients with Crohn's disease may require frequent evaluation, there is a high need for a non-invasive method.

Thickness and structure of the intestinal wall have been studied by B-mode sonography [1–7]. Bowel wall thickening in patients with Crohn's disease can be caused by inflammation or fibrosis, therefore conventional ultrasound does not permit differentiation between active and inactive disease [8]. In earlier studies, the angiographic vascularization pattern was reported to be helpful for the determination of the activity in Crohn's disease. While inflammation is characterized by hypervascularization of bowel wall, fibrotic tissue was found to be hypovascularized [9, 10]. Technological advances have added new ultrasound techniques. Power Doppler sonography is based on the integrated Doppler power spectrum, which is related to the number of red blood cells that produce the Doppler shift. This method is independent of the insonation angle, there is no aliasing, and power Doppler sonography is much more sensitive to low-volume blood flow than conventional color Doppler [11–15]. Recently, a combination of B-mode and power Doppler sonography has been suggested as a method of assessing disease activity in patients with Crohn's disease [16, 17]. The improved depiction of tissue vascularization has potential benefits for the detection of slow blood flow in small vessels. Evaluations of power Doppler criteria for several areas of the abdomen have been published [15, 18–20].

The aim of this prospective study was to evaluate diagnostic criteria for power Doppler sonography in patients with Crohn's disease by blinded comparison with ileocolonoscopy.

Patients and Methods

Patients

Twenty-two consecutive patients who had been referred to the Department of Gastroenterology, Hepatology and Endocrinology of the University Hospital Charité (Campus Mitte) with confirmed Crohn's disease were included in this prospective study (13 women and 9 men). The median age was 33.7 years (range 16–56). The mean duration of time post-diagnosis was 7.3 years. The study protocol was approved by the local ethics committee, and all patients gave their informed consent to participate in the study.

In 4 patients a total of 6 segments could not be evaluated due to prior bowel surgery. These 4 patients had a resection of the terminal ileum and the cecum. In 1 patient, the resection also extended to the ascending colon, and in another patient, it included a longer distance of the ileum, so that the evaluation of the ileum was not possible. All patients were prospectively studied with B-mode and power Doppler sonography as well as ileocolonoscopy.

Table 1. Definition of sonography score

Wall thickness	Vessels		
	no vessels/cm^2	1–2 vessels/cm^2	>2 vessels/cm^2
<5 mm	1	2	3
≤7 mm	2	3	4
>7 mm	2	3	4

Procedures

All procedures were performed by experienced examiners who were blinded to the clinical data and results of other procedures. Sonography was performed within 3 days prior to endoscopy with a high-resolution scanner (dynamic linear scanner 5–12 MHz and dynamic sector scanner 4–7 MHz, HDI 5000, Philips Ultrasound). Defined ultrasound parameters (bowel wall thickness and vascularization pattern) were recorded separately for 6 different segments of bowel in a standardized protocol: the sigmoid colon, descending colon, transverse colon, ascending colon, cecum, and terminal ileum.

Firstly, the abdomen was investigated with the sector scanner by B-mode to search for thickened intestine wall. Thickened bowel loops were then scanned with power Doppler sonography, and the area of highest vascularization was selected (fig. 1). Pulsed Doppler was used to confirm that signals originated from blood vessels and not from movement artifacts (fig. 2). The maximum bowel wall thickness, obtained with compression, was measured (lumen-to-serosa distance) with the linear scanner. Subsequently, the degree of vascularization was determined by power Doppler sonography, based on the number of vessels detected per square centimeter. B-mode (bowel wall thickness) and power Doppler sonography (vascularization pattern) were used to determine a sonographic score of the activity (see table 1) from 1 (none), 2 (mild), 3 (moderate) to 4 (high).

Endoscopic parameters (pattern, extent of typical lesions) were recorded with a standardized protocol for the same 6 segments of bowel: sigmoid colon, descending colon, transverse colon, ascending colon, cecum, and terminal ileum. Subsequently, the endoscopic degree of activity was scored for each bowel segment: 1 (no lesions), 2 (aphtes), 3 (aphtes and ulcers <50%) to 4 (aphtes and ulcers >50%).

Statistics

Weighted κ coefficients were calculated to examine the degree of concordance between the scores of sonography and ileocolonoscopy using StatXact (Version 5.0.3, Cytel software). The scheme for grading the strength of the weighted κ coefficients is presented in table 2 [21].

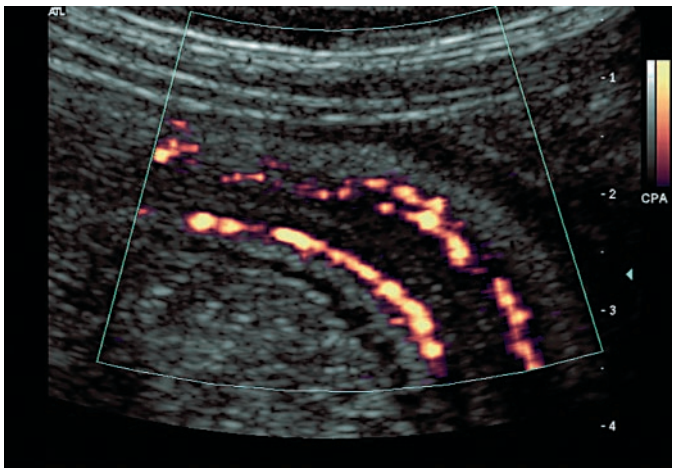

1

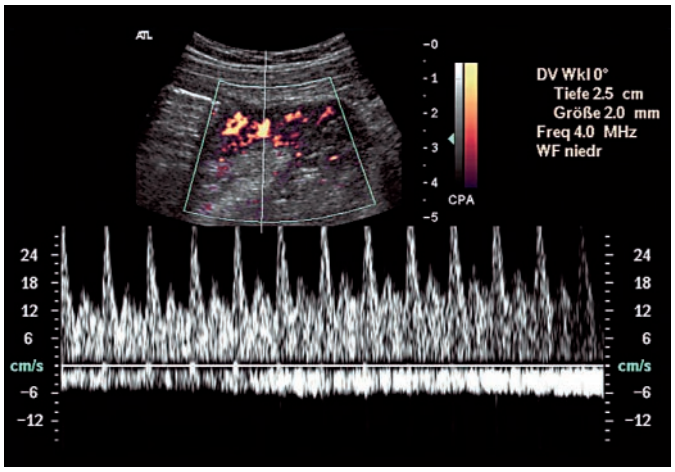

2

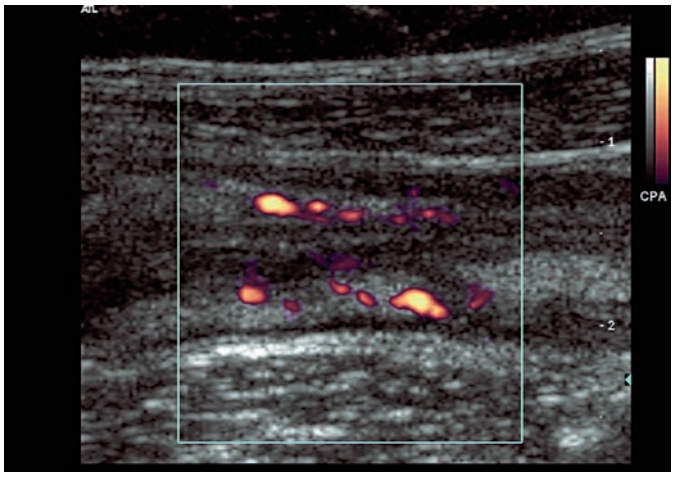

3

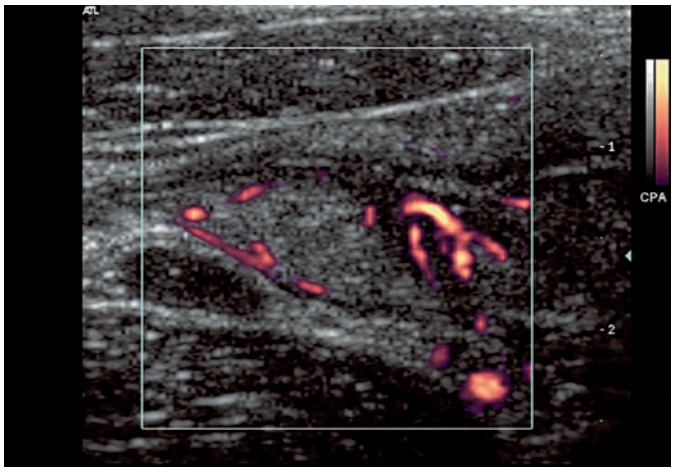

4

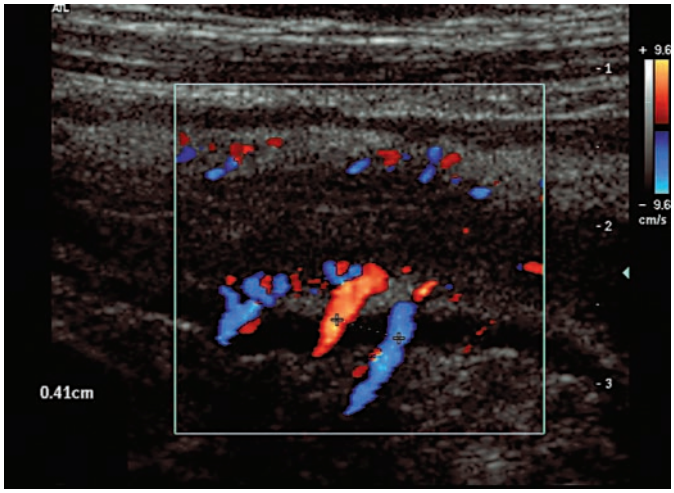

5

Fig. 1. A thickened bowel loop in the sigmoid colon scanned with power Doppler sonography, the area of highest vascularization was selected by sector scanner.
Fig. 2. Pulsed Doppler was used to confirm that signals originated from blood vessels and not from movement artifacts: Doppler spectrum of an artery and a vein.
Fig. 3. Rare vessels in the echo-dense submucosa of the descending colon: score 2.
Fig. 4. Vessels with branches in the thickened wall of the terminal ileum: score 3.
Fig. 5. Hypervascularization with detection of feeding vessels branching off after penetrating the wall: score 4. The flow signal is strong, color Doppler detects flow direction.

Table 2. κ coefficient and strength of concordance

Weighted (κ) coefficient	0	<0.21	0.21–0.40	0.41–0.60	0.61–0.80	>0.81
Strength of concordance	none	slight	fair	moderate	substantial	perfect

Table 3. Results of power Doppler sonography in comparison to ileocolonoscopy

	Sigmoid colon	Descending colon	Transverse colon	Ascending colon	Cecum	Terminal ileum
Identical score	74%	78%	74%	60%	73%	55%
Score difference: 1	22%	22%	22%	36%	27%	45%
Score difference: 2	4%	0%	4%	4%	0%	0%
Score difference: 3	0%	0%	0%	0%	0%	0%
Weighted κ[1]	0.81	0.91	0.78	0.75	0.84	0.82
Confidence interval: 95%	0.63–0.99	0.83–0.98	0.56–0.99	0.56–0.94	0.70–0.97	0.71–0.93

[1] κ coefficient: range 0–1, a higher value indicates a higher concordance.

Results

In total, 126 bowel segments were evaluated by both ultrasound and endoscopy. The study showed a high concordance of power Doppler sonography and ileocolonoscopy, the best match was found in the descending colon. The weighted κ coefficients were: 0.81 (95% confidence interval (CI) 0.63–0.99) for the sigmoid colon; 0.91 (95% CI 0.83–0.98) for the descending colon; 0.78 (95% CI 0.56–0.99) for the transverse colon; 0.75 (95% CI 0.56–0.94) for the ascending colon; 0.84 (95% CI 0.70–0.97), and 0.82 (95% CI 0.71–0.93) for the cecum and of the terminal ileum, respectively. The results are summarized in table 3.

There was no case with a score difference of 3 between both procedures. In 3 out of the 126 bowel segments examined, the difference between the scores was 2, one in the sigmoid colon, one in the transverse colon and one in the ascending colon, respectively. In these 3 cases, activity scores were underestimated or not detected sonographically. A score difference of one was seen in 39 cases. Sonography indicated higher disease activity in 19 cases and a lower activity in 20 cases respectively. Identical scores were found in 84 cases. The distribution of scores is shown in table 4.

Three sonographic images out of these 84 identical evaluations are depicted in figures 3–5. Figure 3 shows rare vessels located in the echo-dense submucosa of the descending colon. Vessels with branches in the thickened wall of the terminal ileum can be seen in figure 4. Figure 5 shows a section of ascending colon with hypervascularization and feeding vessels branching off after penetration of the wall.

Table 4. Summary of scoring results of power Doppler sonography and ileocolonoscopy

Sonography	Ileocolonoscopy				
	Score: 1	Score: 2	Score: 3	Score: 4	Total
Score: 1	54	12	3	0	69
Score: 2	4	7	6	0	17
Score: 3	0	6	11	2	19
Score: 4	0	0	9	12	21
Total	58	25	29	14	126

Discussion

Crohn's disease is characterized by segmental inflammation of the gastrointestinal tract. Currently, endoscopy is the standard for assessing disease activity [22, 23]. A non-invasive method not utilizing ionizing radiation would be a useful tool to monitor disease activity and

treatment of patients with inflammatory bowel disease. Ultrasound is not associated with any deleterious adverse effects. Furthermore, advantages of sonographical examinations include its relatively low cost and wide availability. Nevertheless, the need for histological confirmation and for screening of colon cancer means that ileocolonoscopy remains the definitive diagnostic method.

Several studies have analyzed the value of various ultrasound techniques for the assessment of Crohn's disease. In a pediatric study, bowel wall thickening measured by ultrasound correlated well with Crohn's disease activity in children [24]. In adults, the thickness of bowel wall measured by ultrasound showed only weak correlation with disease activity. Patients with inactive disease and pronounced intestinal thickening on ultrasound have been observed. The accuracy of B-mode sonography for distinguishing between active and inactive disease is most likely limited due to similar findings in patients with inflammatory wall thickening and fibrosis [8]. We hypothesize that the better correlation in children can be attributed to the age of the patients or duration of disease, respectively. Fibrosis is distinctly less common than in adults with Crohn's disease.

Flow measurements of the superior and inferior mesenteric arteries by Doppler ultrasound have been reported as an additional tool to measure disease activity in patients with Crohn's disease [25–27]. This method is complicated by angle dependence of the Doppler shift, high deviations of flow measurements and a high inter-equipment variability [28]. In later studies, Doppler examinations of the mesenteric arteries did not show any statistically significant difference between patients with active and inactive Crohn's disease [22]. Angiography has been the only reliable diagnostic method to detect the vascularization pattern of the gut wall until the development of new ultrasound techniques [9, 10].

With this study, we have addressed the need to evaluate diagnostic criteria for a combination of B-mode and power Doppler sonography which has recently been suggested as a method of assessing disease activity in patients with Crohn's disease [16]. Our findings were comparable with these previously reported studies, inflamed bowel segments had been found to be hypervascularized, no or few vessels had been found in non-inflamed segments (table 4). This study also showed that power Doppler sonography can detect vessels <1 mm in diameter, and that it can also visualize irregular and tortuous vessels in the gut wall. In the future, the direct detection of vessels in the intestinal wall could be the most important advantage of ultrasound contrary to other imaging methods.

The results of this comparative study demonstrated a high concordance of the non-invasive combination of B-mode ultrasound and power Doppler sonography with ileocolonoscopy, the current diagnostic standard, suggesting that it can be a useful tool to monitor disease activity in patients with Crohn's disease.

References

1 Holt S, Samuel E: Grey scale ultrasound in Crohn's disease. Gut 1979;20:590–595.
2 Wellmann W, Gebel M, Freise J, Grote R: Ultrasound in the diagnosis of ileitis terminalis Crohn. Röfo Fortschr Geb Röntgenstr Nuklearmed 1980;133:146–148.
3 Sonnenberg A, Erckenbrecht J, Peter P, Niederau C: Detection of Crohn's disease by ultrasound. Gastroenterology 1982;83:430–434.
4 Kimmey MB, Martin RW, Haggitt RC, Wang KY, Franklin DW, Silverstein FE: Histologic correlates of gastrointestinal ultrasound images. Gastroenterology 1989;96:433–441.
5 Meckler U, Caspary WF, Clement T, Herzog P, Lembcke B, Limberg B, el Mouaaouy A, Nippel G, Reuss P, Schwerk WB: Sonography in Crohn disease – The conclusions of an experts' group. Z Gastroenterol 1991;29:355–359.
6 Hata J, Haruma K, Suenaga K, Yoshihara M, Yamamoto G, Tanaka S, Shimamoto T, Sumii K, Kajiyama G: Ultrasonographic assessment of inflammatory bowel disease. Am J Gastroenterol 1992;87:443–447.
7 Hata J, Haruma K, Yamanaka H, Fujimura J, Yoshihara M, Shimamoto T, Sumii K, Kajiyama G, Yokoyama T: Ultrasonographic evaluation of the bowel wall in inflammatory bowel disease: Comparison of in vivo and in vitro studies. Abdom Imaging 1994;19:395–399.
8 Maconi G, Parente F, Bollani S, Cesana B, Bianchi Porro G: Abdominal ultrasound in the assessment of extent and activity of Crohn's disease: Clinical significance and implication of bowel wall thickening. Am J Gastroenterol 1996;91:1604–1609.
9 Bousen E, Reuter SR: Mesenteric angiography in the evaluation of inflammatory and neoplastic disease of the intestine. Radiology 1966;87:1028–1036.
10 Lunderquist A, Knutsson H: Angiography in Crohn's disease of the small bowel and colon. Am J Roentgenol Radium Ther Nucl Med 1967;101:338–344.
11 Rubin JM, Bude RO, Carson PL, Bree RL, Adler RS: Power Doppler US: A potentially useful alternative to mean frequency-based color Doppler US. Radiology 1994;190:853–866.
12 Newman JS, Adler RS, Bude RO, Rubin JM: Detection of soft-tissue hyperemia: Value of power Doppler sonography. AJR Am J Roentgenol 1994;163:385–389.
13 Bude RO, Rubin JM, Adler RS: Power versus conventional color Doppler sonography: Comparison in the depiction of normal intrarenal vasculature. Radiology 1994;192:777–780.
14 Martinoli C, Derchi LE, Rizzatto G, Solbiati L: Power Doppler sonography: General principles, clinical applications, and future prospects. Eur Radiol 1998;8:1224–1235.
15 Wermke W, Gassmann B: Tumour Diagnostics of the Liver with Echo Enhancers. Berlin, Springer, 1998, pp 8–223.
16 Heyne R, Rickes S, Bock P, Schreiber S, Wermke W, Lochs H: Non-invasive evaluation of activity in inflammatory bowel disease by power Doppler sonography. Z Gastroenterol 2002;40:171–175.

17 Maconi G, Sampietro GM, Russo A, Bollani S, Cristaldi M, Parente F, Dottorini F, Bianchi Porro G: The vascularity of internal fistulae in Crohn's disease: An in vivo power Doppler ultrasonography assessment. Gut 2002;50: 496–500.
18 Rickes S, Unkrodt K, Ocran K, Neye H, Lochs H, Wermke W: Evaluation of Doppler ultrasonography criteria for the differential diagnosis of pancreatic tumors. Ultraschall Med 2000; 21:253–258.
19 Rickes S, Unkrodt K, Neye H, Ocran KW, Wermke W: Differentiation of pancreatic tumours by conventional ultrasound, unenhanced and echo-enhanced power Doppler sonography. Scand J Gastroenterol 2002;37: 1313–1320.
20 Rickes S, Schulze S, Neye H, Ocran KW, Wermke W: Improved diagnosing of small hepatocellular carcinomas by echo-enhanced power Doppler sonography in patients with cirrhosis. Eur J Gastroenterol Hepatol 2003;15: 893–900.
21 Munoz SR, Bangdiwala SI: Interpretation of κ and B statistic measures of agreement. J Appl Stat 1997;24:105–111.
22 Miao YM, Koh DM, Amin Z, Healy JC, Chinn RJ, Zeegen R, Westaby D: Ultrasound and magnetic resonance imaging assessment of active bowel segments in Crohn's disease. Clin Radiol 2002;57:913–918.
23 Scholmerich J: Inflammatory bowel disease. Endoscopy 2003;35:164–170.
24 Haber HP, Busch A, Ziebach R, Stern M: Bowel wall thickness measured by ultrasound as a marker of Crohn's disease activity in children. Lancet 2000;355:1239–1240.
25 Van Oostayen JA, Wasser MN, van Hogezand RA, Griffioen G, de Roos A: Activity of Crohn disease assessed by measurement of superior mesenteric artery flow with Doppler US. Radiology 1994;193:551–554.
26 Van Oostayen JA, Wasser MN, van Hogezand RA, Griffioen G, Biemond I, Lamers CB, de Roos A: Doppler sonography evaluation of superior mesenteric artery flow to assess Crohn's disease activity: Correlation with clinical evaluation, Crohn's disease activity index, and α_1-antitrypsin clearance in feces. AJR Am J Roentgenol 1997;168:429–433.
27 Van Oostayen JA, Wasser MN, Griffioen G, van Hogezand RA, Lamers CB, de Roos A: Diagnosis of Crohn's ileitis and monitoring of disease activity: Value of Doppler ultrasound of superior mesenteric artery flow. Am J Gastroenterol 1998;93:88–91.
28 Zoli M, Merkel C, Sabba C, Sacerdoti D, Gaiani S, Ferraioli G, Bolondi L: Inter-observer and inter-equipment variability of echo-Doppler sonographic evaluation of the superior mesenteric artery. J Ultrasound Med 1996;15: 99–106.

Original Article

Digestive Diseases

Dig Dis 2004;22:73–80
DOI: 10.1159/000078738

Accepted: February 4, 2004

Differential Diagnosis of Focal Liver Lesions in Signal-Enhanced Ultrasound Using BR 1, a Second-Generation Ultrasound Signal Enhancer

R. Peschl A. Werle G. Mathis

Department of Internal Medicine, Landeskrankenhaus Hohenems, Hohenems, Austria

Key Words

Contrast agent · Focal liver lesion · Ultrasound · Ultrasound signal enhancer · Hepatocellular carcinoma · Focal nodular hyperplasia · Metastasis · Haemangioma

Abstract

Aim: The aim was to evaluate the diagnostic value of contrast-enhanced ultrasound in the differential diagnosis of focal liver lesions, in a blinded experiment. In clinical routine the examiner can generally be influenced by the patient's history. ***Method:*** 62 patients with focal liver lesions, which could not be clearly differentiated and diagnosed by conventional ultrasound, were examined with contrast-enhanced (BR1, SonoVue®, Bracco) ultrasound and included in a blinded prospective and randomized study. The examinations performed on a Sequoia 512 (Acuson) in a coherent contrast imaging method were recorded by an S-VHS recorder and afterwards analyzed by an examiner who did not know the patient's history. The basis of the diagnosis was the dynamic appearance and enhancement of the ultrasound contrast enhancer in different phases of liver perfusion. The conformation of the diagnoses was made by corresponding reference methods, as computer tomography, magnetic resonance imaging, biopsy and clinical follow-up. ***Results:*** The following diagnoses were confirmed by reference methods: 18 patients with metastases, 4 hepatocellular carcinomas, 19 haemangiomas, 6 focal nodular hyperplasias, 13 patients with focal fatty infiltration and 2 patients with focal fatty sparing. 59 out of 62 patients with one or more liver lesions were correctly diagnosed by contrast-enhanced ultrasound. ***Conclusion:*** Second-generation ultrasound contrast enhancers improve the differential diagnosis of benign and malignant liver lesions considerably, especially in a blinded study.

Copyright © 2004 S. Karger AG, Basel

Introduction

Although ultrasound has a sensitivity of 90–95% for detecting a focal liver lesion, the correct differentiation of these lesions is still a challenge for any imaging method. In general the correct diagnosis with conventional grey scale ultrasound is only possible in 26 up to 35% of benign lesions and in 28 up to 39% of malignant lesions [1, 2]. In other studies the correct differentiation was even possible in 60 up to 68% [3, 4]. Recently, several studies showed that by the use of ultrasound contrast enhancers, further improvement of the accuracy is possible. In clinical routine the patient's history is often known by the examiner who can consequently be influenced by this knowledge in the differentiation of a focal liver lesion. In a cirrhotic liver, metastases are rare in contrast to a hepatocellular carcinoma. However, this knowledge can be irritating in some cases, as the examiner sees what he is expecting to see [5].

KARGER

Fax + 41 61 306 12 34
E-Mail karger@karger.ch
www.karger.com

© 2004 S. Karger AG, Basel
0257–2753/04/0221–0073$21.00/0

Accessible online at:
www.karger.com/ddi

Dr. med. Robert Peschl
Krankenhaus Hohenems
Bahnhofstrasse 31
AT–6845 Hohenems (Austria)
Tel. +43 5576 703, Fax +43 5576 7032200, E-Mail robert.peschl@aon.at

The aim of this study was to undertake a blinded characterisation of focal liver lesions by using ultrasound contrast media. Thereby no information about the patient was announced to the examiner. He only could do the differentiation by using the information given by the contrast-enhanced ultrasound. Thus we hoped to obtain an objective evaluation of the method by this study design.

Materials and Methods

Patients

In the period from November 2001 to December 2003, 63 patients with not clearly differentiated focal liver lesions underwent a contrast-enhanced ultrasound examination by using a second-generation ultrasound contrast enhancer at the Department of Internal Medicine, General Hospital, Hohenems, Austria. All patients gave their informed consent after they were completely informed about the examination method and any possible complications.

Ultrasound Equipment

The examination was carried out on an Acuson Sequoia 512 ultrasound system, using the coherent contrast inversion (CCI) technique. CCI is based on the pulse inversion harmonic imaging mode. Insonation was done with a curved array transducer, which transmitted at 3.0 MHz.

Ultrasound Contrast Enhancer

The examinations were performed by using BR1 (SonoVue®, Bracco, Italy), a second-generation ultrasound contrast enhancer. BR1 consists of phospholipid-stabilized microbubbles of sulphur hexafluoride (SF6). It is based on perfluorocarbon and is poorly soluble, totally innocuous and inert gas.

Examination

Ultrasound scans were performed by an experienced examiner and recorded on an S-VHS videotape. Before starting the examination the ultrasound contrast enhancer was prepared with 5 ml saline and shaking for 1 min. Previously the focal liver lesion was examined by fundamental grey scale, imaging was optimized and the focus was set at the right depth. In case of several lesions, the largest and most obvious one was chosen. After changing to CCI low MI mode and choosing a mechanical index of 0.16–0.19, a bolus of 2.4 ml BR1 (SonoVue®, Bracco) was injected intravenously into the cubital vein. Afterwards it was immediately flushed with 5 ml of saline to make sure that the whole amount of ultrasound signal enhancer reached the bloodstream. Time measurement was commenced at the end of the injection. Ultrasound scan was performed throughout the whole contrast-enhanced phases without interruption and recorded on S-VHS. Additionally, digital pictures and videoclips were taken from the most important phases, the early arterial phase, arterial phase, portal-venous phase and the late phase.

Examination Analysis

The records were analyzed by an examiner (R.P.) who did not know the patient's history. The order in which the analyzing was performed was given by a protocol. First echogeneity, homogeneity, dimension and amount of the focal liver lesion were described in the fundamental grey scale mode. After injection of the ultrasound contrast agent the transit time from injection to ultrasound contrast enhancer arrival in the hepatic artery was measured. Afterwards, the behaviour of the signal enhancer in the individual vascular phases and the enhancement pattern was judged. The most significant of the individual phases were summarized, resulting in the spaces for placing the diagnosis (table 1). Computer tomography, magnetic resonance tomography, fine needle aspiration biopsy and clinical follow-up were used as reference method (table 2). The clinical follow-up period was on average 14 months, including changes in symptoms, ultrasound change of the lesion in size and texture, and laboratory parameters, e.g. α-fetoprotein.

Table 1. Recorded signal-enhanced ultrasound examinations were analyzed by this protocol

Parameter	Diagnosis
Patient	
Number of focal liver lesions	
Size of focal liver lesion	
Conventional grey scale	
Liver arrival time	
Early arterial phase	
Arterial phase	
Portal venous phase	
Late phase	
Summary	
Diagnosis	

Table 2. Reference methods which were used to confirm the diagnosis set by signal-enhanced ultrasound

	All	Focal fatty changes	Haemangioma	FNH	Metastases	HCC
Clinical follow-up	25	9	8	2	6	0
Computer tomography	24	6	8	3	7	0
Magnetic resonance tomography	1	0	1	0	0	0
Fine needle aspiration biopsy	12	1	1	1	5	4

Results

Sixty-two patients were included with focal liver lesions which could not be clearly differentiated by fundamental grey scale ultrasound. Imaging in the CCI low MI mode took from 1 to 15 min. Each record was assessed twice. In all examinations a significant and homogeneous enhancement of the liver parenchyma was observed. The maximum depth was limited at 13–14 cm. Areas deeper than 14 cm showed weak and inhomogeneous enhancement. Consequently, the characterization of a perfusion pattern was only possible with difficulties.

The mean time the ultrasound contrast enhancer needed to reach the liver was 13.4 s, with a minimum to maximum range from 4 to 30 s. The diagnoses of the contrast media-enhanced ultrasound were verified with reference methods. A computer tomography scan was performed in 24 patients, and due to allergies to iodine-containing contrast media, a magnetic resonance tomography had to be done in 1 case. Fine needle aspiration biopsy and histological examination was performed in 12 patients. In 25 cases the diagnoses were confirmed by clinical follow-up, including 6 cases with metastasis, 9 haemangiomas, 2 focal nodular hyperplasia and 4 patients with focal fatty infiltrations and focal fatty sparings. In 2 cases of a focal nodular hyperplasia, colour-coded duplex sonography showed a significant spoke-wheel sign, so that no further invasive investigations were performed due to a lack of clinical relevance. Clinical follow-up confirmed the diagnosis later.

The records of the contrast-enhanced ultrasound examination were analyzed and a diagnosis was made in every case. These diagnoses were confirmed in 59 of 62 patients by the reference methods outlined above.

Table 3. Differentiation of benign and malignant liver lesions

	Benign liver lesions, % (n = 40)	Malignant liver lesions, % (n = 22)
Sensitivity	95	100
Specificity	100	95
Positive predicted value	100	92
Negative predicted value	92	100
Accuracy	97	97

Differential Diagnosis of Benign and Malignant Lesions

All diagnoses of the 38 benign lesions were confirmed by reference methods, whereas 2 out of 24 diagnoses of malignant lesions were benign. In the end, 38 (95%) out of the 40 benign focal livers lesions were diagnosed correctly. Of these, 2 lesions were false negative of a benign lesion and false positive of a malignant liver lesion. A correct diagnosis was made in 22 (92%) out of 24 malignant liver lesions (table 3).

Malignant Focal Livers Lesions

A malignant diagnosis was made in 24 patients after the signal-enhanced ultrasound examination. These were separated in 19 cases of metastases and 5 cases of hepatocellular carcinoma.

Metastases

Out of the 19 focal liver lesions diagnosed as metastases, 6 cases were confirmed by clinical follow-up, in 5 cases by fine needle aspiration biopsy and in 7 cases by computer tomography. One diagnosed metastasis turned out to be a haemangioma in a computer tomography. Eighteen correctly classified metastases showed a lack of contrast enhancement and blurred margins during the portal-venous phase.

In the arterial phase the enhancement of the ultrasound contrast enhancer was in a wide range variable in metastatic lesions. Hypervascularity was seen in 6 cases as opposed to 3 cases of hypovascularity (fig. 1). Three lesions showed the same enhancement as the surrounding parenchyma. A mix of strong peripheral enhancement and poor central enhancement was visible in 2 metastases (fig. 2). The arterial phase was not visible in 1 case.

Hepatocellular Carcinoma

Five cases were diagnosed as hepatocellular carcinoma and it was possible to confirm the diagnoses by a fine needle aspiration as reference method. One focal liver lesion, misdiagnosed as hepatocellular carcinoma, was classified as a focal nodular hyperplasia by computer tomography. The correctly positive classified hepatocellular carcinomas showed a strong ultrasound contrast enhancer uptake and therefore a strong enhancement in the arterial phase. The enhancement pattern was homogeneous in 2 cases (fig. 3), whereas 2 focal liver lesions showed a chaotic ultrasound contrast enhancer uptake. During the portal-venous phase the same enhancement as in the surrounding parenchyma was visible in the arterial homogeneous lesions. The lesions with the chaotic enhancement pattern

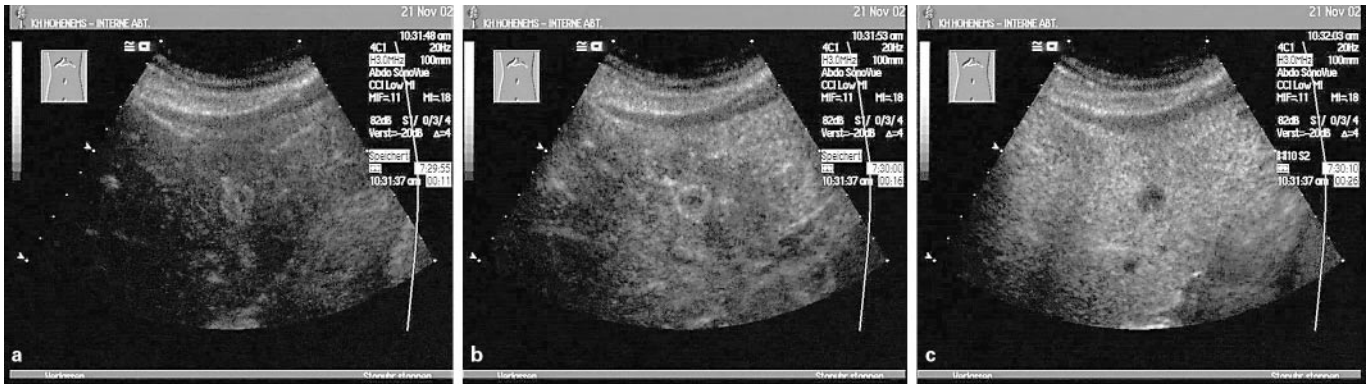

Fig. 1. Metastasis with hypervascularisation in signal-enhanced ultrasound. 11 s after contrast agent injection a strong contrast agent uptake is visible (**a**), which becomes hypoechoic 5 s later (**b**). 26 s after injection the lesion shows a complete lack of contrast enhancement (**c**).

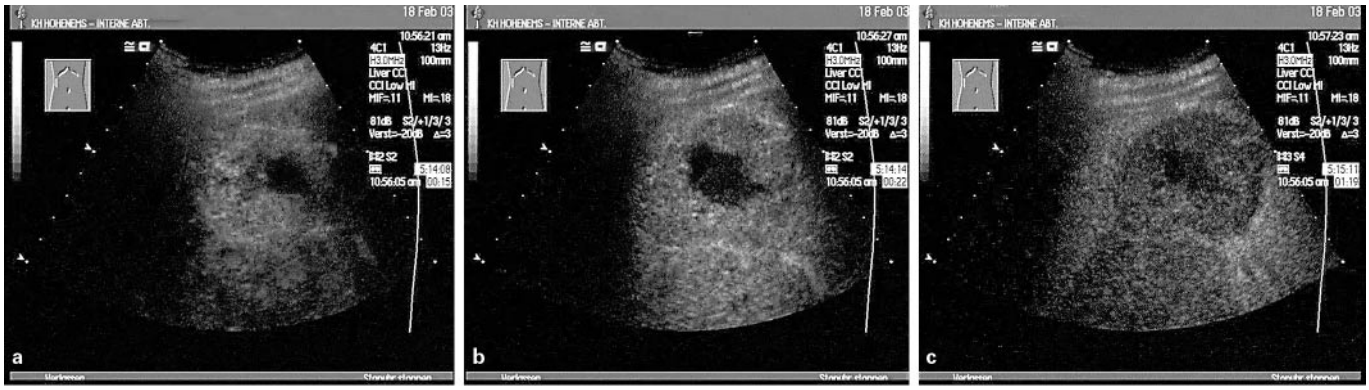

Fig. 2. Metastasis with mixed vascularisation pattern in contrast-enhanced ultrasound. 15 s after injection a hyperechoic lesion with a central lack of contrast enhancement is visible (**a**). 22 s after injection the lesion is isoechoic, except for the central area (**b**) and at 1 min 19 s the lesion becomes hypoechoic (**c**).

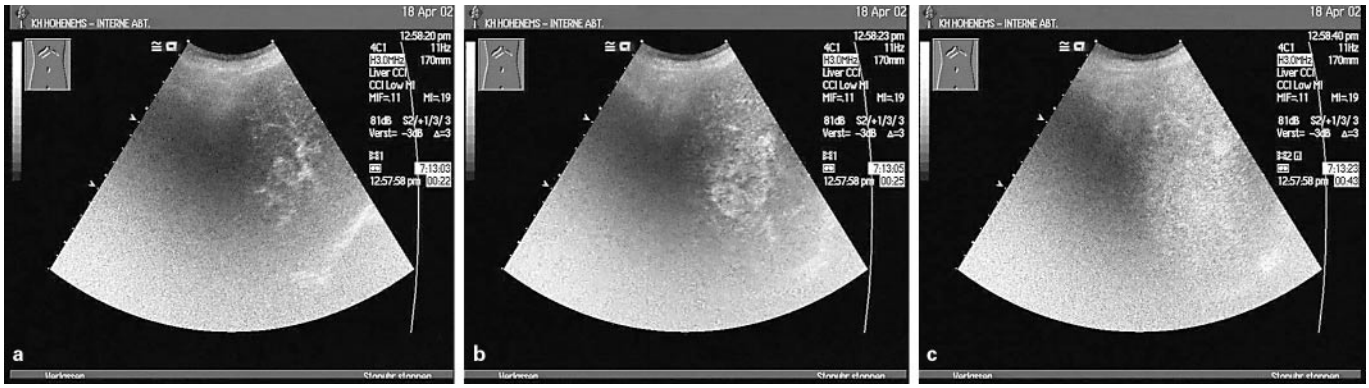

Fig. 3. Contrast-enhanced hepatocellular carcinoma with homogeneous enhancement. 22 s after injection the lesion becomes visible with a strong contrast agent uptake (**a**). 25 s after injection the lesion shows a nodule homogeneous enhancement pattern (**b**). 18 s later in the portal-venous phase the lesion is isoechoic to the surrounding liver parenchyma (**c**).

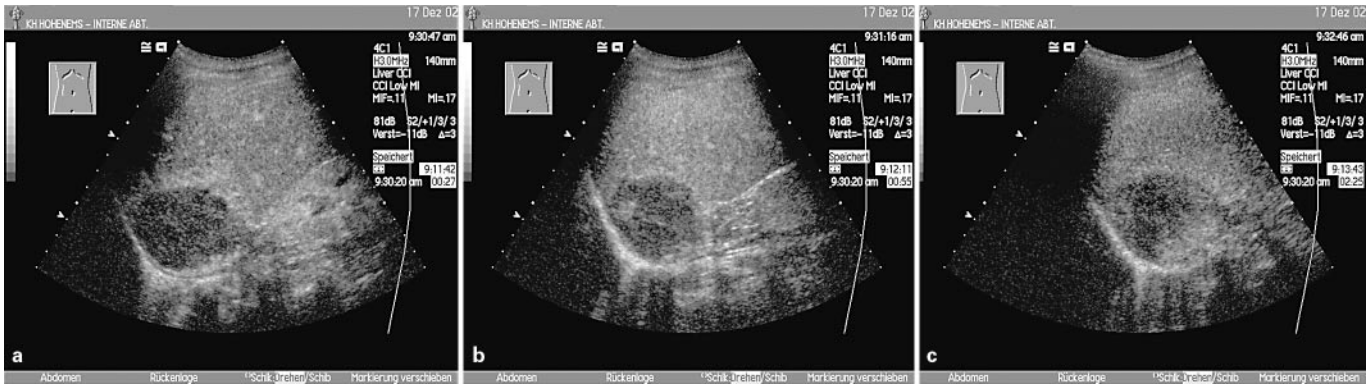

Fig. 4. Signal-enhanced ultrasound of a haemangioma. 27 s after injection a rim-like enhancement is visible (**a**). 55 s after injection it shows a globular enhancement (**b**) with progressive centripetal fill-in, which is not complete in this case (**c**).

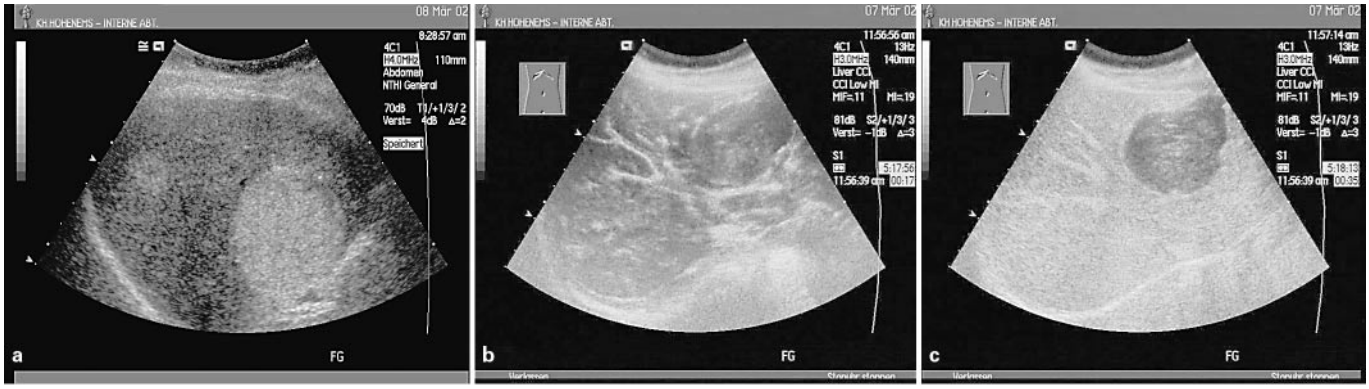

Fig. 5. Thrombosed haemangioma. In the unenhanced grey scale mode a hyperechoic nodule is visible (**a**). In the arterial phase 17 s after injection the lesion shows no signal enhancer uptake (**b**) as well as 35 s after injection (**c**). Conspicious is that the lesion delimits with a clear borderline the surrounding liver parenchyma.

were hypoechoic in the portal-venous phase. Histologically the lesions with the homogeneous pattern corresponded to a high differentiated hepatocellular carcinoma and the lesion with the chaotic pattern to a low differentiated hepatocellular carcinoma.

Benign Focal Liver Lesions

A benign diagnosis was made in 38 cases, which were divided up in 17 haemangiomas, 5 focal nodular hyperplasias, 3 focal fatty infiltrations and 13 focal fatty sparings.

Haemangiomas

Haemangioma was diagnosed in 17 patients and was confirmed by reference methods in all cases. The verification was done in 8 cases by clinical follow-up, in 8 cases by computer tomography, and in another 2 cases by magnetic resonance tomography and fine needle aspiration biopsy. Out of 17 lesions, 16 showed the characteristic peripheral fill-in of ultrasound contrast enhancer (fig. 4), whereas in 1 lesion no signal enhancer uptake was visible (fig. 5). In this case a sharp margin to the surrounding parenchyma was seen and the bases for setting the diagnosis.

Focal Nodular Hyperplasia

The diagnosis of a focal nodular hyperplasia was made in 5 cases and was confirmed in 1 patient by a fine needle aspiration biopsy, 2 cases by computer tomography and in another 2 cases by power Doppler ultrasound examination, following a clinical follow-up. In the arterial phase of the signal-enhanced ultrasound examination a spoke-

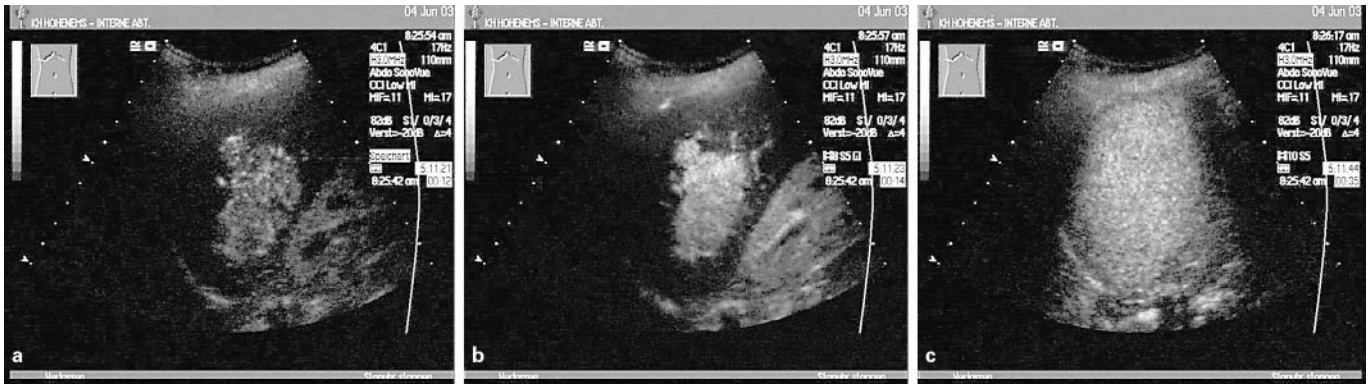

Fig. 6. Focal nodular hyperplasia in CCI low MI mode. 12 s after contrast agent injection (**a**) the lesion shows a strong nodular homogeneous enhancement pattern, which is stronger 2 s later (**b**) and is clearly marked off from the surrounding liver parenchyma. 35 s after signal enhancer injection (**c**) the lesion is no longer visible and is isoechoic.

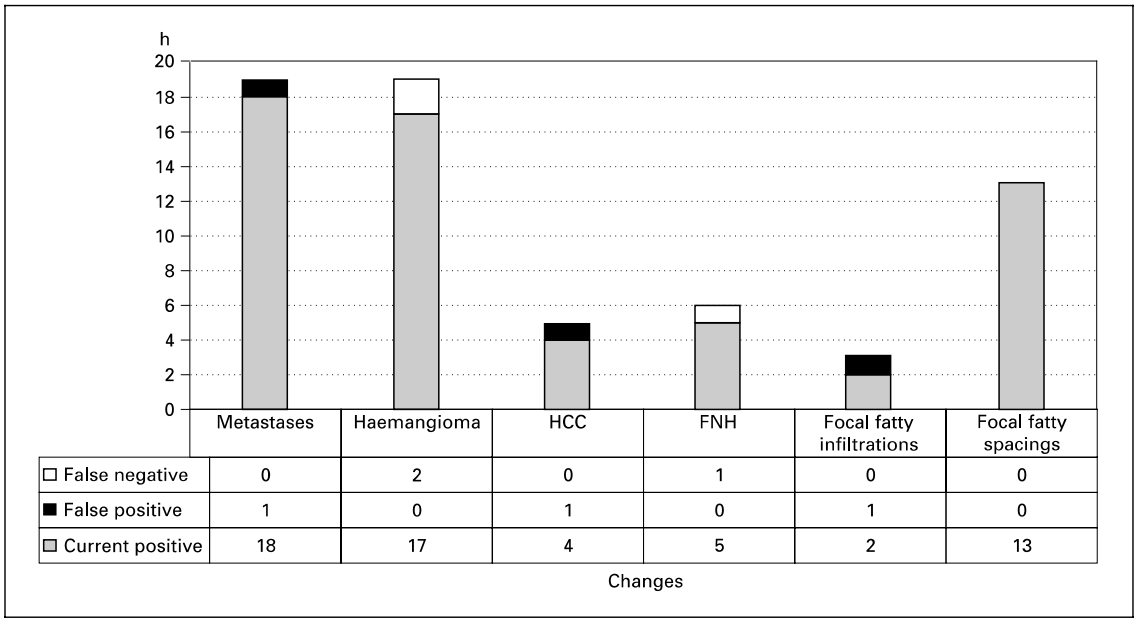

Fig. 7. Distribution of the results.

wheel sign was just seen in 1 case, whereas the other 4 lesions showed a strong and homogeneous enhancement (fig. 6). In the portal-venous phase all 5 lesions had the same enhancement as surrounding area and a central scar was visible just in 1 case.

Benign Metabolic Lesions

In 3 cases, focal fatty infiltration was diagnosed and was confirmed by computer tomography and clinical follow-up in 2 cases. In 1 case the interesting focal liver lesion was classified as haemangioma by computer tomography. Thirteen focal liver lesions were correctly diagnosed as a focal fatty sparing. Verification was carried out by clinical follow-up in 8 cases, computer tomography in 4 cases and in 1 patient by a biopsy.

The lesions showed in all phases the same enhancement as the surrounding liver parenchyma. The differentiation between focal fatty infiltration and focal fatty sparing was made by means of the grey scale image morphology.

In the end, 22 lesions were malignant, divided up into 4 patients with hepatocellular carcinoma and 18 patients with metastases. Out of the 62 examined patients, 40 showed a benign lesion and 22 a malignant liver lesion. The 40 benign lesions were divided up into 19 haemangiomas, 6 focal nodular hyperplasias, 13 focal fatty sparings and 2 focal fatty infiltrations (fig. 7).

Discussion

The main advantage of second-generation ultrasound contrast enhancers compared to first-generation ones results from the use of gas instead of air and from the phospholipid membrane. The sulphur hexafluoride microbubbles remain longer in the bloodstream compared to air-filled ultrasound contrast enhancers because of the poor solubility of gas. Therefore, the liver enhancement is prolonged. The elevated resistance to pressure of the second-generation ultrasound contrast enhancer is based on the use of gas instead of air and furthermore on the phospholipid membrane, which is more flexible than a membrane out of galactose, used in first-generation ultrasound contrast media. A higher resistance to pressure in the capillary system of the chest and also in the left ventricle of the heart is the result [6].

Second-generation ultrasound contrast enhancers have better oscillating qualities in comparison to first-generation ultrasound contrast medias. Therefore, a lower mechanical index is necessary driving the microbubbles to resonance and backscattering harmonic waves [7, 8].

In contrast to the intermittent harmonic imaging method, used by first-generation ultrasound contrast media, the pulse inversion harmonic method allows a continuous ultrasound scan during the whole examination without destroying the microbubbles [9, 10]. Consequently, more information about the enhancement behaviour of different vascular phases of the lesion is obtainable. In the continuous mode it is possible to adjust focus, imaging energy and technical parameters better so that the quality of the ultrasound image is improved and breathing movements of the patient can be compensated more easily [11, 12].

Transit Time from Injection to Ultrasound Contrast Enhancer Arrival in Hepatic Artery (Liver Arrival Time)

According to the literature, time limits for the different phases of liver perfusion are set and very strict [8, 11, 13]. We showed that the liver arrival time of the ultrasound contrast enhancer can be variable, depending on the cardiac output and localisation of the intravenous injection, cubital vein or the dorsum of hand vein. In our study the strict time settings of the several phases were used as an orientation for functional characterization of the liver perfusion. In order to differentiate the perfusion phases, we related the time settings from the literature to the real liver reaching time of the contrast media.

Variability of the Liver Perfusion Pattern

Although according to the literature distinct and characteristic perfusion patterns are associated with each different type of focal liver lesion [11, 14, 15], we could demonstrate in our study that some focal liver lesions can show a variable degree of contrast media enhancement. Especially hepatocellular carcinomas and focal nodular hyperplasia showed overlapping in their perfusion pattern that leads to difficulties in the differential diagnosis. An increased enhancement was visible in both lesions in the arterial phase. However, the increased enhancement of the focal nodular hyperplasia was not associated with the spoke-wheel phenomena in all cases, such as the perfusion pattern of a hepatocellular carcinoma was not always chaotic. The central scar, which is described as characteristic for a focal nodular hyperplasia, was only observed in 1 out of 6 cases of focal nodular hyperplasia. Just as the spoke wheel was only vaguely visible in 1 case, the other 4 showed strong homogeneous arterial enhancement [11, 13]. To conclude, all focal nodular hyperplasias showed a typical strong enhancement in the arterial phase, however in contrast to other authors, a spoke wheel was never by far seen in all cases [4].

The perfusion pattern of a metastasis with good vascularisation can be similar to a hepatocellular carcinoma, which is low differentiated, but in clinical routine this is supposed to be a rather minor problem because of the fact that metastasis seldom occurs in a cirrhotic liver [5]. Additionally, the progressive centripetal fill-in, which is characteristic for haemangioma, is not visible in every case of this lesion [14]. In certain circumstances there is a lack of contrast enhancement in a thrombosed haemangioma and sparing of contrast enhancement occurs in the arterial and portal vein phases, which is normally characteristic for a metastasis [8, 11, 13]. In these cases the spared area of contrast enhancement has very sharp edges in contrast to metastasis with bleared margins. In 1 case of our study, not enough attention was paid to this difference which consequently led to a wrong interpretation. Another interesting point we observed was that as opposed to other authors the arterial perfusion pattern of metastasis was inconclusive of the primary [5, 13].

Limitation of the Maximum Depth

Additional problems occur in liver lesions that are deeper than 12–13 cm. In this depth the enhancement of the contrast medium bubbles is not intensive enough in order to generate a sufficient image. Due to inhomogeneous enhancement it is very difficult to observe a characteristic perfusion pattern. In some cases the distance from surface to the examined liver lesion can be decreased by repositioning the ultrasound transducer. Manufacturers of ultrasound systems offer special software updates for their harmonic imaging method in order to get further improvement in this critical depth.

An extraordinary characteristic of the contrast-enhanced sonography is the possibility of observing and recording of perfusion and behaviour of the ultrasound contrast enhancer in an unclear, possibly pathologic structure [11]. Consequently, characteristic changes of perfusion patterns in time and location are obtained and can be observed in real time. Single pictures are only records of a single moment and lack important information. One study demonstrated that the interpretation of single pictures recorded during a contrast-enhanced ultrasound scan leads to poor results [16]. This is because of the fact that single pictures, especially in contrast-enhanced ultrasound, can be irritating. Therefore, we regard it as mandatory to record the whole examination with an adequate technique.

As an additional advantage of recording the examination, the most interesting sequences, particularly in unclear cases, can be analysed several times in detail. Especially during the introduction period of contrast-enhanced sonography the learning phase of an inexperienced examiner can be shortened and improved. Characteristics of certain lesions can be studied easily and rapidly.

Conclusion

The present study clearly demonstrates that a less experienced examiner without any knowledge of the patient's history can make a correct differential diagnosis in 95% of all cases, even in a blinded study.

References

1 Strobel D, Räkar S, Martus P, Hahn E, Becker D: Nutzen von Harmonic Imaging (Phaseninversionstechnik) in der Differenzierung benigner und maligner Leberläsionen Gastroenterologie. Ultraschall Med 2001;22:S105.

2 Leen E, Becker D, Bolondi L, Steinbach R, Weskott H, Stacul F, Ricci P: Prospective, open-label, multi-centre study evaluating the accuracy of unenhanced versus SonoVue® enhanced ultrasonography in the characterisation of focal liver lesions. Ultrasound Med Biol 2003;29S–S12.

3 Weiss H, Weiss A, Seckinger H: Wie genau ist die morphologische Beschaffenheit umschriebener Leberveränderungen sonographisch bestimmbar? In Walser J et al (eds): Ultraschalldiagnostik '90. Berlin, Springer, 1991, pp 91–93.

4 Hohmann J, Skrok J, Puls R, Albrecht T: Characterization of focal liver lesions with contrast-enhanced low MI real-time ultrasound and SonoVue®. Röfo Fortschr Geb Röntgenstr Neuen Bildgeb Verfahr 2003;175:835–843.

5 Rettenmaier G: Fokale Leberveränderungen; in Rettenmaier G, Seitz K (eds): Sonographie I. Stuttgart, Thieme, 2000, pp 79–162.

6 Bokor D: Diagnostic efficacy of SonoVue®. Am J Cardiol 2000;86S:19G–24G.

7 Correas JM, Bridal L, Lesavre A, Mejean A, Claudon M, Helenon O: Ultrasound contrast agents: Properties, principles of action, tolerance, and artifacts. Eur Radiol 2001;11:1316–1328.

8 Becker D: Kontrastmittelsonographie der Leber mit niedriger Sendeleistung – was ist neu? Ultraschall Med 2002;23:397–402.

9 Heckemann RA, Cosgrove DO, Blomley MJ, Eckersley R, Hervey C, Mine Y: Liver lesions: Intermittent Second-Harmonic Gray-Scale US can increase conspicuity with microbubble contrast material – Early experience. Radiology 2000;216:592–596.

10 Kim AY, Choi BI, Kim TK, Kim KW, Lee JY, Han JK: Comparison of contrast-enhanced fundamental imaging, second-harmonic imaging, and pulse-inversion harmonic imaging. Invest Radiol 2001;36:582–588.

11 Dietrich CF, Becker D: Signalverstärkte Sonographie verbessert Nachweis von Leberraumforderungen. Dtsch Ärzteblatt 1999;24:1410–1415.

12 Solbiati L: From echo-enhancers to ultrasound contrast media: New microbubbles are changing the role of ultrasound. Contrast Enhancement Ultrasound 2001;1.

13 Becker D, Dietrich CF: Leber; in Dietrich CF, Becker D (eds): Signalverstärkte Farbdopplersonographie des Abdomens. Konstanz, Schnetztor, 2002, pp 72–130.

14 Kim TK, Choi BI, Han JK, Hong HS, Park SH, Moon SG: Hepatic tumors: Contrast agent-enhancement patterns with pulse-inversion harmonic US. Radiology 2000;216:411–417.

15 Lim A, Patel N, Eckersley R, Taylor-Robinson S, Martin B, David C: Imaging sciences. Differences in kinetics of SonoVue® and Levovist. Ultrasound Med Biol 2003;29S:11–12.

16 Schuessler G, Ignee A, Dietrich C: Interobserverbeurteilung von Leberraumforderungen – Nativultraschall versus signalverstärkten Ultraschall. Ultraschall Med 2003;S1:V2.3.

Original Article

Digestive Diseases

Dig Dis 2004;22:81–86
DOI: 10.1159/000078739

Accepted: February 7, 2004

Evaluation of Diagnostic Criteria for Liver Metastases of Adenocarcinomas and Neuroendocrine Tumours at Conventional Ultrasound, Unenhanced Power Doppler Sonography and Echo-Enhanced Ultrasound

Steffen Rickes Kenneth W. Ocran Grete Gerstenhauer Holger Neye
Wolfram Wermke

Department of Gastroenterology, Hepatology and Endocrinology, University Hospital Charité (Campus Mitte), Berlin, Germany

Key Words
Liver metastases · Differential diagnosis · Echo-enhanced sonography

Abstract
Purpose: In order to improve the differential diagnosis between liver metastases of neuroendocrine tumours and adenocarcinomas, criteria for the masses at conventional ultrasound, unenhanced power Doppler sonography and echo-enhanced ultrasound were evaluated. ***Methods:*** Seventy-three patients with histologically proven liver metastases of a neuroendocrine tumour (n = 26) or an adenocarcinoma (n = 47) were investigated by conventional ultrasound as well as unenhanced power Doppler sonography and echo-enhanced ultrasound focusing on specific properties of the lesions. ***Results:*** Liver metastases of neuroendocrine tumours and adenocarcinomas showed a different contrast behaviour with echo-enhanced sonography. A hypervascularisation at the arterial and capillary phase were found in 85% of the neuroendocrine metastases, and in 17% of the masses of adenocarcinomas, respectively ($p < 0.05$). ***Conclusions:*** The successful treatment of liver metastases requires a highly sensitive and specific diagnostic procedure for their differentiation. A hypervascularisation of the lesions during the arterial and capillary phase at echo-enhanced ultrasound may point to a neuroendocrine primary tumour. However, histology is the only standard of reference for the differentiation of liver metastases, and is necessary for optimal therapy.

Copyright © 2004 S. Karger AG, Basel

Introduction

Histology is the only standard of reference in the differential diagnosis of liver metastases. Especially it is important to differentiate neuroendocrine tumours from adenocarcinomas because of their relatively good prognosis and special therapy. However, in some patients a percutaneous liver biopsy is impossible because of ascites and/or insufficient coagulation. Furthermore, there is the danger of neoplastic seeding during biopsy. In hepatic masses, the detection and characterisation of tumour vascularity are important for differential diagnosis. Up to now, computed tomography and magnetic resonance imaging have been mainly used as imaging modalities to differentiate

KARGER

Fax + 41 61 306 12 34
E-Mail karger@karger.ch
www.karger.com

© 2004 S. Karger AG, Basel
0257–2753/04/0221–0081$21.00/0

Accessible online at:
www.karger.com/ddi

Dr. S. Rickes, Department of Gastroenterology
Hepatology and Infectiology, Otto von Guericke University Magdeburg
Leipziger Strasse 44, DE–39120 Magdeburg (Germany)
Tel. +49 39 1671 3100, Fax +49 39 1671 3105
E-Mail steffen.rickes@medizin.uni-magdeburg.de

Table 1. Liver metastases of neuroendocrine tumours and adenocarcinomas at conventional ultrasound

Criteria	Liver metastases of neuroendocrine tumours		Liver metastases of adenocarcinomas	
	n	%	n	%
Echogenicity?				
Echogenic	9	35	13	28
Hypoechoic	14	54	26	55
Hyper- and hypoechoic	3	11	8	17
Homogeneity?				
Yes	0	0	1	2
No	26	100	46	98
Hypoechoic margin (halo)?				
Yes	15	58	21	45
No	11	42	26	55
Lobulated margin?				
Yes	26	100	46	98
No	0	0	1	2
Necroses?				
Yes	7	27	9	19
No	19	73	38	81
Calcifications?				
Yes	4	15	8	17
No	22	85	39	83

Table 2. Liver metastases of neuroendocrine tumours and adenocarcinomas at unenhanced power Doppler sonography

Criteria	Liver metastases of neuroendocrine tumours		Liver metastases of adenocarcinomas	
	n	%	n	%
Detection of vessels?				
Yes	12*	46	10*	21
No	14*	54	37*	79
Predominant vessels?				
Arterial vessels	10	83	10	100
Venous vessels	2	17	0	0
Vascular resistance in power Doppler?				
High	0	0	2	20
Low	12	100	8	80
Vessel architecture?				
Peritumoural	6	50	3	30
Intratumoural	3	25	4	40
Peri- and intratumoural	3	25	3	30
Chaotic vascular pattern?				
Yes	7	58	6	60
No	5	42	4	40
Detection of AV shunts?				
Yes	0	0	1	10
No	12	100	9	90
Tumour hypervascularised?				
Yes	6	50	5	50
No	6	50	5	50

* $p < 0.05$.

liver lesions [1]. With conventional transabdominal ultrasound there are no characteristic signs for the differentiation of liver metastases. Echo-enhanced sonography is an increasingly used procedure for the differential diagnosis of liver tumours [2–6].

In the present study, criteria for the differential diagnosis of liver metastases by this procedure were evaluated.

Materials and Methods

Patients

From January 1998 through October 2002, we prospectively studied 73 patients (39 men and 34 women, mean age 58 years, range 26–81 years) with liver metastases of an adenocarcinoma (n = 47) or a neuroendocrine tumour (n = 26). For adenocarcinomas, the primary tumours were located in most cases at the colon and the pancreas. The neuroendocrine primary tumours were found in the pancreas, the ileum and the lung. All malignomas were histologically proven by means of surgery, percutaneous or endoscopic biopsy. The patients gave their informed consent to participate in the study.

Techniques

Conventional Percutaneous Ultrasound. The patients were investigated by an experienced examiner blinded for the patients' history, symptoms and other laboratory and imaging findings. A dynamic 2- to 5-MHz sector scanner (HDI 3000 and 5000, Philips Ultrasound) was used. One corresponding liver lesion per patient was evaluated concerning specific criteria, shown in table 1.

Unenhanced Power Doppler Sonography and Echo-Enhanced Ultrasound. The same liver mass was further investigated using the criteria shown in table 2 with unenhanced power Doppler sonography followed by echo-enhanced ultrasound with 2nd Harmonic or Pulse Inversion Imaging. Echo-enhanced power Doppler sonography with 2nd Harmonic Imaging was commenced immediately after bolus injection of 4 g Levovist® (concentration 300 mg/ml). One focus zone with depth adapted to the area of interest and a mechanical index of 0.8–1.3 were used.

For echo-enhanced sonography with Pulse Inversion Imaging, 2.4 ml SonoVue® was injected, and the mechanical index varies between 0.1 and 0.2. As for echo-enhanced power Doppler sonography the investigation lasted approximately 2 min.

A chaotic vascular pattern was defined as detection of terminated vessels and a irregular course of the vessels. Arteriovenous shunts are characterised by a high diastolic blood flow on the arterial side and pulsatile spectra on the venous side.

Statistical Analysis

Data analysis was done with SPSS® (version 10.0). The percentage of each criteria detected was determined for conventional ultrasound as well as for unenhanced power Doppler sonography and

echo-enhanced sonography. χ^2 test was used to find significant differences between the metastases of adenocarcinomas and neuroendocrine tumours. p values <0.05 were considered to be significant.

Results

Conventional Ultrasound (table 1)

The mean size of the liver metastases investigated was 42 ± 25 mm (range 9–100) for neuroendocrine tumours, and 45 ± 29 mm for adenocarcinomas (range 10–120), respectively (p = n.s.). There was a small higher percentage of echogenic and sharply delineated neuroendocrine metastases compared with the lesions of adenocarcinomas. However, these differences were not significant. With respect to the other criteria investigated, no differences could be found between the lesions of neuroendocrine tumours and adenocarcinomas, respectively.

Unenhanced Power Doppler Sonography (table 2)

With unenhanced power Doppler sonography, vessels were detected in metastases of neuroendocrine tumours more frequently compared with the lesions of adenocarcinomas (46 vs. 21%, $p < 0.05$). In most cases, arteries with a low resistance were found. Peritumoural vessels could be observed in 50% of the neuroendocrine metastases, and in 30% of the lesions of adenocarcinomas, respectively (p = n.s.).

Echo-Enhanced Sonography (table 3)

After injection of an echo-enhancer the liver metastases were found to be hypervascularised in 85% of the neuroendocrine tumours, and in 17% of the adenocarcinomas, respectively ($p < 0.05$). Furthermore, neuroendocrine lesions showed a chaotic vascularisation pattern and a sharp delineation at the capillary phase more frequently ($p < 0.05$). At the portal venous phase, nearly all metastases were visible as a contrast defect. A liver metastasis of a neuroendocrine tumour and an adenocarcinoma of the colon before and after injection of an echo-enhancer are shown in figures 1 and 2, respectively.

Table 3. Liver metastases of neuroendocrine tumours and adenocarcinomas at echo-enhanced sonography

Criteria	Liver metastases of neuroendocrine tumours		Liver metastases of adenocarcinomas	
	n	%	n	%
Arterial and capillary phase (10–35 s after injection)				
Peritumoural signal enhancement?				
Yes	16	62	26	55
No	10	38	21	45
Chaotic vascular pattern?				
Yes	23*	88	30*	64
No	3*	12	17*	36
Detection of AV shunts?				
Yes	0	0	1	2
No	26	100	46	98
Contrast behaviour?				
Centrifugal	0	0	1	2
Centripetal	20	77	44	94
Centripetal and centrifugal	6	23	2	4
Lesion sharply delineated?				
Yes	19*	73	23*	49
No	7*	27	24*	51
Tumour hypervascularised?				
Yes	22*	85	8*	17
No	4*	15	39*	83
Portal venous phase (30–90 s after injection)				
Detection of a contrast defect?				
Yes	25	96	46	98
No	1	4	1	2

* $p < 0.05$.

Discussion

The liver is one of the most common sites of metastases from adenocarcinomas and neuroendocrine tumours. It is important to differentiate between both tumour entities because neuroendocrine metastases have a generally better prognosis and need a special therapy.

Histology is the gold standard in the differentiation of liver lesions. It is accepted that in most cases, percutaneous biopsy is safe, accurate, and enables a definitive diagnosis to be made quickly [7–9]. However, some problems, such as the possibility of neoplastic seeding, present limitations [10, 11]. Furthermore, in some patients a percutaneous liver biopsy is impossible because of ascites and/or insufficient coagulation. On the other hand, differentiation of liver metastases is difficult by imaging techniques.

Up to now, computed tomography and magnetic resonance imaging with newer liver-specific contrast agents are mainly used with good results to diagnose and differentiate liver tumours. Magnetic resonance imaging has become a standard in different departments, where transplantation of the liver is performed [12]. However, computed tomography and magnetic resonance imaging are

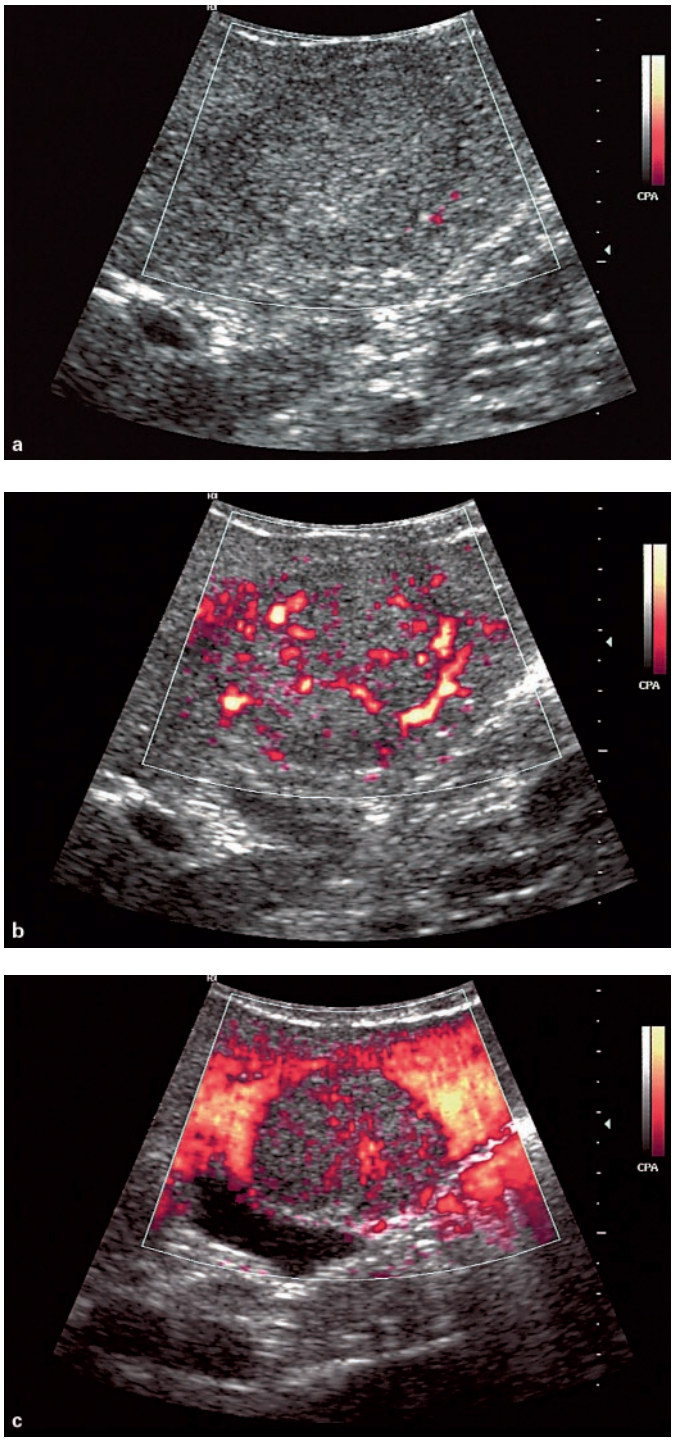

Fig. 1. Liver metastasis of a small bowel neuroendocrine tumour at unenhanced (**a**) and echo-enhanced sonography (**b**, **c**). **a** Hypoechoic lesion with a lobulated margin. **b** Detection of a hypervascularised mass at the capillary phase 30 s after injection of the echo-enhancer. **c** Detection of a contrast defect at the portal venous phase 40 s after injection of the echo-enhancer.

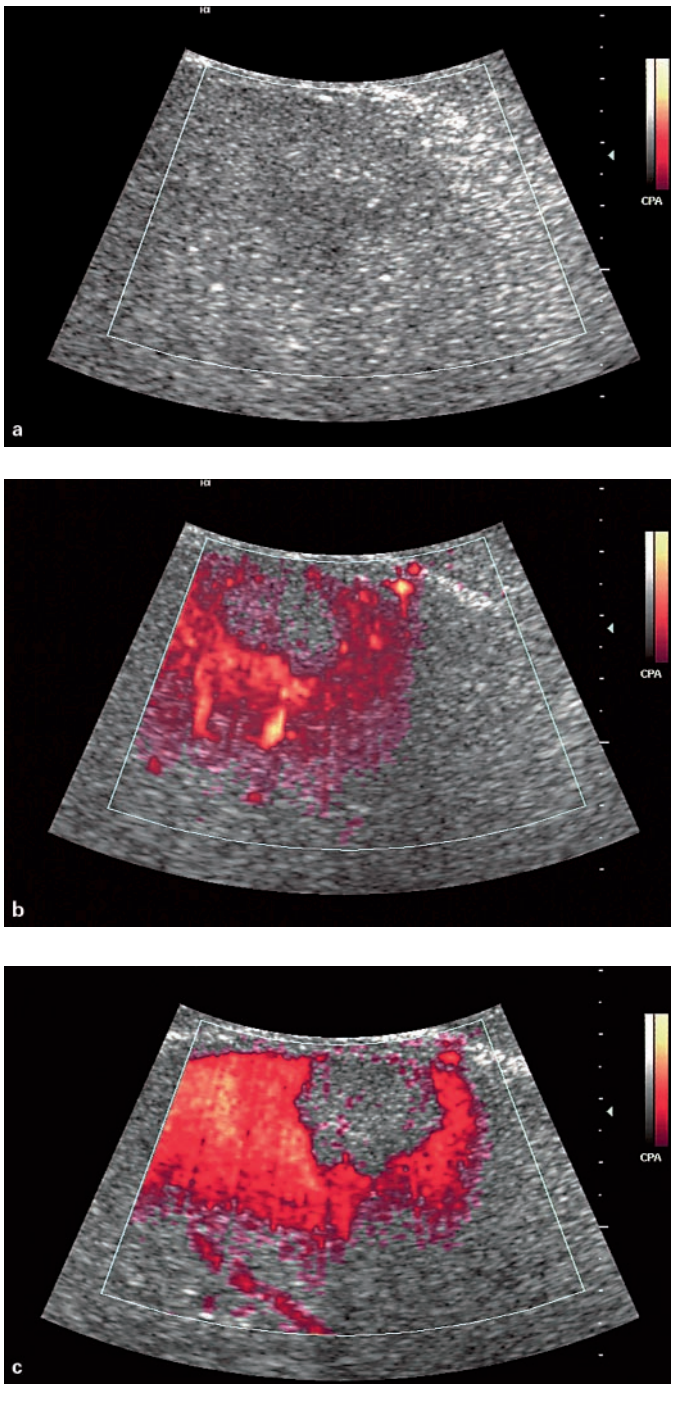

Fig. 2. Liver metastasis of a colorectal adenocarcinoma at unenhanced (**a**) and echo-enhanced sonography (**b**, **c**). **a** Hypoechoic lesion with a lobulated margin. **b** Detection of a hypovascularised mass at the capillary phase 30 s after injection of the echo-enhancer. **c** Detection of a contrast defect at the portal venous phase 40 s after injection of the echo-enhancer.

expensive. A non-invasive and cost-efficient method with high diagnostic accuracy is, therefore, required.

A major problem is that there are no characteristic signs for different liver metastases in conventional ultrasound. Thus, it is difficult to distinguish the lesions with this technique. With respect to the criteria investigated by B-mode sonography, no significant differences were found between the metastases of neuroendocrine tumours and adenocarcinomas in the present study. There was a higher percentage of echogenic and sharply delineated neuroendocrine lesions, but finally both tumour entities may present with an echogenic pattern as well as a hypoechoic and lobulated margin.

Computed tomography and magnetic resonance imaging have the advantage to investigate the vascularisation pattern in the differentiation of liver lesions. Whereas metastases of adenocarcinomas are characterised by their hypovascularisation, lesions of neuroendocrine tumours were found to be often hypervascularised [13].

Unenhanced power Doppler sonography allows the investigation of the vascularisation pattern of liver and pancreatic tumours by ultrasound as well [14–18]. However, there are problems of low sensitivity for detecting small vessels or low blood flow velocity, and the existence of multiple tissue artefacts [2]. In the present study, vessels were detected with this procedure in metastases of neuroendocrine tumours more frequently. However, a differential diagnosis of liver metastases is difficult with this sonographic technique alone.

In recent years, the sensitivity of unenhanced power Doppler sonography for detecting low blood flow velocity or small vessels has improved by echo-enhancers, for example Levovist®. This preparation consists of microbubbles of air which enhance the Doppler signal at 20–30 dB [2, 19, 20]. With echo-enhanced sonography, however, the signal intensity from flowing blood is lower compared to that of tissue movements. 2nd Harmonic Imaging was developed to overcome these difficulties. This method is based on the property of microbubbles to resonate and emit harmonic waves in an ultrasound field with a frequency of 1–5 MHz. If the harmonic frequency is to be detected at twice the transmitted frequency, the procedure is called 2nd Harmonic Imaging. Tissue particles have fewer 2nd harmonic waves than microbubbles, so the signals of echo-enhancers are better distinguishable [2, 19, 20].

Recently, the new contrast agent Sonovue® is being used more frequently for echo-enhanced sonography. Furthermore, 2nd Harmonic Imaging was replaced partially by the Pulse Inversion Imaging technique. There are remarks that with this new procedure more favourable results can be achieved than with 2nd Harmonic Imaging. With 2nd Harmonic Imaging it is impossible to separate the transmitted and received harmonic signal completely because of limited bandwidth. However, Pulse Inversion Imaging avoids these bandwidth limitations by using characteristics specific to microbubble vibrations to subtract rather than filter out the fundamental. Because this imaging transmits two reciprocal pulses, leading to subtract fundamental signals, it can allow the use of broader transmit and receive bandwidths for improved resolution and can provide increased sensitivity to contrast [21]. However, comparative results of large prospective studies are missing.

In the present study a high percentage (85%) of the neuroendocrine metastases was hypervascularised with echo-enhanced sonography. However, a hypervascularisation was observed also in about 20% of the metastases of adenocarcinomas. That means that a reliable differentiation of both tumour entities is impossible with this procedure. Furthermore, in our own experience, liver metastases of other primary tumours, like melanomas, may also be well vascularised.

The successful treatment of liver metastases requires a highly sensitive and specific diagnostic procedure for their differentiation. A hypervascularisation at echo-enhanced ultrasound may point to a neuroendocrine primary tumour. However, histology is the standard of reference for the differentiation of liver metastases, and is necessary for optimal therapy.

References

1 Kanematsu M, Hoshi H, Yamada T, et al: Small hepatic nodules in cirrhosis: Ultrasonographic, CT, and MR imaging findings. Abdom Imaging 1999;24:47–55.

2 Wermke W, Gaßmann B: Tumour Diagnostics of the Liver with Echo Enhancers. Berlin, Springer, 1998, pp 26–194.

3 Fracanzani AL, Burdick L, Borzio M, et al: Contrast-enhanced Doppler ultrasonography in the diagnosis of hepatocellular carcinoma and premalignant lesions in patients with cirrhosis. Hepatology 2001;34:1109–1112.

4 Rickes S, Ocran K, Schulze S, Wermke W: Evaluation of Doppler sonographic criteria for the differentiation of hepatocellular carcinomas and regenerative nodules in patients with liver cirrhosis. Ultraschall Med 2002;23:83–90.

5 Beissert M, Delorme S, Mutze S, et al: Comparison of B-mode and conventional colour/power Doppler ultrasound, contrast-enhanced Doppler ultrasound and spiral CT in the diagnosis of focal lesions of the liver: Results of a multicentre study. Ultraschall Med 2002;23:245–250.

6 Rickes S, Schulze S, Neye H, Ocran KW, Wermke W: Improved diagnosing of small hepatocellular carcinomas by echo-enhanced power Doppler sonography in patients with cirrhosis. Eur J Gastroenterol Hepatol 2003;15:893–900.

7 Buscarini L, Fornari F, Bolondi L, et al: Ultrasound-guided fine-needle biopsy of focal liver lesions: Techniques, diagnostic accuracy and complications. A retrospective study on 2,091 biopsies. J Hepatol 1990;11:344–348.

8 Borzio M, Borzio F, Macchi R, et al: The evaluation of fine-needle procedures for the diagnosis of focal liver lesions in cirrhosis. J Hepatol 1994;20:117–121.

9 Limberg B, Hopker WW, Kommerell B: Histologic differential diagnosis for focal liver lesions by ultrasonically guided fine needle biopsy. Gut 1987;28:237–241.

10 Navarro F, Taourel P, Michel J, et al: Diaphragmatic and subcutaneous seeding of hepatocellular carcinoma following fine-needle aspiration biopsy. Liver 1998;18:251–254.

11 Weimann A, Ringe B, Klempnauer J, et al: Benign liver tumors: Differential diagnosis and indications for surgery. World J Surg 1995;19:13–18.

12 Kim JH, Kim MJ, Suh SH, Chung JJ, Yoo HS, Lee JT: Characterization of focal hepatic lesions with ferumoxides-enhanced MR imaging: Utility of T1-weighted spoiled gradient recalled echo images using different echo times. J Magn Reson Imaging 2002;15:573–583.

13 Chiti A, Fanti S, Savelli G: Comparison of SRI, CT and US in the clinical management of neuroendocrine gastro-entrero-pancreatic tumors. Eur J Nucl Med 1998;25:1396–1403.

14 Koito K, Namieno T, Morita K: Differential diagnosis of small hepatocellular carcinoma and adenomatous hyperplasia with power Doppler sonography. AJR 1998;170:157–161.

15 Rickes S, Flath B, Wermke W, et al: Pancreatic metastases of renal cell carcinomas – Evaluation of the contrast behaviour at echo-enhanced power Doppler sonography in comparison to primary pancreatic tumours. Z Gastroenterol 2001;39:571–578.

16 Rickes S, Unkrodt K, Neye H, Ocran KW, Wermke W: Differentiation of pancreatic tumours by conventional ultrasound, unenhanced and echo-enhanced power Doppler sonography. Scand J Gastroenterol 2002;37:1313–1320.

17 Rickes S, Unkrodt K, Ocran K, Neye H, Wermke W: Differentiation of neuroendocrine tumours from other pancreatic lesions by echo-enhanced power Doppler sonography and somatostatin receptor scintigraphy. Pancreas 2003;26:76–81.

18 Rickes S, Unkrodt K, Wermke W, et al: Evaluation of Doppler sonographic criteria for the differentiation of pancreatic tumours. Ultraschall Med 2000;20:253–258.

19 Calliada F, Campani R, Bottinelli O, Bozzini A, Sommaruga MG: Ultrasound contrast agents. Basic principles. Eur J Radiol 1998;27:157–160.

20 Correas JM, Hélénon O, Pourcelot L, Moreau JF: Ultrasound contrast agents. Examples of blood pool agents. Acta Radiol 1997;38:101–112.

21 Kim AY, Choi BI, Kim TK, Kim KW, Lee JY, Han JK: Comparison of contrast-enhanced fundamental imaging, second-harmonic imaging, and pulse-inversion harmonic imaging. Invest Radiol 2001;36:582–588.

Original Article

Digestive Diseases

Dig Dis 2004;22:87–91
DOI: 10.1159/000078740

Accepted: April 27, 2004

A Community-Based Epidemiologic Study on Gallstone Disease among Type 2 Diabetics in Kinmen, Taiwan

Chi-Ming Liu[a,b] Tao-Hsin Tung[a] Jorn-Hon Liu[b] Wen-Ling Lee[b,c] Pesus Chou[a]

[a]Community Medicine Research Center & Institute of Public Health, National Yang-Ming University, [b]Cheng-Hsin Rehabilitation Medical Center, and [c]Institute of Clinical Medicine, School of Medicine, National Yang-Ming University, Taipei, Taiwan

Key Words
Type 2 diabetes · Gallstone disease, prevalence · Community-based study

Abstract
Background: This study was conducted to assess the prevalence and associated risk factors of gallstone disease (GSD) among type 2 diabetics in Kinmen, Taiwan. ***Methods:*** Based on a total of 858 type 2 diabetics ascertained in 1991–1993, an ultrasound sonography screening was performed by a panel of specialists in 2001. A total of 440 (51.3%) subjects were examined. ***Results:*** Sixty-three out of 440 type 2 diabetics were diagnosed with GSD. The overall prevalence of GSD was 14.4%, including single stone 8.0% (n = 35), multiple stones 3.2% (n = 14), and cholecystectomy 3.2% (n = 14). The significant risk factors of GSD based on multiple logistic regression analysis were age (OR = 1.06, 95% CI: 1.02–1.10) and BMI (OR = 1.11, 95% CI: 1.01–1.22). ***Conclusions:*** Our results found that older age and higher BMI may increase the risk of developing GSD in type 2 diabetics.

Copyright © 2004 S. Karger AG, Basel

Introduction

Gallstone disease (GSD) is one of the most common diseases in developed countries. The prevalence of GSD increases with age and reaches 30% by the age 70 years in Western countries [1, 2]. Based on a community sonographic survey in Taiwan, the prevalence of GSD in the general population aged 30 years or more was 4.3% in 1989 [3]. Another voluntary screening in 1995 showed that the prevalence of GSD had reached 10.7% among healthy subjects [4]. For this reason, due to westernization of diet and environment, GSD was not rare in the Chinese population and had become a major health problem in Taiwan.

The etiology of GSD is multifactorial and associated factors related to GSD include age, sex, genetic factors, obesity, parity, diet, drugs, hyperlipidemia, ileal diseases and hemolytic anemias [5]. In addition, it has been a matter of controversy whether diabetes mellitus is associated with GSD or not. Some epidemiologic studies showed that diabetes was mentioned as a risk factor of GSD, but such an association has not consistently been observed in other population-based studies [6, 7]. From a clinical viewpoint, type 2 diabetes combined with gallstone may induce acute cholecystitis more often, and have a higher

KARGER

Fax + 41 61 306 12 34
E-Mail karger@karger.ch
www.karger.com

© 2004 S. Karger AG, Basel
0257–2753/04/0221–0087$21.00/0

Accessible online at:
www.karger.com/ddi

Dr. Pesus Chou
Community Medicine Research Center
National Yang-Ming University
Shih-Pai, Taipei 112 (Taiwan)
Tel. +886 2 2826 7050, Fax +886 2 2820 1461, E-Mail pschou@ym.edu.tw

probability to progress to septicemia. Furthermore, it is generally believed that diabetics secrete more lithogenic bile than non-diabetics [8]. The previous study also showed that prevalence of GSD among type 2 diabetes was about 2- to 3-fold more common compared with the normal population [9].

In order to identify the prevalence and associated factors of GSD among type 2 diabetics, a community-based screening for early detection of GSD was required. Early cases of GSD can be ascertained from these type 2 diabetics via real-time ultrasound sonography examination. However, there were few community-based epidemiological studies focused on the prevalence of GSD among type 2 diabetics in Taiwan. In the present study, we conducted a community-based screening program for GSD in order to assess the prevalence and associated risk factors with GSD among type 2 diabetics in Kinmen, Taiwan.

Materials and Methods

Data Resources

Data used in this study was derived from a community-based screening in Kinmen, Taiwan. According to population stability, geographic area and local support, Kinmen was selected to carry out the screening concept of community diseases. The details of the study design and execution have been described in full elsewhere [10]. The diagnosis of type 2 diabetes was based on the 1999 WHO definition [11]. A total of 1,123 type 2 diabetics aged 30 and over were found based on the population survey in 1991–1993 carried out in Kinmen. Of 1,123 type 2 diabetics, after excluding those who had migrated or died, the remaining 858 type 2 diabetics formed a cohort to receive abdominal ultrasound sonography. These 858 subjects were invited to receive screening for GSD by telephone calls or invitation letters in 2001. Informed consent was obtained from all participants before the survey.

Data Collecting

Two steps of data collection were conducted in the present study. Firstly, baseline information was collected in 1991–1993. Face-to-face interviews were conducted by the Yang-Ming Crusade, a volunteer organization of well-trained medical students of National Yang-Ming University. Fasting blood samples were drawn by public health nurses. Overnight fasting serum and plasma samples (preserved with EDTA and NaF) were collected and kept frozen (–20°C) until analysis. Fasting plasma glucose (FPG) concentrations were determined using the hexokinase glucose-6-phosphate dehydrogenase method with a glucose (HK) reagent ldt (Gilford Co., Berlin, Ohio, USA). Secondly, the follow-up screening regimen of GSD was performed in 2001. Based on the presence of movable hyperechoic material with acoustic shadow [4, 12], GSD was diagnosed by a panel of specialists using a real-time ultrasound sonography to examine the participants' abdominal region after fasting for at least 8 h. The cases of GSD were classified as follows: single gallbladder stone, multiple gallbladder stones, and cholecystectomy, excluding gallbladder polyps. The non-cases were identified as no GSD among type 2 diabetics.

Table 1. Response rate of screening for GSD among type 2 diabetics in Kinmen, 2001

Variable	Eligible population	Screened population	Response rate, %
Sex			
Male	369	193	52.3
Female	489	247	50.5
Age			
40–49	90	45	50.0
50–59	174	97	55.7
60–69	269	157	58.4
70+	325	141	43.4
Total	858	440	51.3

In order to set up the consistent diagnosis of GSD between specialists, the κ statistic was used to assess the agreement of interobserver reliability among study specialists. The pilot study was performed with 50 random selected type 2 diabetics other than the study subjects. For the interobserver reliability, the κ value for diagnosis of GSD was 0.77 (95% CI: 0.50–0.96).

Statistics Analysis

Statistical analysis was performed using SAS software. In the univariate analysis, independent t-test was applied for continuous variables. Multiple logistic regression was used to investigate the independence of factors associated with GSD. Odds ratio and 95% confidence intervals were used for categorical variables. Findings were considered to be statistically significant at the $p < 0.05$ level.

Results

Of 858 type 2 diabetics, 440 subjects attended the real-time ultrasound sonography for examination of the abdominal region. The overall response rate was 51.3%. The majority of baseline factors associated with the risk of type 2 diabetes in attendants were similar to those in non-attendants except that the age of non-attendants was statistically significant older than attendants. Other baseline biochemical factors (including FPG, SBP, DBP, total cholesterol, triglyceride, HDL, LDL, BUN, creatinine, uric acid, BMI, and waist-hip ratio) associated with the risk of type 2 diabetes for attendants were not significantly different from those for non-attendants. Table 1 shows that males had a slightly higher response rate than females (52.3 vs. 50.5%), and the adults aged 60–69 (58.4%) and 50–69 (55.7%) years had a higher response rate than other age groups.

Table 2 shows that the overall prevalence of GSD among type 2 diabetics aged 40 and over was 14.4%,

Table 2. Prevalence of GSD among type 2 diabetics in Kinmen, 2001

Variable	Total number of diabetics	Gallstone disease							
		subtotal prevalence[1]		single stone prevalence		multiple stones prevalence		cholecystectomy prevalence	
		n	%	n	%	n	%	n	%
Sex									
Male	193	26	13.5	16	8.3	5	2.6	5	2.6
Female	247	37	14.9	19	7.7	9	3.6	9	3.6
Age									
40–49	45	1	4.4	1	2.2	0	0.0	1	2.2
50–59	97	10	10.3	7	7.2	1	1.0	2	2.1
60–69	157	23	14.7	9	5.7	7	4.5	7	4.5
70+	141	28	19.9	18	12.8	6	4.3	4	2.8
Total	440	63	14.4	35	8.0	14	3.2	14	3.2

[1] Cochran-Armitage trend test for age (z = 3.18, p = 0.002).

Table 3. Comparison of characteristics between GSD subjects and controls among type 2 diabetics in Kinmen (mean ± SD)

Variable	Gallstone disease		p value for t test
	yes (n = 63)	no (n = 377)	
Age, years	68.3 ± 9.7	64.3 ± 10.9	0.006
Duration of diabetes years	9.6 ± 2.2	9.4 ± 2.8	NS
FPG, mg/dl	149.3 ± 44.5	142.9 ± 56.0	NS
BMI, kg/m^2	26.3 ± 3.8	25.3 ± 3.6	0.046
SBP, mm Hg	145.4 ± 22.5	139.0 ± 23.2	0.032
DBP, mm Hg	86.8 ± 13.6	84.5 ± 13.3	NS
Triglyceride, mg/dl	116.4 ± 58.9	132.9 ± 80.5	NS
Total cholesterol, mg/dl	219.6 ± 57.7	214.1 ± 41.4	NS
HDL, mg/dl	53.5 ± 30.7	54.2 ± 29.1	NS
AST, U/l	25.9 ± 17.9	23.4 ± 14.4	NS
ALT, U/l	31.7 ± 35.5	125.4 ± 22.0	NS
Uric acid, mg/dl	115.7 ± 1.5	116.0 ± 1.7	NS

Table 4. Multiple logistic regression on the risk factors associated with the GSD among type 2 diabetics in Kinmen

Variable	GSD vs. non-GSD	
	OR	95% CI
Intercept	−8.53	–
Age, years	1.06	1.02–1.10
BMI, kg/m^2	1.11	1.01–1.22

Independent variables: sex, age, duration of type 2 diabetes, fasting plasma glucose, BMI, SBP, DBP, cholesterol, triglyceride, HDL, uric acid, ALT, and AST.

including 8.0% (n = 35) of single stone, 3.2% (n = 14) of multiple stones, and 3.2% (n = 14) of cholecystectomy. The number of females (14.9%) was not statistically higher than males (13.5%) ($p > 0.05$). From the Cochran-Armitage trend test, the prevalence of GSD shows an increase with age (z = 3.18, p = 0.002). In addition, subjects aged 60 years and over (51/298 = 17.1%) had a more than 2-fold risk for GSD as compared with the subjects aged 40–59 years (11/142 = 7.7%).

Table 3 shows the comparisons of baseline (1991–1993) variables between the GSD and non-GSD group. From the independent t-test, baseline factors that were significantly related to GSD included age (cases (68.3 ± 9.7 years) vs. non-cases (64.3 ± 10.9 years), t = 2.74, p = 0.006), BMI (cases (26.3 ± 3.8 kg/m^2) vs. non-cases (25.3 ± 3.6 kg/m^2), t = 2.00, p = 0.046), and SBP (cases (145.4 ± 22.5 mm Hg) vs. non-cases (139.0 ± 23.2 mm Hg), t = 2.15, p = 0.032).

The effects of independent risk factors of GSD were examined by the multiple logistic regression model. Table 4 shows that, after adjustment for other associated confounding factors, the independent risk factors of GSD were age (OR = 1.06, 95% CI: 1.02–1.10), and BMI (OR = 1.11, 95% CI: 1.01–1.22).

Discussion

Implications of Associated Factors for GSD

Our findings revealed that the prevalence of overall GSD was lower than other similar population-based surveys [13]. The underestimation of the prevalence of GSD due to a relative lower response rate and younger age of participants in our study may account for the major cause. Using the different methodology of GSD assessment could also affect the comparison of prevalence. In addition, regarding diabetes mellitus and GSD, evidence from the positive association was still obviously inconclusive because of potential detection bias. In the present study, the prevalence of overall GSD was higher than the general Chinese population in Taiwan when using the same methodology of GSD assessment [4]. Previous population-based studies had resulted in disparate findings on diabetes mellitus and GSD [14]. Like findings in other studies [4, 13, 15], our results also implied that type 2 diabetes could be viewed as one of positive risk factors to GSD.

Most epidemiologic studies had revealed that females had a higher prevalence of GSD than males [16]. Pregnancy and sex hormones could be involved by altering biliary secretion or gallbladder motility, or both maybe play an important role on the sex-related difference in prevalence of GSD [16, 17]. However, our findings also showed similar results, but the prevalence of GSD was not statistically significant different between males and females.

It was not surprising that age was one of the positive risk factors for GSD in the present study. It had been observed that among the elderly, larger amounts of cholesterol were secreted by the liver, and the catabolism of cholesterol to bile acid decreased [18, 19]. It had also been recommended that diabetic subjects should be referred for cholecystography on more liberal grounds than other subjects [20]. The long-term exposure to other risk factors among the elderly also may account for their increased chance of developing GSD, such as longer duration of type 2 diabetes [4, 21]. Furthermore, cholelithiasis was an acquired disease determined by chronic environmental factors plus the aging effect [3].

We simultaneously demonstrated a positive association between BMI and GSD after adjusting for other related confounding factors in the present study. Many epidemiological population-based studies had indicated that GSD was more common in obese subjects [4, 15, 22]. From the clinical perspective, supersaturated bile was the linkage between obesity and cholesterol GSD. Obesity could raise the saturation of bile by increasing biliary secretion of cholesterol – the latter depending probably on a higher synthesis of cholesterol in obese subjects [16, 23].

In addition, the present study showed that SBP was significantly and positively associated with GSD in the univariate analysis but not in the multivariate analysis. The result was consistent with other community-based studies for the general population [4]. Age may possibly dilute the effect of blood pressure for GSD in type 2 diabetic subjects. However, further epidemiological and etiologic investigations were needed to clarify the pathophysiological mechanisms between blood pressure and GSD among diabetic populations.

Methodological Consideration

The present study had several methodological advantages. Firstly, based on the community-based epidemiologic study design, the GSD and non-GSD groups were unselectively evaluated by ultrasonography and selection bias could be prevented. Secondly, biomarker results were assessed by the standard procedures in a central laboratory and possible measurement errors could also be eliminated. Nevertheless, the potential impact on the prevalence and associations with GSD in our estimates were inevitable due to a relatively lower response rate, and non-attendants with older age indicated that subjects may have died or did not return for follow-up. GSD was diagnosed only at follow-up in 2001 and therefore we could not clarify the temporality between biomedical makers and GSD. Another possible drawback in the present study was the initiating screening program for GSD in type 2 diabetics that was conducted after 8 years of mass screening and where the bias due to delayed diagnosis of GSD could have occurred.

Conclusion

In conclusion, we have shown that in type 2 diabetics, an older age and higher BMI may increase the risk of developing GSD in type 2 diabetics. These results suggest that factors related to type 2 diabetes may be important in the pathogenesis mechanism of the increased risk of GSD among type 2 diabetics.

Acknowledgements

This study was supported by the grants from the National Science Council (NSC-91-2320-B-010-056) and Cheng Hsin Rehabilitation Medical Center (90-3).

References

1 Jorgensen T: Prevalence of gallstones in a Danish population. Am J Epidemiol 1987;126: 912–921.
2 Jorgensen T, Kay L, Schultz-Larsen K: The epidemiology of gallstones in a 70-year-old Danish population. Scand J Gastroenterol 1990;25: 335–340.
3 Lu SN, Chang WY, Wang LY, Hsieh MY, Chuang WL, Chen SC, Su WP, Tai TY, Wu MM, Chen CJ: Risk factors for gallstones among Chinese in Taiwan: A community sonographic survey. J Clin Gastroenterol 1990;12: 542–546.
4 Chen CY, Lu CL, Huang YS, Tam TN, Chao Y, Chang FY, Lee SD: Age is one of the risk factors in developing gallstone disease in Taiwan. Age Ageing 1998;27:437–441.
5 Sama C, Labate AMM, Taroni F, Barbara L: Epidemiology and natural history of gallstone disease. Semin Liver Dis 1990;10:149–158.
6 Santis ADE, Attili AF, Ginanni CS, Scafato E, Cantagalli A, Luca DEC, Pinto G, Lisi D, Capocaccia L: Gallstones and diabetes: A case-control study in a free-living population sample. Hepatology 1997;25:787–790.
7 Kono S, Shinchi K, Todoroki I, Honjo S, Sakurai Y, Wakabayashi K, Imanishi K, Nishikawa H, Ogawa S, Katsurada M: Gallstone disease among Japanese men in relation to obesity, glucose intolerance, exercise, alcohol use, and smoking. Scand J Gastroenterol 1995;30:372–376.
8 Ponz de Leon M, Ferenderes R, Carulli N: Bile lipid composition and bile acid pool size in diabetes. Dig Dis Sci 1978;23:710–716.
9 Feldman M, Felman M Jr: The incidence of cholelithiasis, cholesterolosis and liver disease in diabetes mellitus. An autopsy study. Diabetes 1954;3:305–307.
10 Chou P, Liao M J, Kuo HS, Hsiao KJ, Tsai ST: A population survey on the prevalence of diabetes in Kin-Hu, Kinmen. Diabetes Care 1994; 17:1055–1058.
11 WHO: Definition, Diagnosis and Classification of Diabetes mellitus and Its Complications: Report of a WHO Consultation. 1. Diagnosis and Classification of Diabetes mellitus. Geneva, WHO, 1999.
12 Cooperberg PL, Burhenne HJ: Real-time ultrasonography: Diagnosis technique of choice in calculous gallbladder disease. N Engl J Med 1980;302:1277–1279.
13 Haffner SM, Diehl AK, Valdez R, Mitchell BD, Hazuda HP, Morales P, Stern MP: Clinical gallbladder disease in NIDDM subjects. Relationship to duration of diabetes and severity of glycemia. Diabetes Care 1993;16:1276–1284.
14 Sasazuki S, Kono S, Todoroki I, Honjo S, Sakurai Y, Wakabayashi K, Nishiwaki M, Hamada H, Nishikawa H, Koga H, Ogawa S, Nakagawa K: Impaired glucose tolerance, diabetes mellitus, and gallstone disease: An extended study of male self-defence officials in Japan. Eur J Epidemiol 1999;15:245–251.
15 Pacchioni M, Nicoletti C, Caminiti M, Calori G, Curci V, Camisasca R, Pontiroli AE: Association of obesity and type II diabetes mellitus as a risk factor for gallstones. Dig Dis Sci 2000; 45:2002–2006.
16 Sama C, Labate AMM, Taroni F, Barbara L: Epidemiology and natural history of gallstone disease. Semin Liver Dis 1990;10:149–158.
17 Bennion LJ, Mott DM, Spagnola AM: A biochemical basis for the higher prevalence of cholesterol gallstone in women. Clin Res 1978;26: 496.
18 Einarsson K: Why do humans secrete too much of cholesterol into their bile? Hepatol Rap Lit Rev 1992;22:11.
19 Méndez N, Cárdenas R, Ponciano G, Uribe M: Pathophysiology of cholesterol gallstone disease. Arch Med Res 1996;27:433–441.
20 Persson GE, Thulin AJG: Prevalence of gallstone disease in patients with diabetes mellitus. A case-control study. Eur J Surg 1991;157:579–582.
21 Chen CY, Lu CL, Lee PC, Wang SS, Chang FY, Lee SD: The risk factors for gallstone disease among senior citizens: An oriental study. Hepatogastroenterology 1999;46:1607–1612.
22 Chapman BA, Wilson IR, Frampton CM, Chisholm RJ, Stewart NR, Eagar GM, Allan RB: Prevalence of gallbladder disease in diabetes mellitus. Dig Dis Sci 1996;41:2222–2228.
23 Bouchier IAD: Gallstones: Formation and epidemiology; in Blumgart LH (ed): Surgery of the Liver and Biliary Tract. Edinburgh, Churchill Livingstone, 1998, pp 503–516.

Clinical Images

Digestive Diseases

Dig Dis 2004;22:92–93
DOI: 10.1159/000079371

Spoke-Like Vascular Pattern – A Characteristic Sign of Focal Nodular Hyperplasias in the Liver

Steffen Rickes Kerstin Schütte Matthias Ebert Peter Malfertheiner

Department of Gastroenterology, Hepatology and Infectiology, Otto von Guericke University, Magdeburg, Germany

A 35-year-old asymptomatic woman presented with an inhomogeneous liver tumour found at a routine sonography by her general practitioner. Tumour size was 7 cm. There were no risk factors for hepatocellular carcinoma. At conventional ultrasound the mass was more hypoechoic than the surrounding tissue and had a central stellate scar (fig. 1). A spoke-like vascular pattern was found at power Doppler sonography (fig. 2). The Doppler spectrum of a feeding artery showed low vascular resistance (fig. 3). Because of this classic vascularisation pattern, the mass was suspected as focal nodular hyperplasia. The diagnosis was confirmed by histology.

Focal nodular hyperplasia is a benign hepatic lesion common in women. Its differentiation from other hepatocellular tumours is important because the treatment is usually conservative, given the absence of live-threatening complications and malignant transformation. CT scan, magnetic resonance imaging, and radionuclide scanning can all be used for diagnosis. However, power Doppler sonography is an inexpensive technique that is increasingly used for the differentiation of liver tumours. For patients with focal nodular hyperplasias, the spoke-like vascular pattern is a characteristic sign. Further studies have to find out if histology is necessary for lesions with clear sonographic detection of this feature.

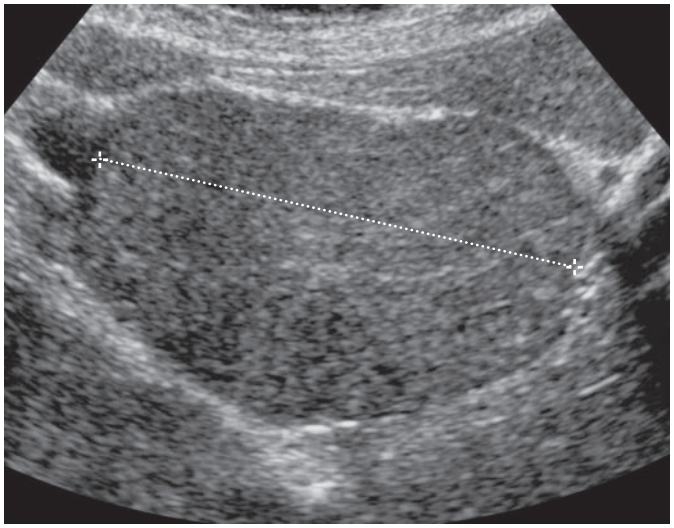

Fig. 1

KARGER

Fax + 41 61 306 12 34
E-Mail karger@karger.ch
www.karger.com

© 2004 S. Karger AG, Basel
0257–2753/04/0221–0092$21.00/0

Accessible online at:
www.karger.com/ddi

Dr. S. Rickes, Otto von Guericke University Magdeburg
Departments of Gastroenterology, Hepatology and Infectiology
Leipziger Strasse 44, DE–39120 Magdeburg (Germany)
Tel. +49 391 671 3100, Fax +49 391 671 3105
E-Mail steffen.rickes@medizin.uni-magdeburg.de

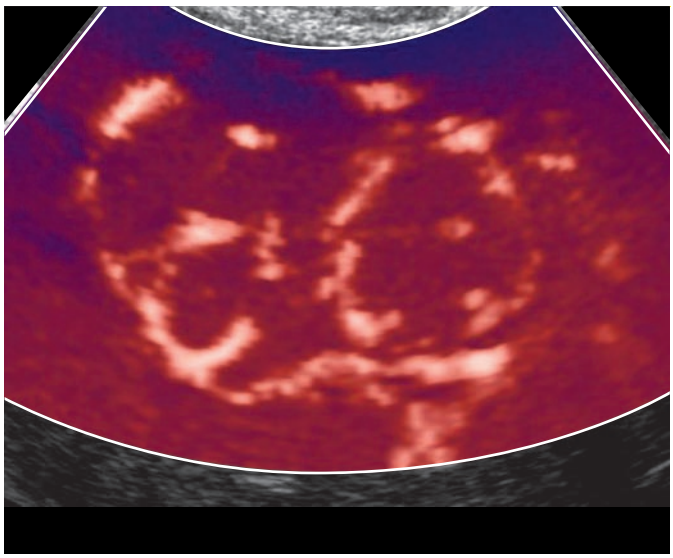

Fig. 2

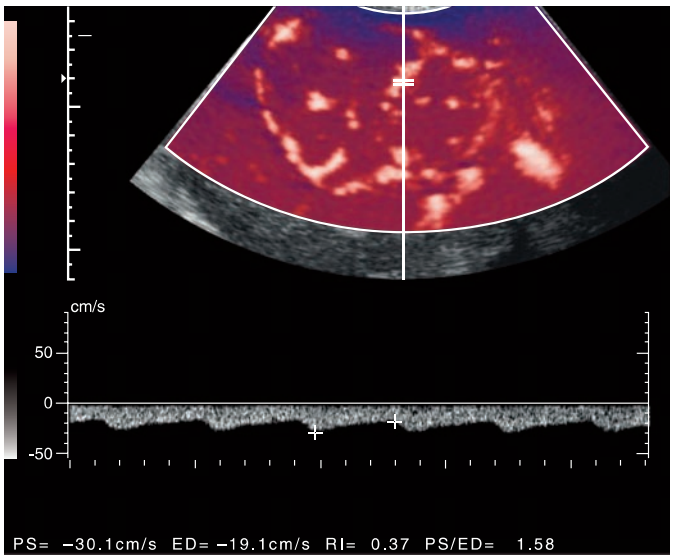

Fig. 3

Digestive Diseases

Author Index Vol. 22, No. 1, 2004

Subject Index Vol. 22, No. 1, 2004

KARGER

Fax + 41 61 306 12 34
E-Mail karger@karger.ch
www.karger.com

© 2004 S. Karger AG, Basel

Accessible online at:
www.karger.com/ddi